A cross-disciplinary analysis of the materials used in the making of Irish works of art

Thesis presented by

Veronica Biolcati

for the degree of

Doctor of Philosophy

University College Cork

Tyndall National Institute

Head of School/Department: Dr. Fatima Gunning

Supervisors: Dr. Daniela Iacopino & Prof Pádraig Ó Macháin

July 1, 2023

Declaration

This is to certify that the work I am submitting is my own and has not been submitted for another degree, either at University College Cork or elsewhere. All external references and sources are clearly acknowledged and identified within the contents. I have read and understood the regulations of University College Cork concerning plagiarism and intellectual property.

01/07/2023

Veronica Biolcati Date

Acknowledgment

I wish to extend my gratitude to my supervisors, Dr Daniela Iacopino and Prof Pádraig Ó Macháin, for patiently sharing their knowledge without any reservations and for strongly encouraging me in my career development. The research could not have been completed without the support of the collaborators in the project. Many thanks to Anna Grace Hoffmann, for having suggested references or called my attention to particular materials for consideration; Dr John Gillis, for providing a unique moral support and for sharing unpublished results; Timothy O'Neill, for his wealth of knowledge and experience; Dr Sarah Fiddyment for her willing help while she was dealing with her own projects.

I would like to express my gratitude to Dr Richard Unitt, Dr Michael McAuliffe, Prof Małgorzata Krasnodębska-D'Aughton, and Richard Keyes McDonnell for their time and willingness in this study. I wish to extend warm thanks to Dr Emeline Pouyet, Prof Élodie Lévêque, and Prof James Woolley for pushing me to do my best and for their constant encouragement which made increase my self-confidence. Dr Fenella France, Meghan Wilson, and Dr Cynthia Connelly Ryan, for their help on the way. I am also grateful to Irish Research Council for the opportunity and for the fellowship given to me.

The biggest thanks goes to my family who greatly inspired and supported me during my life and studies, as well as to all my friends for their continuous care.

Thesis abstract

Nowadays, the fields of cultural heritage preservation and heritage science are experiencing a growing demand for non-invasive analytical methodologies. These approaches aim to minimize direct interaction with artefacts in order to minimize any potential damage. In fact, non-invasive analytical techniques, by virtue of their non-destructive nature, do not induce modifications in the physical or chemical constitution of the art objects, and they often obviate the need for sampling. Since decades, X-ray fluorescence spectroscopy (XRF) is routinely used as preliminary step in most analytical surveys of artworks.

This publication-based thesis, under the auspices of the Inks & Skins project, presents three case studies which used XRF for the elemental characterization of the materials under analysis. XRF plaid a key role in all investigations, as it informed about material availability, artistic techniques, and manufacturing technologies among others.

Following the introduction on the principle of XRF and a brief overview on inks and metals, chapter two presents the multi-analytical investigation of the Irish Gaelic manuscript on animal skin, the Book of Uí Mhaine. The presented publication was the culmination of an interdisciplinary analysis of the composing material and manufacturing techniques of the largest Gaelic Books surviving from the medieval vernacular period. XRF elucidated the elemental composition of inks, pigments, and parchment support. The extensive data collected in this study served as comparative tool for the undergoing research on the materials and techniques used in other (27 at the time of this thesis) medieval Irish manuscripts from different traditions.

Chapter three presents the publication raising from the study of inks used to write nineteen satiric poems in Harward's Almanac, a 17th century Dublin book. In this specific case XRF aided to establishing the original order in which the verses were written. Again, this work would have not been possible without a transdisciplinary approach which included paleography, codicology, material science, and statistical analysis.

The fourth chapter offers a detailed description of an XRF-based analysis of three gold and silver medieval Irish chalices. This technical study was performed in order to put into historical contest a gilded silver chalice recently sold on auction as to be of medieval and Irish origin. This was done by comparing its materiality with two other late medieval silver-gilt chalices. The study helped to reveal their manufacturing technique, the nature of the decorating enamels and glass, and their story they went through. This work could have not been possible without the essential work and research of art historians.

Finally, to highlight the enormous potential of XRF technique, all the analysis were performed on-site at partner institutions, libraries, and museums.

Contents

List of acronyms

I&S Ink & Skin project

CPU Central Processing Unit

DNA Deoxyribonucleic Acid

FORS Fiber-Optic Reflectance Spectroscopy

FPM Fundamental Parameter Method

MCA Multichannel Analyser

MSI Mulstispectral Imaging

XRF X-Ray Fluorescence spectrscopy

List of figures

List of tables

1. Introduction

1.1 Scope of the project and thesis overview

Inks & Skins project (I&S), a humanities-driven endeavour supported by scientific research, served as the foundation for this thesis. Its primary objective was to employ state-of-the-art analytical techniques to investigate the materiality and composition of medieval Irish Gaelic books written on animal skin. By conducting codicological studies on the constituent materials of these works of art, examining the methods employed in their assembly, and scrutinizing evidence of notable events, it became possible to shed light on questions concerning the availability and origins of specific materials, as well as hypothesise the procedures employed by scribes.

This preliminary examination was done in conjunction with a scientific method of investigation, which used X-Ray Fluorescence spectroscopy (XRF), Fiber-Optic Reflectance Spectroscopy (FORS), Multispectral Imaging (MSI), Hyperspectral imaging (HSI), Raman micro-spectroscopy, protein and DNA analyses. The aim was to elucidate the chemical composition of inks and pigments, and the genetic make-up of the writing support made of animal skin, in order to support the conjectures formulated during the visual and codicological assessment. The outcome of one of the project's target manuscripts, the Book of Uí Mhaine, was published in Heritage (MDPI) in 2023[1] and constitute the second chapter of this thesis.

The information obtained through the study of the Book of Uí Mhaine and other books belonging to the Gaelic, Ecclesiastical, and Municipal Irish traditions, is intended to serve as a tool for conducting comparative analysis of Irish manuscripts from the medieval time. The analyses within the project were conducted on-site at the institutions where the manuscripts are hosted. Several partners participated in the project, including

UCC Boole Library, Royal Irish Academy, Representative Church Body Library, Marsh's Library, Medieval Mile Museum, Waterford Treasures, National Library of Ireland, and National Museum Ireland. I&S was also supported by a team of research fellows and associates, which included paleographers, conservators, curators, archivists, and art historians.

Efforts to digitize the majority of Irish manuscripts[1] have persisted since the late '90s, ushering in new technologies like high-resolution scanners. This transition from physical manuscripts to digital formats has not only expanded scholarly accessibility through repositories and digital libraries, but also underscored the value of integrating technology into humanities research, emphasizing the historical, societal and scientific impact of the I&S endeavor. This momentum extended from the earlier phase of digitizing Irish books.

The possibility of combining the analytical method to humanities research has proven to be crucial for the success of this project. In heritage science, mere acquisition of analytical data falls short; collaborative contributions from diverse fields such as analytical bibliography, paleography, conservation, and codicology have been essential in forming accurate conclusions. The symbiotic effort of experts form seemingly distinct areas have catalysed new ideas and additional projects. This included a comprehensive study of a printed book from 17th century Dublin, the Harward's Almanac, and the stylistic and elemental characterization of three medieval silver chalices associated to Ireland.

An interdisciplinary approach characterized the study of Harward's Almanac, a book containing rare satirical Irish poems. Examining the book, during its disassembly for conservation at the National Library Ireland, unveiled insights into its creation, binding, and reordering of pages. XRF analysis of inks corroborated historical hypotheses about inscription and dating, while statistical analysis grouped similar inks by their elemental composition, linking them to their circulation date. The outcome of this project was submitted for publication to Journal of Cultural Heritage (Elesevier) in 2023 and constitute the third chapter of this work.[2]

The same interdisciplinary strategy extended to studying three late medieval Irish chalices – the Ó Learghusa, de Burgo-O'Malley, and TP-IEP chalices – housed in the

[1] https://www.isos.dias.ie/

National Museum of Ireland. The investigation aimed to compare their artistic execution and elemental composition, revealing insights into their manufacturing technology. The findings provided, for the first time, historical and artistic insights into medieval Irish ecclesiastical silverware, enriching their significance in Irish art and history. The work was submitted for publication to Journal of Cultural Heritage (Elesevier) in 2023 and constitute the fourth chapter of this thesis.[3]

Incorporating these three interdisciplinary studies into this work served to highlight the necessity of multifaceted approaches to research. Insights from materials science, codicology, statistics, paleography, conservation, and art history converge to tackle complex research questions such as reconstructing ancient artistic manufacturing technologies and artistic practices. Attempting to address such complex questions solely through individual disciplines would result in an incomplete understanding of the matter. Instead, a synergistic approach outperforms individual investigations.

It is noteworthy that within an analytical survey, the most pivotal aspect lies in the treatment of data, which holds significantly more weight than the initial data acquisition.

A well planned investigation begins with a profound understanding of the materials under study. This is typically initiated by scholars, which collect historical information, conservation reports, photographs, and conduct literature research on similar artworks. These factors wield substantial influence over the formulation of the appropriate scientific protocol, essential for the success of an analytical project. This significance arises from the fact that the protocol is heavily reliant on the research questions. Moreover, neglecting the historical context of the artefact, including their time and place of production, the ageing processes of materials and their products, and any modern materials used in previous conservation treatments, can lead to misleading analytical data and erroneous interpretations. Thus, a comprehensive and meticulous research of the artworks stands as an indispensable prerequisite for the application of a robust scientific methodology, and that is why historical research and extensive visual assessment comes first in the analytical protocol.

In summary, the journey explored in this thesis was fuelled by the I&S project and nurtured through collaborative holistic endeavors. This approach offered a range of benefits that significantly enhanced the quality, scope, and depth of this research. Finally,

this work showcased the vital role of diverse approaches in uncovering the secrets of the past and reshaping how we see and understand it.

1.2 X-Ray fluorescence spectroscopy

X-ray Fluorescence Spectroscopy (XRF) is a widely employed analytical technique for determining the elemental composition of art materials.[4] It operates by generating an X-ray beam that interacts with the surface of the sample, inducing characteristic fluorescence from its constituent elements. This emitted fluorescence takes the form of secondary X-rays, which are subsequently collected, measured, and presented in a spectrum for analysis. In the XRF spectrum, the energy (x-axis) corresponds to the chemical element interacting with the incident X-rays, while the peak intensity (y-axis) approximately indicates the concentration within the material being studied.

A significant advantage of XRF is its non-invasive nature, eliminating the need for destructive sampling or altering of the analysed material. Moreover, its portability facilitates *in situ* investigations, reducing the risks associated with transporting valuable artworks to dedicated laboratories. Additionally, XRF provides rapid results, typically within seconds or minutes. Finally, a semi–quantitative approach to XRF data can be employed.[5]–[10] This approach involves utilizing the intensity of the emitted X-ray fluorescence signals to estimate the relative concentrations of elements present in the sample. While not providing absolute quantitative values, this semi-quantitative method is valuable for gaining insight into the elemental composition and understanding changes in composition across different samples.

However, like any analytical technique, XRF has inherent limitations. The primary drawback arises from the reduction in energy of fluorescent lines for elements with low atomic numbers (Z). Consequently, elements with $Z<11$ (sodium), which are the fundamental components of organic compounds including carbon-based inks, organic colorants, and ink/pigments' binders, cannot be characterized.[11] A second limitation,

as previously said, pertains to precise quantitative analysis, as the intensity of the fluorescent lines of an element depends on two main factors. The first factor is the overall composition of the analysed area, referred to as the matrix effect, which remains partly unknown, particularly for lighter elements. The second factor concerns the depth distribution of elements due to the X-ray excitation and fluorescence screening effect exerted by each material layer on those beneath.[12], [13] Several studies were performed with the aim of correcting for these effects, rendering the quantification quite precise.[14]–[17]

Finally, XRF is capable of elemental characterization but not compound identification. Despite these constraints, XRF frequently serves as a preliminary means of examination and may even be the sole analysis performed when investigating objects that cannot be sampled. In some cases, it may suffice as the only analysis required to address specific inquiries.

1.3 XRF working principle and instrumental components

When high-energy X-rays impact the surface of an object, they can interact with matter in different ways. The photoelectric effect is the physical phenomena utilized in XRF spectroscopy, in which the incident photon is fully absorbed by the atom of interest, prompting the emission of X-ray fluorescence.[18] The X-rays emitted from the instrument's X-ray source (the X-ray tube) possess enough energy to dislodge an electron from the core shells of atoms within the material. This creates a vacancy, inducing the atom into an excited state (refer to Figure 1.1).

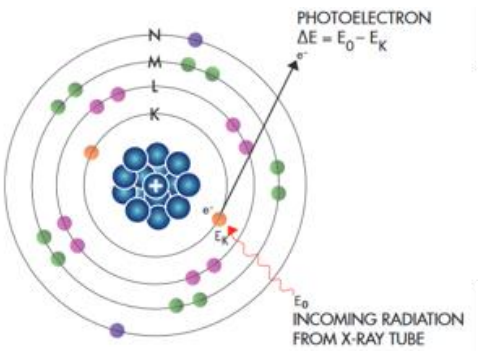

1.1 - Schematic showing the photoelectric effect induced by the collision of an X-ray to the atom. X-ray impacting the atom and creating the vacancy. Image reproduced from Bezur et al. 2020 [19].

To resolve this excited state, electrons from the outer orbitals move to the inner ones to fill the vacancy. This process, known as the electronic cascade, is triggered by the initial vacancy induced by the primary X-ray (Figure 1.2). However, the movement of electrons from outer shells creates additional vacancies that require occupation by other outer electrons, setting off a cascade effect. This process continues until the outermost

orbital is filled by a free electron in the material, ultimately returning the atom to its ground state.

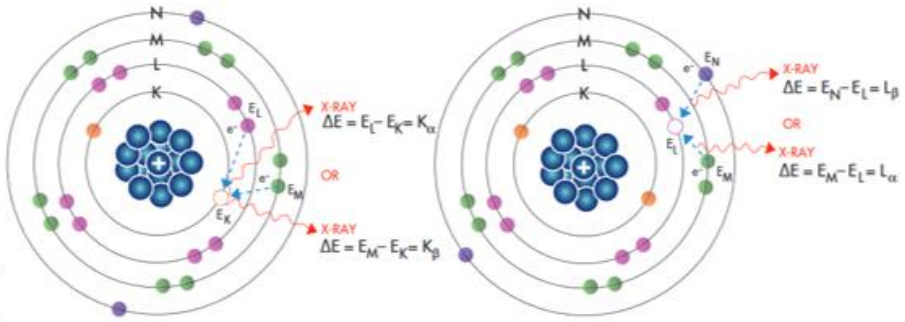

Figure 1.2. Left: Movement of electrons from L and M shells to K shells with consequent emission of Kα and Kβ photons with energy corresponding to the difference between their shells' energy levels. These transitions fill the vacancy in the K shell and, in turn, create vacancies in the L and M shells. Right: Electronic transition from L and N shells to fill a vacancy in the M shell. Image reproduced from Bezur *et al*. 2020 [19].

To name all these possible transitions, the Siegbahn notation is generally used (K, L, M, N, and others, in descending order of occurrence probability). This nomenclature is still in use despite having been replaced by the IUPAC denomination in 1991.[20], [21] In the Siegbahn notation the shell being "filled" are named with a letter (i.e. K, L, M) followed by a Greek letter (i.e. α, β, γ) which define the specific transition (see Figure 1.3).

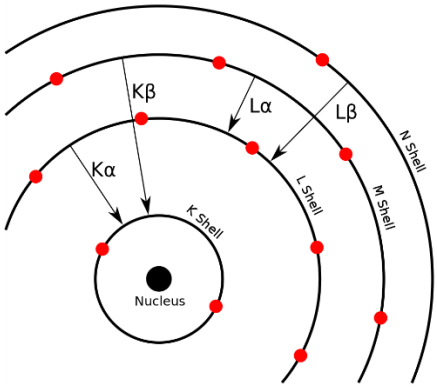

Figure 1.3- Diagram illustrating the Siegbahn notation

K, L, M, and others transitions emit distinct energies, which correspond to the energy level difference between the involved shells. In addition, the electronic orbital structure is elemental-specific. Therefore, every element will exhibit a distinct set of characteristic emission peaks in the spectrum, enabling elemental differentiation. It is

worth noting that, in presence of multiple elements, the overlapping of emission peaks may complicate the interpretation of the spectrum. For instance, the Kα line for arsenic (As) appears at 10.543 keV, which overlap with the lead (Pb) Lα at 10,549 keV. In case of high Pb concentration, only the Kβ emission peak for As will reliably indicate the presence of As.

XRF spectrometers are basically composed of a source of X-ray (X-ray tube) and of a detecting system for the collection of the secondary radiation emitted by the matter under analysis. In Figure 1.4 the main components of a handheld XRF spectrometer are illustrated.

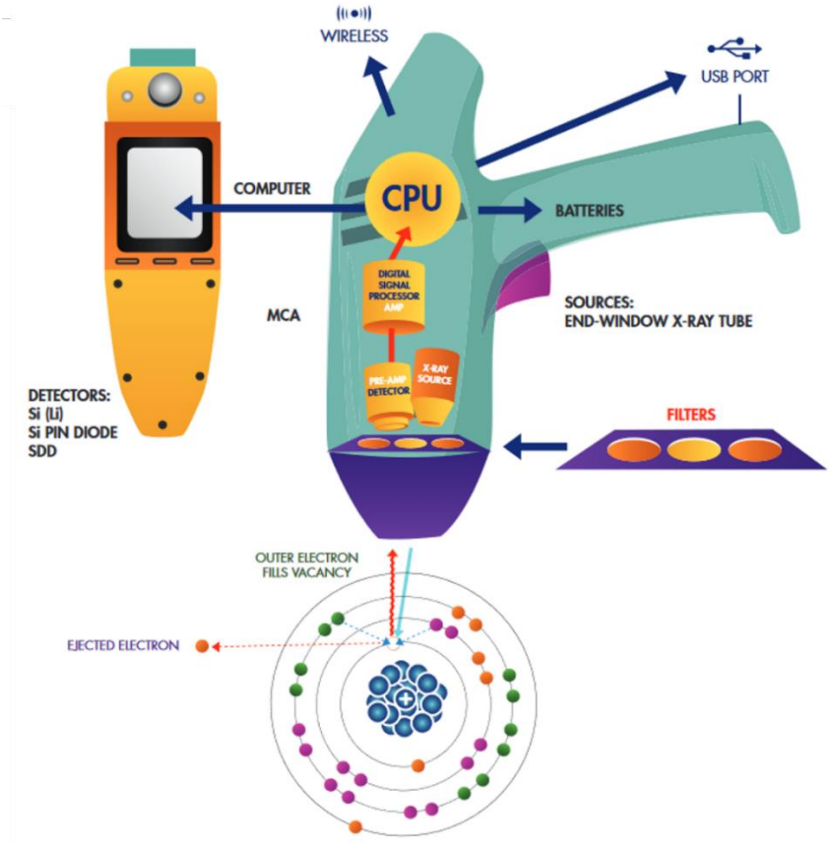

Figure 1.4 - Graphic representation of a handheld XRF spectrometer. Image reproduced from Bezur et al. 2020 [19].

The primary radiation, product of the X-ray tube, leaves the instrument through a beryllium window and a collimator (if present) and irradiates the material under analysis. The collimator has the function of reducing the beam cross-section size and to point it toward the area of interest. Every diffused or fluorescence photon that reach the detector

interact with it by yielding its energy. This causes the emission of an electric impulse with an amplitude proportional to the given energy. All these impulses are detected and pre-amplified by the digital signal processor or multichannel analyser (MCA), then sent to the central processing unit (CPU) which select and memorize these signals based on their amplitude. The results is an XRF spectrum with the energies of the photons in the x-axes and their corresponding counts on the y-axes (Figure 1.5).[19]

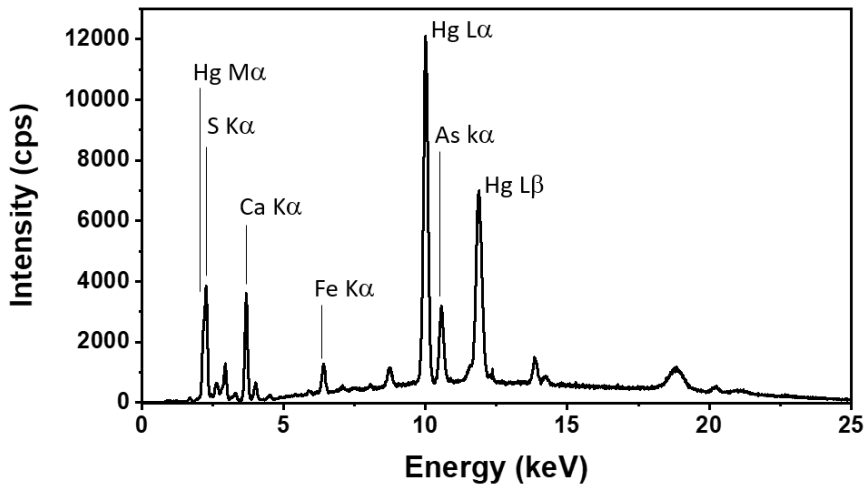

Figure 1.5 – Example of an XRF spectrum. In the x-axes the energy of the emission peaks is expressed in kiloelectron volt (keV), in the y-axes the intensity of the peaks is expressed in count per second (cps). Spectrum from red decoration in the Book of Uí Mhaine, folio 48r.

The primary component of the instrument that warrants further attention and explanation is the X-ray tube. The X-ray tube is comprised of a filament wire, which is heated to incandescence by controlling an electric current (A) that passes through it. This induces electrons to be emitted. The application of a potential difference (kV) between the filament (the cathode) and the target material (the anode), induces the acceleration of these electrons from the cathode to the anode. The amount of energy produced (in keV) by this movement is equal to the potential between cathode and anode; for instance, a potential of 50 kV produces X-rays in a range 0-50 keV.

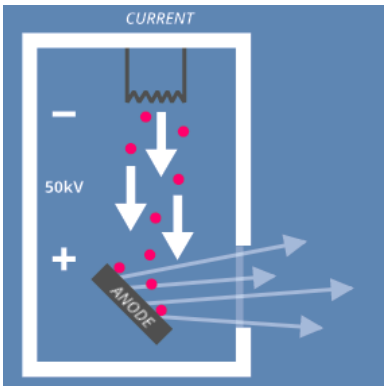

Figure 1.6 - Schematic of an X-ray generator. The red dots represent the accelerated electrons and the arrows represent the emitted X-rays. Image reproduced from https://www.horiba.com/int/scientific/technologies/energy-dispersive-x-ray-fluorescence-ed-xrf/xrf-key-components/

The deceleration of these electrons when they impact the anode produces a broad X-ray continuum. This is called bremsstrahlung (breaking radiation). A part of these electron will also cause characteristic X-ray fluorescence from the anode material itself.

In other words, the accelerating voltage (kV) determines the range of energies produced by the X-ray tube, while the current (A) controls the quantity of electrons bombarding the anode, resulting in the output intensity of the bremsstrahlung and characteristic radiation of the excited elements under analysis. This is significant because each element in the periodic table has an optimal energy for the fluorescence effect to occur, referred to as the absorption edge. The absorption edge represents a distinct point of discontinuity in the substance's absorption spectrum. As previously explained, electronic shells possess precisely defined energy levels. Consequently, the absorption of electromagnetic radiation occurs only at specific frequencies of radiation. This necessitates the impacting X-ray to have adequate energy, closely matching and slightly exceeding the electron-nucleus binding energy. This implies that by tuning the voltage of the X-ray tube, it becomes possible to selectively excite specific elements. This is crucial, as instrument settings must be tailored to the composition of the material under analysis. For instance, when analyzing metal alloys containing heavier elements or inks and parchment composed of lighter elements, optimal settings will differ. In cases involving metal analysis, where metallic elements are particularly susceptible to the photoelectric effect, the voltage will span the full range to detect all possible elements, while lower amperage will be employed to minimize artifacts in the spectrum including pile-up peaks. Pile-up peaks arise at high count rates: when two photons simultaneously reach the

detector are interpreted as a photon of characteristic energy equal to the sum energy of both photons. On the contrary, when examining manuscripts consisting of inks, parchment, and/or paper – materials comprised of lighter elements that emit weak low-energy fluorescence photons – it becomes necessary to enhance the X-ray beam intensity (and long exposure time). This can be achieved by employing high amperage. Meanwhile, the voltage can be maintained at a lower level, as the goal is to excite elements with low electron-nucleus binding energy, and, as was already said, the process is maximized when the energy is close to the element's absorption edge.

Despite the fact that high-energy X-rays can penetrate deeply or even pass through materials, the secondary X-rays detected by the detectors originate from the surface layer of the analysed area. The depth of penetration is determined by the absorption properties of the materials involved. For instance, metals and metal alloys, which have a higher density compared to composing elements of parchment or paper, primarily yield a signal from the few superficial microns of material. However, when examining manuscripts, it is possible to capture signal from subsequent pages as well. This consideration is crucial when selecting the optimal area for analysis and for addressing X-ray safety concerns. When analysing a manuscript, maintaining the page in a vertical position, or at an angle that prevents interference from subsequent folios, is suggested. Furthermore, the presence of other detectable materials on the reverse side of the page must also be avoided. On the contrary, when analysing a metal artefact, the density of metals, and their absorption, results in a characterization limited to the superficial layer. For instance, the presence of corrosion products, which accumulate on top of the metal to be analysed, challenges the analysis of the underlying metal. Finally, it is important to note that due to the high reflectivity of metals, maintaining a safe distance from the instrument while working is necessary.

1.4 X-Ray fluorescence for the study of manuscript and metal artefacts

XRF allows for the characterization of the elemental makeup of the areas under analysis and offers a quick and non-invasive way for knowing the majority of the elements in the periodic table. The understanding of the smaller components of the matter, the atoms, constitutes the first step in nearly all analytical endeavours concerning artworks.[22] This powerful techniques has allowed art and conservation stakeholders to investigate a wide array of materials including metal, pigments, inks, parchment and paper, photographs, ceramics, among many others. The adoption of XRF as a standard technique for artwork analysis stems from numerous compelling factors. Beyond its rapid, non-invasive, and multi-elemental material characterization capabilities, the widespread integration of XRF within heritage science is attributed to the extensive range of applications it offers, establishing its status as a routine method. The analytical surveys, which use XRF in combination with other techniques, often seek to reveal the intricate cultural and historical milieu during the creation phase of the artworks[23]. It is possible to investigate paper and parchment support and reveal the materials used for their preparation.[24]–[26] For instance, Wolff *et al*. measured the elemental composition of parchments fragments and used chlorine/bromine ratios to differentiate between fragments originating in the Dead Sea region and those originating in other geographical areas.[27]

Delving into the pigment composition within manuscript illuminations can give rise to hypotheses about the availability and trade of materials at the time of production,[23] provenance,[28], [29], evolution of pigment use in time and space,[19] as well as later additions and modification.[30] For instance, the non-destructive

capability of XRF instrumentation, along with the possibility of being used on-site, was exploited by Cesareo,[31] and Devezeaux de Lavergne *et al.* to investigate pigments, inks and gold used for the illumination of the folios in a medieval French manuscripts. Deneckere *et al*. used a multi-analytical approach for unveiling the use of pigments in the 12th century manuscript *Liber Floridus*,[32] and Burgio *et al*. identified the pigments used in Islamic manuscripts, where they established that the same pigments were used from the 16th to the 17th century, while they began to change in the 18th century with the introduction of synthetic pigments.[33] Similarly, it is possible to get a better understanding of the use of material within the works of a single artist. Mulholland *et al.* adopted a holistic strategy, leveraging XRF, Fiber Optic Reflectance Spectroscopy (FORS), and hyperspectral imaging to thoroughly characterize Bauer's palette in his coloured annotations.[34]

XRF can also be effectively employed for the examination of inks in manuscripts and printed books. Specifically, it allows for the characterization of the inks, it enables the evaluation of degradation to the underlying supports, and can facilitate the recovering of palimpsests.[35] Hahn *et al*. introduced the practice of using XRF for differentiating among iron-gall inks based on the detection of trace elements present in the iron sulfate of the inks.[36] The technique allowed recognition of different iron-based inks, based on their fingerprint elements, used by artists and scribes.[37], [38] Consequently, it became possible to establish a chronology of their use[39] and later additions.[40], [41] In addition, XRF allows to propose groupings of different manuscripts by using the similarities of their writing inks composition.[42] Turner *et al*. were able to visualize and reconstruct the iron-based ink underdrawings in the manuscript's illuminations using XRF mapping, revealing the working process of the artist.[12] Using a combination of ink fingerprinting and XRF mapping, Gerken *et al*. were able to reveal that iron-based inks were not only used for writing but also for the underdrawings of several German medieval panel paintings.[43] Kanngießer *et al*. studied the degradation of paper support in manuscripts caused by iron-gall inks using an entire X-ray-based protocol. Using XRF (point an mapping), and micro X-ray absorption near edge structure spectroscopy (micro-XANES) they were able to identify that Cu play a role in the photo-reduction process of iron, known to effect paper degradation and embrittlement.[44] Therefore, XRF finds utility in comprehending the artwork's journey through time, aiding the assessment of the

materials' conservation state, and providing conservators with insights for selecting the optimal conservation interventions.

Similarly to what is done for manuscripts, XRF has been widely used in characterizing historical metal alloys due to the inherent suitability of metallic elements for this technique.[45], [46] Metallic elements possess high atomic number, resulting in prominent emission peaks during XRF analysis. This explain why, in the late '60s, the first attempts to apply XRF for the study of cultural heritage mainly focused on the use of this technique for the characterization of metal alloys. Additionally, the nature of more complex samples, such as pigments or inks, is not always fully resolved by using this technique alone and often requires investigations at the molecular level.

The unveiling of metal artefacts elemental composition can add to the knowledge of their composition and production technology, as well as the dynamic evolution of metallurgical methodologies in ancient time, and their geographical spread. [47]–[49] For example, Hložek *et al*. proved the production of brass in the South Moravian Region. Until recently, the majority of their aged objects displaying a green patina were commonly categorized as bronze (copper-tin alloy); however, upon conducting XRF analyses, it was revealed that the alloy was, in fact, brass (copper-zinc alloy).[50]

There are several XRF studies of coins and jewellery in literature, from ancient to modern time.[51]–[53] For instance, Sándor *et al*. used quantitative XRF for knowing the gold, silver, and copper content in medieval coins in Hungary and Byzantium and related these contents to the coins' provenance.[54]

XRF can help to shed light on modern materials applied during previous conservation treatments, aiding the discerning of original materials form later additions.[55] In a similar way, the elemental characterization can help the identification of modern or medieval counterfeit.[56]

Moreno-Suárez *et al*. utilized XRF both before and after employing various cleaning methods on copper-silver alloys to identify the least aggressive approach.[57] Also Porcinai *et al*. proposed an XRF analysis with an application to conservation of silverware. They were able to assess the thickness of application of protective coatings on metal depending on the means of application either brush or spray.[58]

1.5 Quantitative analysis of X-Ray fluorescence data

Quantitative XRF analysis allows for the accurate determination of elemental concentrations in the sample under analysis. This can be achieved through two methods.

The first technique, commonly applied to metal alloys, involves comparing analytical data with data obtained from the analysis of alloy standards.[59], [60] A mathematical curve/model, derived from known alloy standards, represents the intensity of elemental peaks against their concentrations. This curve is used as a reference to infer the elemental concentrations of the alloys being analyzed.

The second method, known as the fundamental parameter method (FPM),[61] employs a standardless semi-quantitative approach that is particularly suited for unknown materials with complex matrices, such as inks, or materials lacking reference standards.[36], [38] The FPM is rooted in the fundamental physical principles of XRF and considers the complexities of the sample matrix, providing more accurate and reliable results for elemental concentrations.[17], [62]

The conversion of peak intensities to elemental concentrations can be accomplished using various software tools, including AXIL[63] and PyMca[64]. PyMca, developed at the European Synchrotron Radiation Facility, stands out as the most comprehensive solution for quantitative XRF. This open-source software boasts a user-friendly interface. A typical procedure utilizing PyMca involves the calibration of the experimental XRF spectrum, identification of the elemental peaks present, extraction of peak areas through the spectrum fitting tool and the “fit configuration” dialog, and, finally, quantification of the concentrations of the elements.

In greater detail, the initial noise fluctuations in the raw experimental data are subjected to smoothing, such as the Savitsky-Golay method. This smoothing operation models the region of interest in the spectra using a polynomial line. The net peak area of the elements is then obtained after correction for the continuum background. For this correction, the preferred approach is SNIP (Statistical Nonlinear Iterative Peak Clipping).

Next, the peak shapes are examined to assess whether the fitting function accurately models the raw spectra, making it suitable for subsequent steps, such as batch fitting. This fitting procedure, which aims at minimizing the difference between the fitting line representing the experimental data and the raw spectra, is repeated until the optimal set of parameters is determined.

Following the spectrum fitting, the elements of interest are selected. Parameters such as the X-ray tube emission profile for the XRF spectrometer, primary beam filter, thickness of the beryllium window, and the active area of the detector need to be provided to the PyMca software through a configuration file or by populating with these data the fit configuration dialog, enabling their consideration in the analysis. Experimental parameters, including time exposure, acquisition geometry, and XRF tube flux, are adjusted according to the setup employed during data acquisition. Once a satisfactory agreement is achieved between the fitting line and experimental data, the concentrations of the elements of interest can be extrapolated.

Hahn *et al*. extensively employed FPM to discriminate between writing inks and identify manuscript passages containing inks of similar elemental composition.[65] Manso *et al*. successfully determined and quantified the elemental composition of the paper support and writing inks in the Third Secret of Fátima. This enabled them to verify the document's originality and confirm that no alterations to the original manuscript had been made.[10] Similarly, Pessanha *et al*. used FPM for the analysis of XRF data from paper and inks in the early 20th-century Austrian book *Civilprocessordnung*, demonstrating the applicability of quantitative XRF in forensic studies.[66] Cappuccio *et al*. applied the FPM to XRF data to comprehend the stoichiometry of colors used in two Japanese scrolls. This furnished conservators with a tool to optimize the formula for consolidating adhesive in the conservation treatment, based on elemental concentrations obtained from XRF.[67]

Heginbothan and Solé designed a protocol for the quantification of copper alloys using both alloys standards and FPM using eight XRF spectrometers available in the market. This was done to maximize the reproducibility of results from various institutions that run analysis on metal artefacts with different XRF instruments.[8], [9]

1.6 Inks

The term ink originates from the ancient Greek word *enkauston*, which signifies burnt or cooked. This is likely a reference to carbon black, the primary historical source of black inks, derived from the combustion of various wood species or plant residues.[68] Inks typically consist of a coloring agent and a medium. The coloring agent can be either an inorganic pigment or an organic dye. The medium enables the colorants to stay suspended during application and also promotes the ink adherence to the surface once it dries. Throughout history, diverse types of ink have been utilized, each with distinct recipes that vary based on the time period and origin.

Since 2500 BC, Chinese scribes used inks made of lamp black or carbon black mixed with a vegetal oil, in liquid or solid form. Ancient Egyptian also employed carbon-based blacks but with different binders: gum arabic, vegetal oil, or animal glue.

The methods for ink production appears to have spread from Egypt to Greece and eventually reached Rome. This is supported by the writings of Pliny and Vitruvius, who, in the first century after Christ, detailed the process of ink-making.[69] The ingredients were carbon-based black, extracted from burning fruit pitches or various types of wood mixed with gum arabic, honey, egg white, or animal glue. These ink recipes included vinegar, extract from garlic and cloves as preservative.[70] Pliny was the first to describe an alternative recipe for carbon-based inks: iron-based inks. His formulation included iron salts, a solution of gallnuts and peel of pomegranates. Even in that era, the potential issue with carbon ink was evident, as it could be easily removed by scraping it off the surface. This characteristic finds its origin in the ink's nature: carbon-based ink is a dispersion of particles in a medium. Consequently, if the binder is removed through scraping, the coloring agent is also eliminated. In contrast, iron-based inks include a component that stains the substrate, enhancing their resistance to erasure.

In Middle Age Europe, despite being produced using several recipes, mainly three types of inks were used: carbon-based inks in gum arabic or animal glue, mixed inks of carbon-based and gallic-metal compounds in gum arabic, and pure gallic-metal inks in gum arabic.[71]

Gum arabic, is derived from several *Acacia* species, is a polysaccharide-based tree exudate.[72] Gum arabic is one of the most used ink binder due to its water solubility. This property allows to form a viscous gel when mixed with water and act as a glue after moisture evaporation.

Carbon-based inks were crafted through the mixture of a binder (often gum arabic) with water and carbon-based compounds procured from various sources. Carbonaceous materials exist in nature in diverse forms: the crystalline allotrope is known as graphite, while flame carbons, cokes, chars, and coal are considered disordered materials.[73] Flame carbon and soots consist of carbon generated in the gaseous phase through incomplete combustion of hydrocarbons; chars are the outcome of wood pyrolysis, a process characterized by the thermal decomposition of wood under controlled conditions; cokes are synthetic materials derived through the carbonization of bituminous coals or bitumen; coal is an organic rock composed of lithified plant remains.[74], [75]

Coccato *et al*., in their Raman spectroscopic studies of carbonaceous materials, proposed a classification of carbon-based blacks used in art, and therefore with a possible use in ink making, based on their production processes: carbon black of mineral and natural origin (i.e. graphite, black heart, humic heart, sepia), blacks obtained from firing vegetable or animal materials (i.e. charcoal, carbon-black, peach black, grape black, cherry black, ivory/bone black, atramentum, bistre), and blacks obtained in the form of smokes and soots (i.e. furnace black, lamp black).[76]

To counteract the ease with which carbon-based inks could be erased, scribes likely began experimenting by mixing various materials into their inks. Eventually, they discovered that adding iron sulfate, which is soluble, facilitated the ink's penetration between the skin fibers, resulting in better resistance to rubbing. Consequently, there might have been a period during which both carbon-based inks and iron-based inks coexisted, frequently being used in combination to achieve desired optical and physical properties. For instance, carbon-based inks required continuous stirring to keep the carbon particles suspended in the ink container, therefore an addition of iron-based ink, since it

is a dark liquid with no apparent particles, was possibly providing the impression of not having to stir so frequently. On the other hand, iron-based inks were not very dark upon application, possibly prompting the practice of blending them with carbon-black to enhance ink visibility during use.

While a precise transition from carbon- to iron-based inks cannot be pinpointed, and while these two ink types were likely used in combination, evidence indicates that by the late Middle Ages, the prevalent choice of ink shifted towards iron-based inks.[77] The constituents of iron-based inks typically comprised water, often with the addition of wine or vinegar to modify the pH of the aqueous solution, along with tannins (from plants parts including bark and galls among others), and an iron source, either iron sulfate (vitriol) or iron fillings.[39], [78], [79] A binder like gum arabic was not consistently employed. The interaction between gallotannin-containing extracts and iron sulfate led to the formation of a water-soluble ferrous complex. Upon application and exposure to oxygen, this complex transforms into an insoluble dark compound known as the ferric gallate pigment.[80] This transformation is pivotal in endowing iron-based inks with their resistance to erasure. The ink penetrates deeply into parchment or paper fibers, rather than merely residing on the surface, and transforms in situ into an insoluble compound.

Iron-gall inks are a type of iron-based ink that utilize tannins derived from gall nuts. These nuts result from the actions of parasitic insects, which puncture various types of vegetation to lay their eggs. The galls produced by gall wasp larvae on oak trees are particularly esteemed for ink production due to their high tannin content, specifically gallotannic acid responsible for the chemical reaction.

As previously explained, one of the essential components of iron-based inks is vitriol. Vitriol is a mixture of metal sulfates composed for the majority of iron sulfate ($FeSO_4$) and with minor components of copper, manganese and zinc sulfates. Vitriol provide iron(II) ions which react with organic gallotannic acid to form the iron complex.[81] The elemental components of vitriol (iron, copper, manganese, and zinc) are detectable using XRF, and allow for the discrimination among various inks and vitriol sources.[80] The reaction, in presence of humidity and especially when there is an excess of iron sulfate over gallic acid, produces sulfuric acid (H_2SO_4) known to be responsible of the damaging “corrosion” of the substrate (especially in the case of paper supports).[82] This explains the reason numerous elemental and molecular studies of

iron-gall inks, which attempt to characterize the reaction taking place and mitigate the damage.[83]

1.7 Historical silver alloys and their decoration

Metal artifacts have been crafted since ancient times. They were used both for practical purpose as well as artistic production. Metalwork stands as invaluable source of information into the practices of ancient metallurgy, as well as for historical and cultural understanding regarding their place and time of production.

Medieval metal crafts, with regards to ecclesiastical metal objects, were primarily made of gold, silver, copper, and their alloys. These religious objects were often commissioned by patrons and donated to the local church as a symbol of their wealth.[84] In view of this increasing demand, and easier access to raw materials, the medieval period witnessed the refinement and expansion of metalworking techniques, leading to advancements in areas such as blacksmithing, casting, and alloying.[85]

The physical properties of metals are what have led to their choice as construction materials. In the case of artworks, they are valued for being precious, hard, and durable substances. Moreover, metals can undergo various forms of manipulation, such as alloying, quenching, casting, and shaping through hammering, enabling artisans to craft them into desired forms and structures.[86]

Metals, with the exception of mercury, exist as cohesive collections of atoms that have a solid state at standard room temperature conditions. These atoms are intricately united through metallic bonds, a consequence of their sharing of accessible electrons.[86] Generally metals have a poly-crystalline structure (they are composed of grains), but when the molten metal is rapidly cooled their structure change form a crystalline phase to near-amorphous solid phase.[87]

Metals can be alloyed, leading to the creation of a mixture comprising two or more distinct metals. This practice is employed for various purposes, including altering the properties of the base metal (the component present at higher concentration). These

alterations can encompass lowering the melting point, enhancing strength, hardness, or ductility, while also preserving aesthetic attributes. For instance, silver is a soft metal easy to work. To reduce its malleability, and to reduce cost, silver was often alloyed with copper.

Since metals in alloys have different melting points, they solidify at varying rates and their crystals expand until they meet each other. This microstructural heterogeneity is referred to as dendritic. The dimension and configuration of these dendrite, resembling miniature fern-like structures, depend on the rate of molten cooling. Rapid cooling yields smaller dendrites, while slower cooling results in larger ones.[86] This phenomenon instigates phase-segregation, whereby one of the alloy components becomes localized within the inner or outer sections of the dendritic arm or the outer surface. As previously elucidated, when XRF analysis is conducted on metals and metal alloys, the examination is limited to the surface layer, which may not accurately reflect the overall composition.

When subjected to stretching or hammering, metals initially experience elastic deformation, followed by plastic deformation before reaching a point of fracture. Plastic deformation, utilized in craftsmanship, results from the movement of atomic layers within the metal and is facilitated by weak points/imperfections in the lattice known as dislocations. A metal can be manipulated until a tangle of dislocations impedes further plastic deformation, indicating the need for high-temperature treatment. This elevated temperature induces the crystal lattice to relax and re-crystalise, thus restoring the dislocations. This process, termed annealing, enables further manipulation of the metal piece.[88]–[90]

That explain why, when shaping silver-alloy objects through hammering, twisting, or rolling, the metal becomes brittle. To counter this, the metal must be heated to around 650°C. In this process, the copper present in the alloy oxidises and forms a black oxide scale called firescale. This is removed by post-manufacture acid treatments or abrasion, leading to a change of composition, a silver-enrichment, of the surface. Since the annealing process can be iterated multiple times, the surface layers do not accurately represent the composition of the underlying alloy, and this is reflected in the XRF results. Instead, the surface will consist of several layers, varying in copper/silver content depending on the extent of annealing and applied abrasion/acid treatments.[91] This also explains why conservation treatments for silver objects should avoid surface polishing,

as it leads to the removal of original material that also serves as protection for the underlying layers.[92], [93]

Silver, along with other noble metals, is relatively resistant to corrosion and oxidation when exposed to air. [94] This quality renders it an ideal choice for crafting enduring objects that are frequently handled and utilized. Silver offers a more cost-effective alternative to gold while maintaining its durability and preciousness. This explains why silver artefacts were frequently coated with a layer of gold using various techniques.

While surviving examples are scarce, the oldest gilding technique entailed applying a layer of gold foil onto the surface of wood, bronze, or silver, and securing it by trapping the edges within grooves. This method, though wasteful and resulting in limited detailing due to the thickness of the gold foil, led to the introduction of an alternative technique using thinner gold foil.[95] Known to ancient civilizations such as the Egyptians, Persians, and ancient Greeks since the first millennium BC, and later adopted by the Romans, this alternative technique involved heating the gold foil, applied on other metals, to facilitate the diffusion of gold into the underlying metal. The Roman period saw the widespread adoption in Europe of the fire-gilding technique, which continued to be extensively used throughout the Middle Ages.[96]

Fire-gilding, also known as the mercury-amalgam technique, entailed applying a paste made of liquid mercury and gold (in the form of leaves or filings) onto the metals intended for gilding. The metal surface was initially treated with an acid solution containing alum and acetic acid to dissolve the layer of copper oxide that formed during the manufacturing process (depletion gilding).[97], [98] Subsequently, the paste was spread onto the metal and heated briefly to temperatures ranging from 250°C to 350°C, causing the surface to transition from gray to a yellow hue.[99]

Because of the mercury evaporation, the resultant surface was porous and did not possess a shiny appearance, thus necessitating a burnishing step. This step typically involved using a stone to smooth out the micro-cavities and enhance the reflective and glossy quality of the gold. This final process often left marks that are frequently discernible to the naked eye.

The surface of metal artifacts constitutes their interface with the surrounding environment and is the site where alterations and corrosion products develop. Several factors contribute to the initiation of metal transformation, including air, soil, sulfur-based

compounds, acids, oxidizing agents, salts, organic substances, and elevated temperatures. Among these, air and water play pivotal roles in the corrosion process, exerting significant influence on the condition and longevity of metal artifacts.[100], [101] For instance, silver tarnishing is a result of the growth of a corrosion layer comprising various compounds that impact the reflective properties of the metal. This phenomenon can take place on both silver and silver-gilt objects, as the gilding layer's porosity enables gas exchange with the surrounding environment. The primary constituent of this tarnish film has been identified as acanthite (Ag_2S), formed through the interaction of silver with sulfur-containing gases such as hydrogen sulfide (H_2S) and carbonyl sulfide (OCS).[102] Silver can also react with chloride-containing airborne, leading to the formation of chloroargyrite (AgCl).[103] In silver-copper alloys, selective corrosion can occur. Copper, being more reactive than silver, tends to react preferentially with the surrounding environment, and depending on the conditions, may result in the development of a green patina composed of copper carbonates ($Cu_2CO_3(OH)_2$) or dark red concretions of copper oxides. In addition, stress-induced corrosion can occur. This is often associated with extensive cold work, can selectively affect the metal from areas that have undergone substantial deformation, retaining residual stress and exhibiting weaker characteristics where impurities and minor phases tend to accumulate.[104] For guidance on the materials and methods employed in the conservation and restoration of silver artworks, one can refer to the work of Palomar *et al*.[105], [106], Liu *et al*.[88], Costa,[101], Degrigny *et al*.[107], Fariselli *et al*.[108]

1.8 Experimental methods overview

This thesis embarks on a multidisciplinary exploration, employing an array of advanced analytical techniques to unravel the intricacies of the subject matter. The experimental methods utilized include XRF (X-ray Fluorescence), multispectral imaging (MSI), Raman spectroscopy, FORS (Fiber Optic Reflectance Spectroscopy), and protein analysis for the study of manuscripts on paper and animal skin, and metal artifacts. Although the detailed application is discussed primarily for XRF, as this was the primary focus of the author of this thesis, the integration of these techniques, highlighted in this chapter, offers a comprehensive analytical approach. This integrated approach promises a richer understanding of the samples, offering a more nuanced narrative. The core of this holistic approach specifically lies in the synergy of analytical methods, each contributing a distinct layer of understanding. XRF, with its elemental revelations, forms the foundation. MSI then steps forward, adding a visual dimension that extends beyond the elemental composition. Raman spectroscopy follows suit, delving into molecular structures and shedding light on pigments and inks. FORS and protein analysis contribute further, offering insights into optical properties of pigments and organic components. This collective methodology achieves a level of material insight that surpasses the limitations of any individual technique. This multifaceted understanding holds profound value not only for scientists but also for various stakeholders in the art field, notably historians, conservators, and curators, each finding unique avenues of enrichment in the treasure trove of information. For historians and curators the data serves as a time-traveling toolkit, enabling them to delve deeper into historical contexts. For instance, the data gained through a combined application of XRF, Raman spectroscopy, MSI, and FORS allows historians to extract a wealth of information about the composition, construction, alterations, and historical context of manuscripts, contributing to a richer understanding

of the cultural and artistic landscapes of the past. For instance, MSI may reveal annotations or marginalia that have faded over centuries. This provides insights into the thoughts and reactions of contemporary readers, allowing historians to reconstruct the intellectual environment of the time. Manuscripts may contain erased or overwritten content, a palimpsest. MSI can distinguish between the underlying and overlying texts. This allows to recover lost knowledge, reconstructing narratives or information intentionally erased in different historical periods. In addition, as XRF can identify the elemental composition of pigments and inks, historians can use these data to determine regional styles and availability of specific materials during a particular era. Changes in pigment use over time may reflect shifts in trade routes, technological advancements, or cultural influences. In the case of ink analysis, variations in the iron and other elemental concentrations can provide information about ink recipes, revealing regional or chronological differences in writing practices. If a bigger sample set is analysed, for instance a collection of illuminated manuscripts, historians and curators may use the scientific data to identify differences in material composition, suggesting diverse sources or workshops involved in their production. This sheds light on the socio-economic dynamics and cultural exchange during the artworks' creation. The same applies to metal artifacts or any other media. For conservators the detailed insights into the materiality act as a cornerstone, guiding precise preservation strategies. An holistic approach enhances their ability to assess, preserve, and restore historical artifacts, contributing to the longevity and understanding of these invaluable cultural heritage. For instance, by knowing the chemical composition of materials they can find hidden features and vulnerabilities in these materials. This integrated approach empowers conservators with a holistic view, ensuring that preservation efforts are not only based on visual assessment but also encompass the broader structural aspects of the artifacts.

In conclusion, emphasizing the significance of a holistic approach in art studies is paramount. It is crucial to recognize the importance of building a bridge between scientific methodologies and cultural narratives. Beyond the individual benefits each technique provides to the specific disciplines mentioned earlier, this integrated approach serves as a connective bridge, linking scientific methodologies with the intricate stories embedded in the artifacts under study. The collaborative potential between scientific communities and cultural heritage professionals is evident, creating a space for dialogue

and mutual enrichment. The synthesis of scientific rigor and cultural insight promises a holistic and profound appreciation of the historical, cultural, and artistic significance of the examined artifacts.

X-ray Fluorescence XRF

This thesis initiated its analytical journey with XRF, a powerful non-destructive technique. XRF employed to unveil the elemental composition of the samples, providing insights into the material's chemical makeup. The comprehensive data derived from XRF served as a foundation for subsequent analyses, guiding the exploration into other dimensions of the samples. The XRF experimental data were acquired and processed solely by the author of this work.

Multispectral Imaging (MSI)

Building upon the elemental insights from XRF, MSI was introduced to capture detailed spatial and spectral information. MSI images were acquired by experts from the Library of Congress, Washington, and processed in collaboration with the author of this thesis. This technique allowed for the visualization of variations in colour and intensity of ink and pigment applications, providing a deeper understanding of the manuscripts' surface characteristics. The integration of MSI complemented the elemental data obtained from XRF, offering a holistic perspective. One of the primary applications of MSI in manuscript studies is the enhancement of text and image visibility. By capturing images at various wavelengths beyond the visible spectrum, MSI can reveal details that are often imperceptible to the human eye. Faded or obscured text, illustrations, or annotations become more legible, providing scholars with a clearer understanding of the manuscript's content. MSI is guided by the strategic capture of images at diverse wavelengths across the electromagnetic spectrum. Operating beyond visible light, it employs tailored light sources emitting ultraviolet (UV), visible, and infrared (IR) wavelengths. Specific filters isolate targeted wavelengths, and detectors record the reflected or emitted light. By processing captured images with specialized software, MSI creates a multispectral dataset. This dataset, analysed for reflectance and absorption, reveals hidden details within manuscripts.[109]

Fiber Optic Reflectance Spectroscopy (FORS)

FORS was introduced to delve into the reflective properties of the samples. This technique, performed and processed by experts from the Library of Congress, aids in understanding the interaction of light with the material's surface, offering valuable insights into its optical characteristics. The integration of FORS enhances the spectral information, fostering a more complete analysis of the samples. FORS stands as a powerful analytical tool, particularly for the characterization of pigments. Its application provides valuable insights into the composition and nature of pigments used in artworks, manuscripts, and historical artifacts. FORS operates on the principle of measuring the reflectance of light across a range of wavelengths including UV, visible, and IR regions. A fiber optic probe is employed to illuminate the sample, and the reflected light is analysed to generate a reflectance spectrum. The resulting spectrum offers information about the interaction between light and the material's surface, providing details about its composition. One of the primary applications of FORS in pigment characterization is the identification of specific pigments used in artworks.[110] Different pigments exhibit characteristic absorption features in the reflectance spectrum, allowing for their identification. By comparing the observed spectrum with reference databases, scientist, conservators, and researchers can discern the presence of various pigments and even differentiate between different shades or types of the same colour. FORS excels in detecting pigment mixtures within a single layer or across multiple layers of paint. The technique's sensitivity allows for the identification of subtle variations in pigments that might be challenging to distinguish visually. This capability is crucial for understanding an artist's layering techniques, as well as for unravelling later alterations or overpainting. The reflectance spectra obtained through FORS can also reveal information about the state of pigment preservation. Changes in the reflectance patterns may indicate pigment fading or degradation over time due to environmental factors, exposure to light, or other deteriorative processes. This information is pivotal for conservators in developing strategies for the preservation and restoration of artworks. This additional layer of analysis enhances the overall understanding of the artistic techniques employed.

Raman Spectroscopy

The journey into molecular characterization took a significant leap with Raman spectroscopy, conducted by experts at UCC with the subsequent data treatment carried

out by the author of this thesis. This technique enables the identification of molecular structures based on their vibrational modes. It identifies specific chemical bonds and molecular structures, offering details about the organic and inorganic compounds present in inks and pigments. In studying metal artworks, Raman spectroscopy helps in studying corrosion products. By analysing the chemical composition of corrosion layers, conservators can develop targeted conservation strategies to prevent further deterioration. Raman spectroscopy operates on the principle of inelastic scattering of light. When a sample is illuminated with a monochromatic light source (usually laser light), the photons interact with the molecular vibrations in the sample. The scattered light undergoes a shift in frequency, known as the Raman shift, which corresponds to the energy levels of molecular vibrations. By analyzing the scattered light, specifically the shifts in frequency, Raman spectroscopy provides information about the molecular composition and structure of the sample. The resulting spectrum reveals vibrational modes, offering insights into the chemical bonds and molecular arrangements present in the material.[111] The complementary use of XRF and Raman spectroscopy offers one of the most powerful approaches for a more holistic understanding of materials. Together, they cover a broad spectrum of compounds, combining the strengths of both elemental and molecular analysis. In summary, the integration of XRF, with MSI, FORS, and Raman spectroscopy creates a powerful analytical approach. XRF offers elemental data, FORS provides pigment and organic material details, MSI enhances visualization, and Raman offers molecular insights.

Protein Analysis

Shifting the focus to biological components, protein analysis was incorporated to explore the presence and characteristics of proteins within the folios of the manuscripts under study. This aspect broadens the scope of the thesis, providing a bridge between the physical and biological dimensions of the subject. Protein analysis was performed by experts at Cambridge University with samples collected by the author of this thesis. Protein analysis of animal skin in manuscripts is a specialized method that provides insights into the parchment used in the creation of manuscripts. Animal skin used as writing support in manuscripts is typically derived from sheep, goats, deers, or calves, and is composed of proteins such as collagen. Collagen is the primary protein present in

animal skin used for parchment or vellum. Protein analysis can assist in differentiating between parchment made from various animal species. For protein analysis, techniques like MALDI-TOF (Matrix-Assisted Laser Desorption/Ionization Time-of-Flight) mass spectrometry are commonly used. In MALDI-TOF, proteins are ionized and accelerated in an electric field, with the resulting time-of-flight data providing information about their mass and structure. Scientists and historians utilize protein analysis to gain insights into the material composition of artifacts, particularly organic materials like parchment or binding adhesives in manuscripts. By analysing the proteins present, scientists can determine the type of animal skin used, assess the condition of manuscripts, and understand historical techniques in manuscript production.[112] This information contributes to a deeper understanding of cultural practices, trade networks, and the technological aspects of manuscript creation, aiding in historical contextualization and preservation efforts.

1.8 References

[1] V. Biolcati *et al.*, "The Book of Uí Mhaine: An Interdisciplinary Analysis of the Materiality of the Gaelic Manuscript Tradition," *Heritage*, vol. 6, no. 7, pp. 5393–5409, Jul. 2023, doi: 10.3390/heritage6070284.

[2] Biolcati, Veronica *et al.*, "Establishing the original order of the poems in Harward's Almanac using paleography, codicology, X-ray fluorescence spectroscopy, and statistical analysis," *J. Cult. Herit.*, forthcoming 2023.

[3] Biolcati, Veronica, Keyes McDonnell, Richard, Krasnodębska-D'Aughton, Małgorzata, Hoffmann, Anna Grace, Ó Macháin, Pádraig, and Iacopino, Daniela, "Comparing the elemental composition of three late medieval silver gilt chalices to reveal their manufacturing technique and potential dating," *J. Cult. Herit.*, Forthcoming 2023.

[4] A. Shugar, "Advancements in portable and lab based XRF instrumentation for analysis in cultural heritage: A change in perspective," *Microsc. Microanal.*, vol. 27, no. S1, pp. 2552–2553, Aug. 2021, doi: 10.1017/S1431927621009077.

[5] R. Sitko, "Quantitative X-ray fluorescence analysis of samples of less than 'infinite thickness': Difficulties and possibilities," *Spectrochim. Acta Part B At. Spectrosc.*, vol. 64, no. 11, pp. 1161–1172, Nov. 2009, doi: 10.1016/j.sab.2009.09.005.

[6] N. Ekinci, F. i. El-Agawany, and E. Kavaz, "Quantitative Analysis in X-Ray Fluorescence System," in *X-Ray Fluorescence in Biological Sciences*, John Wiley & Sons, Ltd, 2022, pp. 287–294. doi: 10.1002/9781119645719.ch19.

[7] L. de Viguerie, V. A. Sole, and P. Walter, “Multilayers quantitative X-ray fluorescence analysis applied to easel paintings,” *Anal. Bioanal. Chem.*, vol. 395, no. 7, pp. 2015–2020, Dec. 2009, doi: 10.1007/s00216-009-2997-0.

[8] A. Heginbotham and V. A. Solé, “CHARMed PyMca, Part I: A Protocol for Improved Inter-laboratory Reproducibility in the Quantitative ED-XRF Analysis of Copper Alloys,” *Archaeometry*, vol. 59, no. 4, pp. 714–730, 2017, doi: https://doi.org/10.1111/arcm.12282.

[9] A. Heginbotham *et al.*, “CHARMed PyMca, Part II: An evaluation of interlaboratory reproducibility for ED-XRF analysis of copper alloys,” *Archaeometry*, vol. 61, no. 6, pp. 1333–1352, 2019, doi: 10.1111/arcm.12488.

[10] M. Manso, S. Pessanha, M. Guerra, J. L. Figueirinhas, J. P. Santos, and M. L. Carvalho, “Unveiling the Third Secret of Fátima: μ-XRF quantitative characterization and 2D elemental mapping,” *Spectrochim. Acta Part B At. Spectrosc.*, vol. 130, pp. 35–38, Apr. 2017, doi: 10.1016/j.sab.2017.02.006.

[11] M. Mantler and M. Schreiner, “X-ray Fluorescence Spectrometry in Art and Archaeology,” *X-Ray Spectrom.*, vol. 29, pp. 3–17, Jan. 2000, doi: 10.1002/(SICI)1097-4539(200001/02)29:13.3.CO;2-F.

[12] N. K. Turner, C. S. Patterson, D. K. MacLennan, and K. Trentelman, “Visualizing underdrawings in medieval manuscript illuminations with macro-X-ray fluorescence scanning,” *X-Ray Spectrom.*, vol. 48, no. 4, pp. 251–261, Jul. 2019, doi: 10.1002/xrs.2956.

[13] K. Trentelman, C. Patterson, and N. Turner, “XRF analysis of manuscript illuminations,” 2013, pp. 159–190. doi: 10.2307/j.ctt9qdzfs.9.

[14] M. Wang, Y. Gu, H. Lu, L. Ge, Q. Zhang, and G. Zeng, “Matrix effect correction method based on the main spectral parameters for rock samples in an in situ energy dispersive X-ray fluorescence analysis,” *Spectrochim. Acta Part B At. Spectrosc.*, vol. 193, p. 106438, Jul. 2022, doi: 10.1016/j.sab.2022.106438.

[15] A. G. Revenko, A. L. Tsvetyansky, and A. N. Eritenko, “X-ray fluorescence analysis of solid-state films, layers, and coatings,” *Radiat. Phys. Chem.*, vol. 197, p. 110157, Aug. 2022, doi: 10.1016/j.radphyschem.2022.110157.

[16] V. Laperche and B. Lemière, “Possible Pitfalls in the Analysis of Minerals and Loose Materials by Portable XRF, and How to Overcome Them,” *Minerals*, vol. 11, p. 33, Dec. 2020, doi: 10.3390/min11010033.

[17] J. Kawai, K. Yamasaki, and R. Tanaka, “Fundamental Parameter Method in X-Ray Fluorescence Analysis,” in *Encyclopedia of Analytical Chemistry*, John Wiley & Sons, Ltd, 2019, pp. 1–14. doi: 10.1002/9780470027318.a9666.

[18] S. Piorek, “Principles and applications of man-portable X-ray fluorescence spectrometry,” *TrAC Trends Anal. Chem.*, vol. 13, no. 7, pp. 281–286, Aug. 1994, doi: 10.1016/0165-9936(94)87065-9.

[19] A. Bezur, *Handheld XRF in Cultural Heritage: A Practical Workbook for Conservators*. Los Angeles: The Getty Conservation Institute, 2020.

[20] R. Jenkins, R. Manne, R. Robin, and C. Senemaud, “IUPAC—nomenclature system for x-ray spectroscopy,” *X-Ray Spectrom.*, vol. 20, no. 3, pp. 149–155, 1991, doi: 10.1002/xrs.1300200308.

[21] R. Jenkins, R. Manne, R. Robin, and C. Senemaud, “Nomenclature, symbols, units and their usage in spectrochemical analysis - VIII. Nomenclature system for X-ray spectroscopy (Recommendations 1991),” *Pure Appl. Chem.*, vol. 63, no. 5, pp. 735–746, Jan. 1991, doi: 10.1351/pac199163050735.

[22] K. Janssens *et al.*, “Use of Microscopic XRF for Non-destructive Analysis in Art and Archaeometry,” *X-Ray Spectrom. - X-RAY SPECTROM*, vol. 29, pp. 73–91, Jan. 2000, doi: 10.1002/(SICI)1097-4539(200001/02)29:13.3.CO;2-D.

[23] E. Aloupi, A. G. Karydas, and T. Paradellis, “Pigment analysis of wall paintings and ceramics from Greece and Cyprus. The optimum use of x-ray spectrometry on specific archaeological issues,” *X-Ray Spectrom.*, vol. 29, no. 1, pp. 18–24, 2000, doi: 10.1002/(SICI)1097-4539(200001/02)29:1<18::AID-XRS397>3.0.CO;2-5.

[24] T. Barrett, R. Shannon, J. Wade, and J. Lang, “XRF analysis of historical paper in open books,” in *Handheld XRF for Art and Archaeology*, vol. 3, A. N. Shugar, J. L. Mass, A. N. Shugar, and J. L. Mass, Eds., Leuven University Press, 2012, pp. 191–214.

[25] M. Manso, M. L. Carvalho, I. Queralt, S. Vicini, and E. Princi, “Investigation of the Composition of Historical and Modern Italian Papers by Energy Dispersive X-Ray Fluorescence (EDXRF), X-Ray Diffraction (XRD), and Scanning Electron

Microscopy Energy Dispersive Spectrometry (SEM-EDS)," *Appl. Spectrosc.*, vol. 65, no. 1, pp. 52–59, 2011, doi: 10.1366/10-06105.

[26] M. Manso, M. A. Reis, J. Candeias, and M. L. Carvalho, "Portable energy dispersive X-ray fluorescence spectrometry and PIXE for elemental quantification of historical paper documents," *Nucl. Instrum. Methods Phys. Res. Sect. B Beam Interact. Mater. At.*, vol. 298, pp. 66–69, Mar. 2013, doi: 10.1016/j.nimb.2013.01.008.

[27] T. Wolff *et al.*, "Provenance studies on Dead Sea scrolls parchment by means of quantitative micro-XRF," *Anal. Bioanal. Chem.*, vol. 402, no. 4, pp. 1493–1503, Feb. 2012, doi: 10.1007/s00216-011-5270-2.

[28] L. M. Smieska, R. Mullett, L. Ferri, and A. R. Woll, "Trace elements in natural azurite pigments found in illuminated manuscript leaves investigated by synchrotron x-ray fluorescence and diffraction mapping," *Appl. Phys. A*, vol. 123, no. 7, p. 484, Jun. 2017, doi: 10.1007/s00339-017-1093-0.

[29] I. M. Cortea, L. Ghervase, R. Rădvan, and G. Serițan, "Assessment of Easily Accessible Spectroscopic Techniques Coupled with Multivariate Analysis for the Qualitative Characterization and Differentiation of Earth Pigments of Various Provenance," *Minerals*, vol. 12, no. 6, Art. no. 6, Jun. 2022, doi: 10.3390/min12060755.

[30] S. Mosca *et al.*, "Identification of pigments in different layers of illuminated manuscripts by X-ray fluorescence mapping and Raman spectroscopy," *Microchem. J.*, vol. 124, pp. 775–784, Jan. 2016, doi: 10.1016/j.microc.2015.10.038.

[31] R. Cesareo *et al.*, "Portable Systems for Energy Dispersive X-Ray Fluorescence Analysis or Works of Art," *J. Trace Microprobe Tech.*, vol. 14, pp. 711–725, Jan. 1996.

[32] A. Deneckere *et al.*, "The use of a multi-method approach to identify the pigments in the 12th century manuscript Liber Floridus," *Spectrochim. Acta. A. Mol. Biomol. Spectrosc.*, vol. 80, no. 1, pp. 125–132, Oct. 2011, doi: 10.1016/j.saa.2011.03.005.

[33] L. Burgio, R. J. H. Clark, V. S. F. Muralha, and T. Stanley, "Pigment analysis by Raman microscopy of the non-figurative illumination in 16th- to 18th-century

Islamic manuscripts," *J. Raman Spectrosc.*, vol. 39, no. 10, pp. 1482–1493, 2008, doi: 10.1002/jrs.2027.

[34] R. Mulholland, D. Howell, A. Beeby, C. E. Nicholson, and K. Domoney, "Identifying eighteenth century pigments at the Bodleian library using in situ Raman spectroscopy, XRF and hyperspectral imaging," *Herit. Sci.*, vol. 5, no. 1, p. 43, Oct. 2017, doi: 10.1186/s40494-017-0157-y.

[35] E. Pouyet *et al.*, "Revealing the biography of a hidden medieval manuscript using synchrotron and conventional imaging techniques," *Anal. Chim. Acta*, vol. 982, pp. 20–30, Aug. 2017, doi: 10.1016/j.aca.2017.06.016.

[36] O. Hahn, B. Kanngießer, and W. Malzer, "X-ray Fluorescence Analysis of Iron Gall Inks, Pencils and Coloured Crayons," *Stud. Conserv.*, vol. 50, no. 1, pp. 23–32, Jan. 2005, doi: 10.1179/sic.2005.50.1.23.

[37] O. Hahn, H.-O. Feistel, M. Beit-Arié, I. Rabin, and T. WOLFF, "The Erfurt Hebrew Giant Bible and the experimental XRF analysis of ink and plummet composition," *Gaz. Livre Médiév.*, pp. 16–29, 2007.

[38] W. Malzer, O. Hahn, and B. Kanngiesser, "A fingerprint model for inhomogeneous ink–paper layer systems measured with micro-x-ray fluorescence analysis," *X-Ray Spectrom.*, vol. 33, no. 4, pp. 229–233, Jul. 2004, doi: 10.1002/xrs.676.

[39] O. Hahn, W. Malzer, B. Kanngiesser, and B. Beckhoff, "Characterization of iron-gall inks in historical manuscripts and music compositions using x-ray fluorescence spectrometry," *X-Ray Spectrom.*, vol. 33, no. 4, pp. 234–239, 2004, doi: https://doi.org/10.1002/xrs.677.

[40] G. Nehring, "Writing and Correcting a Torah Scroll in Germany of the Thirteenth and Fourteenth Centuries," 2021.

[41] G. Nehring, N. Gordon, and I. Rabin, "Distinguishing between seemingly identical inks using scanning μXRF and heat maps," *J. Cult. Herit.*, vol. 57, pp. 142–148, Sep. 2022, doi: 10.1016/j.culher.2022.07.007.

[42] Z. Cohen, J. Olszowy-Schlanger, O. Hahn, and I. Rabin, "Composition Analysis of Writing Materials in Geniza Fragments: New Perspectives," in *Jewish Manuscript Cultures*, 2017. doi: 10.1515/9783110546422-013.

[43] M. Gerken, J. Sander, and C. Krekel, "Visualising iron gall ink underdrawings in sixteenth century paintings in-situ by micro-XRF scanning (MA-XRF) and LED-

excited IRR (LEDE-IRR)," *Herit. Sci.*, vol. 10, no. 1, p. 78, Jun. 2022, doi: 10.1186/s40494-022-00696-4.

[44] B. Kanngießer, O. Hahn, M. Wilke, B. Nekat, W. Malzer, and A. Erko, "Investigation of oxidation and migration processes of inorganic compounds in ink-corroded manuscripts," *Spectrochim. Acta Part B At. Spectrosc.*, vol. 59, no. 10, pp. 1511–1516, Oct. 2004, doi: 10.1016/j.sab.2004.07.013.

[45] M. Ferretti, "The investigation of ancient metal artefacts by portable X-ray fluorescence devices," *J Anal Spectrom*, vol. 29, no. 10, pp. 1753–1766, 2014, doi: 10.1039/C4JA00107A.

[46] A. G. Karydas, "Application of a Portable XRF Spectrometer for the Non-Invasive analysis of Museum Metal Artefacts," *Ann. Chim.*, vol. 97, no. 7, pp. 419–432, 2007, doi: 10.1002/adic.200790028.

[47] T. Kearns, M. Martinón-Torres, and T. Rehren, "Metal to mould: alloy identification in experimental casting moulds using XRF," *Hist. Metall.*, vol. 44, no. 1, pp. 48–58, 2010.

[48] A. Vianello and R. H. Tykot, "Investigating Technological Changes in Copper-Based Metals Using Portable XRF Analysis. A Case Study in Sicily," *Open Archaeol.*, vol. 3, no. 1, pp. 392–408, Dec. 2017, doi: 10.1515/opar-2017-0025.

[49] F. Garrido and T. Li, "A handheld XRF study of Late Horizon metal artifacts: implications for technological choices and political intervention in Copiapó, northern Chile," *Archaeol. Anthropol. Sci.*, vol. 9, no. 5, pp. 935–942, Aug. 2017, doi: 10.1007/s12520-016-0315-2.

[50] M. Hložek, B. Komoróczy, and T. Trojek, "X-ray fluorescence analysis of ancient and medieval brass artifacts from south Moravia," *Appl. Radiat. Isot. Data Instrum. Methods Use Agric. Ind. Med.*, vol. 70, pp. 1250–3, Nov. 2011, doi: 10.1016/j.apradiso.2011.11.023.

[51] R. Linke, M. Schreiner, and G. Demortier, "The application of photon, electron and proton induced X-ray analysis for the identification and characterisation of medieval silver coins," *Nucl. Instrum. Methods Phys. Res. Sect. B Beam Interact. Mater. At.*, vol. 226, no. 1–2, pp. 172–178, Nov. 2004, doi: 10.1016/j.nimb.2004.03.084.

[52] M. Chiti, A. Esposito, A. Gorghinian, M. Ferretti, and F. Catalli, “Micro X-ray fluorescence analysis of Roman Imperial coins from Nero,” *J. Archaeol. Sci. Rep.*, vol. 37, p. 102940, Jun. 2021, doi: 10.1016/j.jasrep.2021.102940.

[53] F. Armetta *et al.*, “The silver collection of San Gennaro treasure (Neaples): A multivariate statistic approach applied to X-ray fluorescence data,” *Spectrochim. Acta Part B At. Spectrosc.*, vol. 180, p. 106171, Jun. 2021, doi: 10.1016/j.sab.2021.106171.

[54] Z. Sándor, I. Gresits, and M. Juhász, “X-ray fluorescence analysis of medieval gold coins and jewellery,” *J. Radioanal. Nucl. Chem.*, vol. 256, no. 2, pp. 283–288, Nov. 2004, doi: 10.1023/a:1023941502521.

[55] M. van Bellegem, Röhrs, Stefan, and McLeod, Bet, “A Spanish Medieval altar ‘set’: new investigation and assessment of its date and manufacture,” 2008, Accessed: Jul. 30, 2023. [Online]. Available: https://www.academia.edu/2496766/A_Spanish_Medieval_altar_set_new_investigation_and_assessment_of_its_date_and_manufacture

[56] M. Hložek and T. Trojek, “Silver and tin plating as medieval techniques of producing counterfeit coins and their identification by means of micro-XRF,” *Radiat. Phys. Chem.*, vol. 137, pp. 234–237, Aug. 2017, doi: 10.1016/j.radphyschem.2016.08.013.

[57] A. I. Moreno-Suárez *et al.*, “Feasibility of different cleaning methods for silver-copper alloys by X-ray fluorescence: Application to ancient Greek silver coins,” *Spectrochim. Acta Part B At. Spectrosc.*, vol. 116, pp. 85–91, Feb. 2016, doi: 10.1016/j.sab.2015.11.007.

[58] S. Porcinai and A. Heginbotham, “Thickness mapping of organic layers applied on sterling silver by means of X-ray fluorescence scanning,” *Spectrochim. Acta Part B At. Spectrosc.*, vol. 180, p. 106158, Jun. 2021, doi: 10.1016/j.sab.2021.106158.

[59] A. Heginbotham *et al.*, “The Copper CHARM Set: A New Set of Certified Reference Materials for the Standardization of Quantitative X-Ray Fluorescence Analysis of Heritage Copper Alloys*,” *Archaeometry*, vol. 57, no. 5, pp. 856–868, 2015, doi: 10.1111/arcm.12117.

[60] M. Milazzo and C. Cicardi, “Simple Methods for Quantitative X-Ray Fluorescence Analysis of Ancient Metal Objects of Archaeological Interest,” *X-Ray Spectrom.*,

vol. 26, no. 4, pp. 211–216, 1997, doi: 10.1002/(SICI)1097-4539(199707)26:4<211::AID-XRS214>3.0.CO;2-G.

[61] A. Rindby, P. Engström, S. Larsson, and B. Stocklassa, “Microbeam technique for energy-dispersive x-ray fluorescence,” *X-Ray Spectrom.*, vol. 18, no. 3, pp. 109–112, 1989, doi: 10.1002/xrs.1300180307.

[62] I. Szalóki, D. G. Lewis, C. A. Bennett, and A. Kilic, “Application of the fundamental parameter method to the in vivo x-ray fluorescence analysis of Pt,” *Phys. Med. Biol.*, vol. 44, no. 5, pp. 1245–1255, May 1999, doi: 10.1088/0031-9155/44/5/012.

[63] B. Vekemans, K. Janssens, L. Vincze, F. Adams, and P. Van Espen, “Analysis of X-ray spectra by iterative least squares (AXIL): New developments,” *X-Ray Spectrom.*, vol. 23, no. 6, pp. 278–285, 1994, doi: 10.1002/xrs.1300230609.

[64] V. A. Solé, E. Papillon, M. Cotte, Ph. Walter, and J. Susini, “A multiplatform code for the analysis of energy-dispersive X-ray fluorescence spectra,” *Spectrochim. Acta Part B At. Spectrosc.*, vol. 62, no. 1, pp. 63–68, Jan. 2007, doi: 10.1016/j.sab.2006.12.002.

[65] O. Hahn, “Analyses of Iron Gall and Carbon Inks by Means of X-ray Fluorescence Analysis: A Non-Destructive Approach in the Field of Archaeometry and Conservation Science,” *Restaur.-Int. J. Preserv. Libr. Arch. Mater. - Restaur.*, vol. 31, pp. 41–64, Jan. 2010, doi: 10.1515/rest.2010.003.

[66] S. Pessanha, M. Manso, A. Guilherme, M. Costa, and M. L. Carvalho, “Investigation of historical documents for forensic purposes by x-ray fluorescence spectrometry,” *Surf. Interface Anal.*, vol. 42, no. 5, pp. 419–422, 2010, doi: 10.1002/sia.3085.

[67] G. Cappuccio *et al.*, “PolyCO in XRF analysis: Fundamental Parameter Method applied for Japanese Buddhist scroll studies,” *Radiat. Phys. Chem.*, vol. 188, p. 109660, Nov. 2021, doi: 10.1016/j.radphyschem.2021.109660.

[68] A. Gusmano, *Gli inchiostri nella storia della scrittura e della stampa: storie, strumenti, collezionismi*. Bibliografica, 2011.

[69] T. Christiansen, “Manufacture of Black Ink in the Ancient Mediterranean,” *Bull. Am. Soc. Papyrol.*, vol. 54, pp. 167–195, 2017.

[70] C. A. (Charles A. Mitchell and T. C. Hepworth, *Inks: their composition and manufacture*. London : C. Griffin & company, limited, 1904. Accessed: Aug. 08, 2023. [Online]. Available: http://archive.org/details/inkstheircomposi00mitcrich

[71] C. Cennini and F. Frezzato, *Il libro dell'arte*, 3. ed. in Colibrì (Vicenza, Italy). Vicenza: Neri Pozza, 2006. Accessed: Aug. 08, 2023. [Online]. Available: https://www.loc.gov/catdir/toc/casalini01/02705729.pdf

[72] J. S. Mills and R. White, *The organic chemistry of museum objects*. London: Butterworths, 1987.

[73] J. Winter, "The Characterization of Pigments Based on Carbon," 2023.

[74] C. P. Marshall and R. W. Fairbridge, *Encyclopedia of Geochemistry*. Springer Science & Business Media, 1999.

[75] H. Jüntgen, "Review of the kinetics of pyrolysis and hydropyrolysis in relation to the chemical constitution of coal," *Fuel*, vol. 63, no. 6, pp. 731–737, Jun. 1984, doi: 10.1016/0016-2361(84)90058-9.

[76] A. Coccato, J. Jehlicka, L. Moens, and P. Vandenabeele, "Raman spectroscopy for the investigation of carbon-based black pigments," *J. Raman Spectrosc.*, vol. 46, no. 10, pp. 1003–1015, 2015, doi: 10.1002/jrs.4715.

[77] "The Iron Gall Ink Website." Accessed: Aug. 08, 2023. [Online]. Available: https://irongallink.org/iron-gall-ink-history.html

[78] T. Ghigo, I. Rabin, and P. Buzi, "Black Egyptian inks in Late Antiquity: new insights on their manufacture and use," *Archaeol. Anthropol. Sci.*, vol. 12, no. 3, p. 70, Feb. 2020, doi: 10.1007/s12520-019-00977-3.

[79] C. Colini *et al.*, "The Quest for the Mixed Inks," *Christ. Brockmann Oliver Hahn Volker Märgner Ira Rabin H Siegfried Stiehl Eds Proc. Second Int. Conf. Nat. Sci. Technol. Manuscr. Anal. Manuscr. Cult. 11 2018 41-48*, Jan. 2018, Accessed: Feb. 09, 2022. [Online]. Available: https://www.academia.edu/38120349/The_Quest_for_the_Mixed_Inks

[80] C. Krekel, "The chemistry of historical iron gall inks: understanding the chemistry of writing inks used to prepare historical documents," 1999. Accessed: Jul. 17, 2023. [Online]. Available: https://www.semanticscholar.org/paper/The-chemistry-of-historical-iron-gall-inks%3A-the-of-Krekel/c5bae6e449a9ab22380a48ff6fa7e7aa9f8514ca

[81] R. J. Díaz Hidalgo *et al.*, “New insights into iron-gall inks through the use of historically accurate reconstructions,” *Herit. Sci.*, vol. 6, no. 1, p. 63, Dec. 2018, doi: 10.1186/s40494-018-0228-8.

[82] J. G. Neevel and C. T. J. Mensch, “The behaviour of iron and sulphuric acid during iron-gall ink corrosion,” 1999. [Online]. Available: https://api.semanticscholar.org/CorpusID:101320441

[83] J. G. Neevel, “Phytate: a Potential Conservation Agent for the Treatment of Ink Corrosion Caused by Irongall Inks,” *Restaurator*, vol. 16, no. 3, 1995, doi: 10.1515/rest.1995.16.3.143.

[84] R. E. Sullivan, “The Medieval Church and the Patronage of Art,” *Centen. Rev.*, vol. 33, no. 2, pp. 108–130, 1989.

[85] I. Blanchard, *Mining, Metallurgy, and Minting in the Middle Ages: Continuing Afro-European Supremacy, 1250-1450*. Franz Steiner Verlag, 2001.

[86] D. A. Scott, *Metallography and microstructure of ancient and historic metals*. Marina del Rey, CA: Getty Conservation Institute in association with Archetype Books, 1991.

[87] H. Jones, “Splat cooling and metastable phases,” *Rep. Prog. Phys.*, vol. 36, no. 11, p. 1425, Nov. 1973, doi: 10.1088/0034-4885/36/11/002.

[88] S. Liu *et al.*, “Optimizing the thermal treatment for restoration of brittle archaeological silver artifacts,” *Herit. Sci.*, vol. 10, no. 1, p. 21, Feb. 2022, doi: 10.1186/s40494-022-00657-x.

[89] A. Giumlia-Mair, “Plating and Surface Treatments on Ancient Metalwork,” *Adv. Archaeomaterials*, vol. 1, no. 1, pp. 1–26, Dec. 2020, doi: 10.1016/j.aia.2020.10.001.

[90] P. Northover, S. Northover, and A. Wilson, “Microstructures of ancient and historic silver,” 2013.

[91] J. Mass and C. Matsen, “Quantitative non-destructive analysis of historic silver alloys: X-ray fluorescence approaches and challenges,” *Handheld XRF Art Archaeol.*, pp. 215–248, Jan. 2012.

[92] G. Wharton, S. L. Maish, and W. S. Ginell, “A Comparative Study of Silver Cleaning Abrasives,” *J. Am. Inst. Conserv.*, vol. 29, no. 1, pp. 13–31, 1990, doi: 10.2307/3179588.

[93] P. Storme, O. Schalm, and R. Wiesinger, “The sulfidation process of sterling silver in different corrosive environments: impact of the process on the surface films formed and consequences for the conservation-restoration community,” *Herit. Sci.*, vol. 3, no. 1, p. 25, Aug. 2015, doi: 10.1186/s40494-015-0054-1.

[94] C. Rehren, M. Muhler, X. Bao, R. Schlögl, and G. Ertl, “The Interaction of Silver with Oxygen,” *Z. Für Phys. Chem.*, vol. 174, no. 1, pp. 11–52, Jan. 1991, doi: 10.1524/zpch.1991.174.Part_1.011.

[95] A. Oddy, “Gilding through the ages: An outline history of the process in the old world,” *Gold Bull.*, vol. 14, no. 2, pp. 75–79, Jun. 1981, doi: 10.1007/BF03214601.

[96] W. A. Oddy, “Gold in Antiquity: Aspects of Gilding and of Assaying,” *J. R. Soc. Arts*, vol. 130, no. 5315, pp. 730–744, 1982.

[97] H. Lechtman, “Ancient Methods of Gilding Silver : Examples from the Old and the New Worlds,” Accessed: Aug. 09, 2023. [Online]. Available: https://www.semanticscholar.org/paper/Ancient-Methods-of-Gilding-Silver-%3A-Examples-from-Lechtman/e40674a3327c6955314f5f310853258cafe7d0b0

[98] A. C. Sparavigna, “Depletion Gilding: An Ancient Method for Surface Enrichment of Gold Alloys,” *Mater. Sci.*, 2016.

[99] E. Ottenwelter, C. Josse, A. Proietti, and L. Robbiola, “Fire gilding investigation on early medieval copper-based jewellery by focused ion beam (FIB) on FEG-SEM,” *J. Archaeol. Sci. Rep.*, vol. 46, p. 103602, Dec. 2022, doi: 10.1016/j.jasrep.2022.103602.

[100] Mazzeo, Rocco, “Patine su Manufatti Metallici,” in *Le patine. Genesi, significato, conservazione*, Tian, Piero and Pardini, Carla, Eds., Nardini Editore, 2017, pp. 29–43.

[101] V. Costa, “The deterioration of silver alloys and some aspects of their conservation,” *Rev. Conserv.*, Jan. 2001, Accessed: Aug. 09, 2023. [Online]. Available: https://www.academia.edu/33280672/The_deterioration_of_silver_alloys_and_some_aspects_of_their_conservation

[102] T. E. Graedel, J. P. Franey, G. J. Gualtieri, G. W. Kammlott, and D. L. Malm, “On the mechanism of silver and copper sulfidation by atmospheric H2S and OCS,” *Corros. Sci.*, vol. 25, pp. 1163–1180, 1985.

[103] Y. Fukuda *et al.*, “Indoor Corrosion of Copper and Silver Exposed in Japan and ASEAN1 Countries,” *J. Electrochem. Soc.*, vol. 138, no. 5, p. 1238, May 1991, doi: 10.1149/1.2085766.

[104] O. Oudbashi and R. Wanhill, “Long-Term Embrittlement of Ancient Copper and Silver Alloys,” *Heritage*, vol. 4, no. 3, Art. no. 3, Sep. 2021, doi: 10.3390/heritage4030130.

[105] T. Palomar, B. Ramírez Barat, E. García, and E. Cano, “A comparative study of cleaning methods for tarnished silver,” *J. Cult. Herit.*, vol. 17, pp. 20–26, Jan. 2016, doi: 10.1016/j.culher.2015.07.012.

[106] T. Palomar *et al.*, “Evaluation of laser cleaning for the restoration of tarnished silver artifacts,” *Appl. Surf. Sci.*, vol. 387, pp. 118–127, Nov. 2016, doi: 10.1016/j.apsusc.2016.06.017.

[107] C. Degrigny, R. Jeanneret, D. Witschard, C. Baudin, G. Bussy, and H. Carrel, “A new electrolytic pencil for the local cleaning of silver tarnish,” *Stud. Conserv.*, vol. 61, no. 3, pp. 162–173, May 2016, doi: 10.1179/2047058415Y.0000000015.

[108] A. C. Fariselli *et al.*, “Archaeometric analyses and restoration of silver jewellery from the punic necropolis of Tharros – Capo San Marco (Sardinia, Italy),” *Int. J. Conserv. Sci.*, vol. 13, pp. 771–792, 2022.

[109] C. Jones, C. Duffy, A. Gibson, and M. Terras, “Understanding multispectral imaging of cultural heritage: Determining best practice in MSI analysis of historical artefacts,” *J. Cult. Herit.*, vol. 45, pp. 339–350, Sep. 2020, doi: 10.1016/j.culher.2020.03.004.

[110] M. Picollo *et al.*, “Fiber Optics Reflectance Spectroscopy: A Non-destructive Technique for the Analysis of Works of Art,” in *Optical Sensors and Microsystems: New Concepts, Materials, Technologies*, S. Martellucci, A. N. Chester, and A. G. Mignani, Eds., Boston, MA: Springer US, 2000, pp. 259–265. doi: 10.1007/0-306-47099-3_23.

[111] H. G. M. Edwards, P. Vandenabeele, and P. Colomban, *Raman Spectroscopy in Cultural Heritage Preservation*. in Cultural Heritage Science. Cham: Springer International Publishing, 2023. doi: 10.1007/978-3-031-14379-3.

[112] Q. Wu, B. Zhang, and Y. Hu, “Comparison and Research Progress of Protein Detection Technology for Cultural Relic Materials,” *Coatings*, vol. 13, no. 8, Art. no. 8, Aug. 2023, doi: 10.3390/coatings13081319.

2. The Book of Uí Mhaine: An Interdisciplinary Analysis of the Materiality of the Gaelic Manuscript Tradition

As published in Heritage (MDPI):

Biolcati, V.; Wilson, M.; Fiddyment, S.; Unitt, R.; Ryan, C.C.; Hoffmann, A.G.; Gillis, J.; France, F.; Ó Macháin, P.; Iacopino, D. The Book of Uí Mhaine: An Interdisciplinary Analysis of the Materiality of the Gaelic Manuscript Tradition. *Heritage* 2023, 6, 5393–5409. https://doi.org/10.3390/heritage6070284

2.1 Abstract

This paper presents the findings of the first multi-analytical investigation of the Book of Uí Mhaine, one of the largest Gaelic Books surviving from the medieval vernacular period. A combination of protein analysis, point X-ray fluorescence spectroscopy (XRF), multispectral imaging (MSI), point Fiber-Optic Reflectance Spectroscopy (FORS) and point Raman spectroscopy was used to perform a systematic investigation of the Book of Uí Mhaine's constituent materials, including parchment, inks and pigments. The analysis revealed that the parchment was made of calfskin, both blunt tools and Pb-containing materials were used for ruling the pages throughout the manuscript, and iron-based inks were used to write the content of the book. The decoration was restricted to the initial letters and rubrication across the body text. The decoration color palette was limited to yellow and red, comprising arsenic-, mercury- and lead-based pigments. A copper-based green pigment was found only on one folio. The scientific knowledge acquired through this multi-analytical approach complemented a substantial corpus of knowledge already built by Gaelic scholars, paleographers, codicologists and conservators. This work not only allowed for the consolidation of existing information on methods and materials used for the production of medieval Gaelic manuscripts but also laid the basis for future comparative work with other contemporary traditions in Ireland and Europe.

2.2 Introduction

Among an estimated three hundred surviving vernacular Gaelic vellum manu-scripts, the Book of Uí Mhaine (Leabhar Ua Maine: Royal Irish Academy MS D ii 1) is one of the most important examples of late medieval Irish books. The Book of Uí Mhaine is a large (42 × 26.5 cm) manuscript written towards the end of the fourteenth century. It derives its name from the ancient tribal area of Uí Mhaine in east Co. Galway and south Co. Roscommon in Connacht. Today, the book consists of 157 leaves, estimated to be less than half of its original size [1]. The contents comprise a collection of traditional Irish learning in the form of genealogies, prose-tales and poetry. Ten different scribal contributions, divided across twenty-five quires, have been identified through paleographic investigation [2]. Because of its large size, scope, extent, and variety of contents, the Book of Uí Mhaine is considered one of the most outstanding productions of Irish scholarship in the vernacular tradition.

A number of analytical techniques are routinely used for the material investigation of medieval books. For example, multispectral imaging (MSI) is widely used to enhance the readability of ancient texts. MSI is also the technique of choice for rapid and non-invasive initial assessment of manuscripts, which is crucial to inform and direct the application of complementary analytical techniques [3–6]. X-ray Fluorescence spectroscopy (XRF) has been shown to be diagnostic for the identification of the elemental content of both pigments and writing inks, often in conjunction with further data processing such as finger-printing analysis or principal component analysis [7–9]. Fiber-optic reflectance spectroscopy (FORS) is an invaluable method for the identification of organic and inorganic pigments and inks [10–14]. Recently, proteomic analysis has also emerged as a powerful tool for the non-invasive investigation of

parchment origins in medieval manuscripts. For example, Fiddyment et al. have used proteomic approaches to reveal the animal origins of parchments used for the making of 13th-century bibles across Europe [15–17]. Additionally, Toniolo et al. have used protein analysis to analyze the making of a pocket bible donated by a Franciscan friar to the Chinese Mogul Emperor in the 13th century [18]. In contrast to mono-analytical approaches, the combined application of multi-analytical techniques has recently gained popularity, whereby elemental, molecular and imaging techniques are used in combination to gain a complete picture of the materials and methods used by ancient parchment producers, scribes and decorators. For example, Ricciardi et al. effectively applied imaging spectroscopy and in situ analytical methods for the identification of materials in a 15th-century illuminated manuscript [13]. Cucci et al. have used a combination of hyperspectral imaging, FORS and XRF to investigate the attribution of the Corale 43 manuscript to Beato Angelico [19]; de Viguerie et al. have investigated 15th-century illuminated manuscripts by a combination of XRF and hyperspectral imaging [20]; whereas Calá et al. used a combination of UV-Vis diffuse reflectance spectroscopy, XRF, optical microscopy and protein mass spectrometry to build a holistic picture of the 14th-century Messale Rosselli [21]. In spite of the large availability of multi-analytical approaches, up until now, Gaelic manuscripts have been investigated only at the macro-level, through the codicological and paleographic investigation of used materials and marking events. The information gathered from such investigations, together with other available historical information, has contributed to building a corpus of data on the choice and availability of materials and on processes used for the manufacture of parchment and ink. Some questions on Gaelic medieval book manufacturing remained open, however, such as the choice of animal species used for parchment production, the processes employed to obtain the parchment folios, the types of ruling techniques, and the nature and origin of constituent inks and pigments. The aim of this work was to carry out a multi-analytical study of the materiality of a representative Gaelic vellum manuscript for the first time in order to gain a better understanding of how manuscripts of the vernacular tradition were written and constructed. The choice of analytical methods was deter-mined by the requirement for minimally invasive analysis. Therefore, MSI, FORS, XRF and optical microscopy were the techniques used more extensively throughout the book. Mass spectrometry-based protein analysis was

performed using eraser crumbs collected with conventional PVC erasers. Raman spectroscopy was only used on two microfragments discovered loose on the page or in the gutter of the book during analysis.

2.3 Results and discussion

In order to conduct a systematic investigation of the constituent materials, the Book of Uí Mhaine's main features were classified as shown in Figure 1.

Figure 2.1. Representative photographic images of the Book of Uí Mhaine's analyzed features: (a) Entire page of the book, folio 50 r; (b) Rubricated initial, folio 48 r; (c) Display and main text, folio 49 r; (d) Pricking marks, folio 2 r; (e) Graphic ruling, folio 88 v.

Specifically, Figure 1a shows a representative folio, displaying written text and decorated initials on the vellum support. Figure 1b shows the largest and most outstanding example of a decorated initial letter in the manuscript, colored in red and yellow pigments, indicating the beginning of a new quire. Figure 1c shows an example of the large-format lettering, called display text, typically found at the beginning of a new section of the content. An example of pricking marks puncturing the parchment folios found in the

margins of some pages is shown in Figure 1d. The pricking method is used to demarcate the position of the guidelines. Ruling lines, known as guidelines, were drawn on each page in order to guide the writing of the manuscript. Examples are shown in Figure 1e. The details of the Book of Uí Mhaine's structure and the division of hands by scribe, quire, and folio are reported in Table S1 in the Supplementary Materials. All the parts of the Book of Uí Mhaine listed above were analyzed by a combination of different analytical techniques. Specifically, the parchment was examined by a combination of protein analysis, MSI and XRF; ruling was analyzed by MSI and XRF; writing inks, including inks used for the writing of the main text, display text, marginalia and initial letters, were examined by MSI and XRF; pigments were examined by MSI, XRF, and FORS. Raman spectroscopy was performed on micro-fragments of ink and red pigment discovered loose on the page during the visual assessment. Microscopy and photographic images were taken throughout the book to support the findings.

Parchment

As a first approach to the analysis of the parchment, MSI imaging was used throughout the manuscript to capture characteristics at full-page magnification scale. An example is shown in Figure 2a, where a reflectance image at 365 nm of folio 55 r clearly displays water stain damage appearing as dark areas over a light gray background. The origin of the dark appearance of water-damaged areas under UV illumination is still under debate.

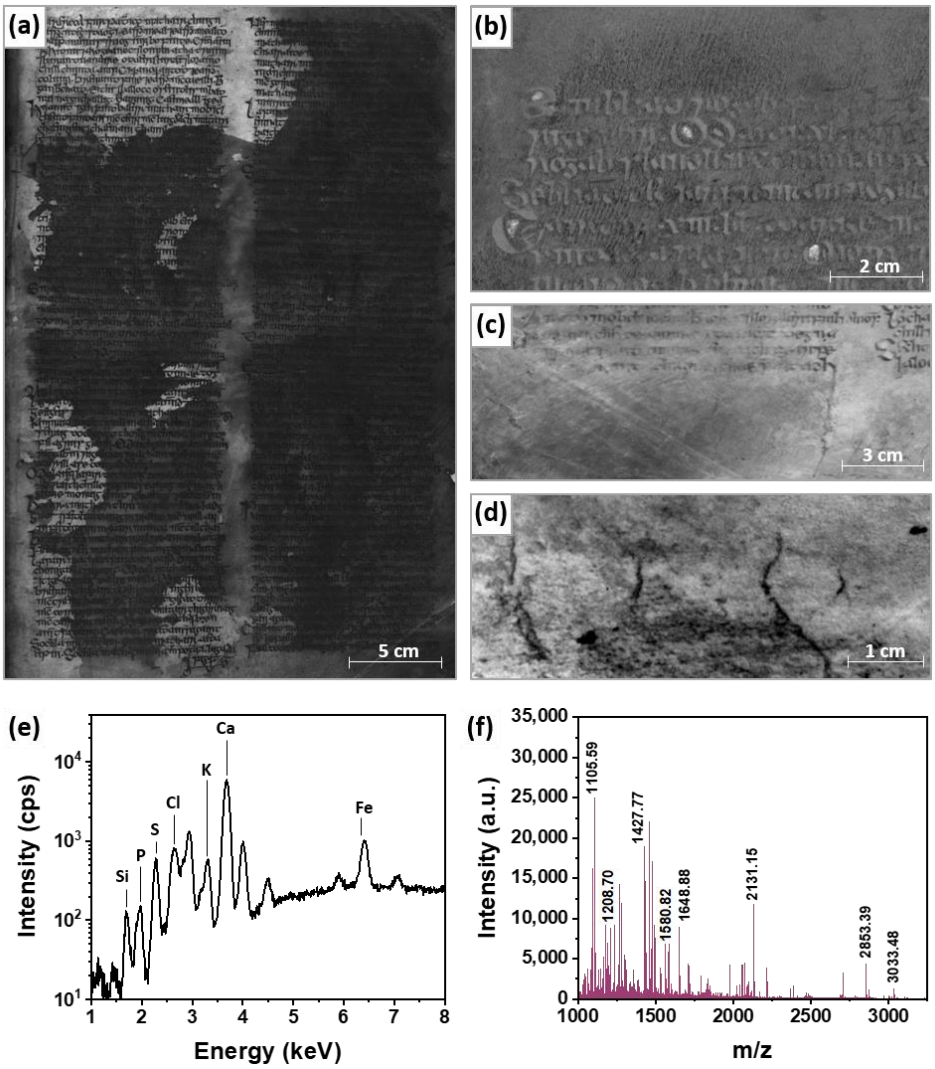

Figure 2.2 (a) UV reflectance image (365 nm) of folio 55 r showing staining caused by dampness or water; (b) PCA projection of a detail of folio 48 v enhancing scrape marks; (c) PCA projection of a detail of folio 53 v enhancing page folds; (d) IR image (940 nm) detail of folio 50 r enhancing animal veins; (e) Representative XRF spectrum of parchment taken in folio 38 v; (f) Representative MALDI-TOF mass spectrum taken in folio 1 v.

The availability of page-by-page images from the MSI analysis allowed the identification of peculiar water stains across the book. In particular, it was possible to group similarly shaped water stains and identify discrepancies in the current binding order of the quires. For example, a break in similarly shaped water stains was observed between folio 18 v and folio 19 r, corresponding to the transition from quire 4 to 5 (Figure S1 in Supplementary Materials). This break is likely the result of the loss of a single folio at this point. In contrast, continuity of stain marks was observed from folio 47 v to 48 r, marking the transition from quire 9 to 10 (Figure S2 in Supplementary Materials). This might be an indication that these two quires were housed together in a very similar

environment even before they were bound together. This aligns with the fact that the Book Uí Mhaine was in a disbound state until the 19th century. It also confirms the known historical connection between the scribes of quires 9 and 10: quire 9, written by Adam Cusin (scribe C), contains a copy of a poem by the scribe of quire 10, Faelán Mac an Ghabann na Scéal (Scribe F).

The MSI data collected were processed and subjected to Principal Component Analysis (PCA) as required in order to highlight different features of the Book and select areas for further analysis. The use of this procedure facilitated better visualization of the scrape marks left on the parchment during the manufacturing process, consistent with the scraping phase observed and reported to be typical of all manuscripts made from skin. This process involved manually removing the flesh and hair after soaking the skin in a lime bath or an organic solution [25]. The scrape marks, caused by the use of rounded knives, appeared in Figure 2b as diagonal parallel lines in the background of the text. Page folds were also visible in Figure 2c, indicating the events the book underwent after its production. These lines emerged from the background parchment; they intersected at similar locations, usually in the corners of the folios. MSI imaging also provided enhanced visualization of parchment veins, suggesting the preferential use of skins from young animals. In younger animals, the vein trails remain more visible due to less-developed skin layers [26]. Figure 2d shows veins as thin, dark trails against a clearer background. A comprehensive visual and microscopy analysis was conducted on the veins within the parchment. The observed findings lead to the most plausible conclusion that the deposition of dust and dirt primarily occurs on collapsed veins. This alignment between dirt deposition and the vein structures may contribute to the dark appearance under IR illumination. The use of juvenile animals was confirmed by protein analyses of 23 samples collected across the entire length of the book, which revealed that parchment folios were constituted by calf (young *bos taurus*) skin (see Figure 2f). The ability to identify the skin's physical features displayed by MSI analysis is based on the comparison with modern skins, where these features are not obscured by content on the page, ageing or events that adversely affect their clarity. Discussions with parchment makers and practical exercises in parchment manufacture also hone observation skills. XRF was used to complement the information gained by protein analysis with the elemental composition of the parchment folios. In order to avoid contamination from the parts containing ink,

XRF measurements were taken from the margins. A representative parchment XRF spectrum is shown in Figure 2e and was characterized by the presence of silicon (Si), phosphorus (P), sulphur (S), chlorine (Cl), potassium (K), calcium (Ca) and iron (Fe). The intense Ca peaks, ubiquitous in all analyzed areas, supported the use of a lime (calcium hydroxide, $Ca(OH)_2$) solution for the dehairing process of the pelts. Ca is ascribable either to the presence of calcite (calcium carbonate, $CaCO_3$), as with time $Ca(OH)_2$ becomes $CaCO_3$, due to reaction with atmospheric CO_2, or is to be attributed to the use of gypsum ($CaSO_4 \cdot 2H_2O$) for surface smoothing, which would also explain the presence of S. It is known that parchment was rubbed with gypsum to avoid the inks bleeding and being absorbed onto the parchment surface and to give it a silky appearance [27]. The presence of K may indicate the use of some form of alum, K-Al-CO_3 (or K-CO_3), as an abrasive or whitening agent used in the curing of the skin. It is known that some skins were desiccated using either sodium or potassium chloride and the pH was adjusted by treating with ammonium chloride or sulphate with lime and applying potash alum [28]. Accordingly, chlorine (Cl), also omnipresent, was ascribed to the treatments above and/or to the practice of using salt for the preservation of the hides from biological attack [29]. Si may be indicative of the use of pumice powder (high in silicon dioxide, SiO_2) for rubbing the flesh side of the skin [30] or may arise from dirt deposition caused by ageing. Trace quantities of mercury (Hg), arsenic (As), and lead (Pb) were also found and were ascribed to humidity-induced dissolutions and migration of the constituent ruled lines and pigments. Traces of copper (Cu) and zinc (Zn) were also detected in all parchment folios. However, due to their low concentrations and similar intensities found in both the clean parchment and inked areas, it was challenging to determine their specific origin—whether they originated from the parchment or the ink. Hg, As, Pb, Cu, and Zn were particularly evident in the XRF spectra taken from heavily water-damaged folios. These elements, not related to parchment content, were found to be particularly high in intensity, and evidence of ink transfer from one page to another was observed (See Figures S3 and S4 in Supplementary Materials).

Ruling

Before the writing phase, the parchment folios were ruled to ensure consistent horizontal and vertical alignment for the written content in each line. During medieval times, guidelines and bounding lines were commonly created through the methods of wet- or dry-ruling. Wet ruling involved the use of inks to trace the lines on the parchment. Dry-ruling, on the other hand, encompassed two techniques: inscribing graphic lines or indenting the parchment with a blunt tool. The graphic line technique involved the use of a lead or silver stylus to create the ruling lines. In such cases, identifiable traces were left on the folio, which would be detected through XRF analysis. Alternatively, a linear indentation was made on the parchment using a blunt stylus, typically crafted from wood or bone. In this second scenario, no detectable elemental traces would be discernible through XRF analysis. A page-by-page visual assessment of the Book Uí Mhaine showed that the ruling practice varied across the book. The majority of the manuscript was ruled in a two-column format. The gatherings written by the scribes G1 and G2, assigned to genealogies, were usually laid out in a multi-column format, the most common style for lists. The nature of the ruling lines was investigated by microscopy, MSI and XRF. Two representative examples of guidelines are shown in Figure 3.

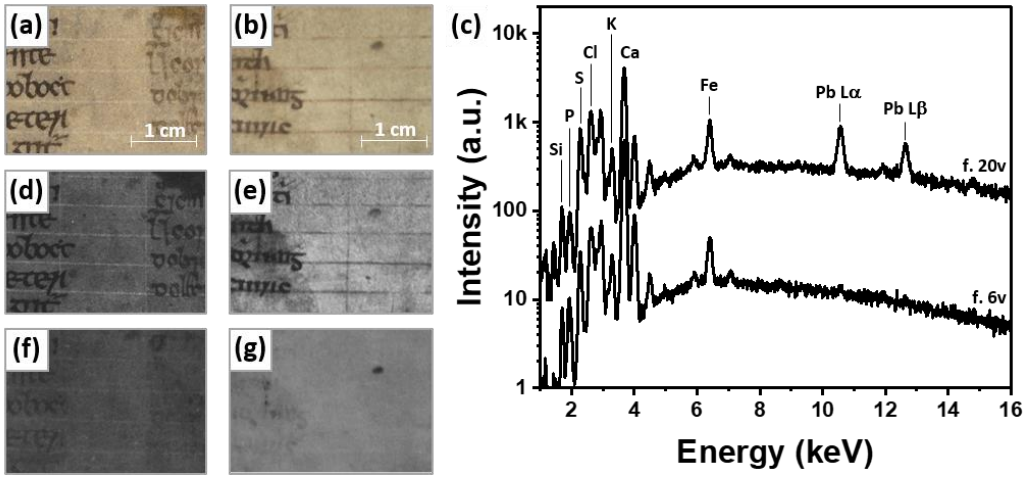

Figure 2.3. (a) Photograph, (d) UV (365 nm), and (f) IR (940 nm) of dry-ruling, detail of f. 6 v; (b) Photograph, (e) UV (365 nm), and (g) IR (940 nm) of lead-pin ruling, detail of f. 20 v; (c) XRF spectra of lead-pin ruling (top, f. 20 v), and dry-ruling (bottom, f. 6 v).

Folio 6 v exhibited distinctive white underlining lines (Figure 3a), characterized by a groove-like appearance. Under UV and IR illumination (Figure 3d,f), these lines appeared bright on a dark background. In contrast, folio 20v showcased dark graphic lines

under both visible and UV illumination (Figure 3b,e). However, these lines vanished under IR illumination (Figure 3g). Studies on drawing media suggest that lines made using a silver-based metal point disappear at 940 nm IR, while lead-based media remains visible at that wavelength [31,32]. To investigate the ruling lines throughout the book, ten areas with varying shades from whitish to gray were subjected to elemental characterization. The spectra analysis revealed the presence of Si, P, S, Cl, K, Ca, and Fe in all areas, attributed to the parchment composition in the background. As anticipated, the indented lines (of a whitish color under visible light) did not exhibit any elemental variation from the parchment. On the other hand, lead (Pb) was detected in the spectra of the graphic lines that appeared dark under visible and UV light and disappeared under IR illumination, while silver (Ag) was not present. The intensity of the Pb peak varied depending on the thickness of the line, suggesting the use of a Pb-based tool or a Pb-containing ink for creating these dark markings.

Microscopic examination of these areas (See Figure S5 in Supplementary Materials) uncovered physical characteristics such as the presence of what appears to be ink infiltrating between the skin fibrils, suggesting that the material may have been applied in a wet state. In the case of a dry application using a lead-based stylus, it would be expected that the material would adhere to the texture created by the fibrils, remaining on the surface of the rough skin without staining the background. Based on the XRF data, we can preliminarily state that both blunt (wood/bone?) and Pb-containing materials were used throughout the book. However, no discernible correlation was found between these ruling techniques and the contributions of the scribes. For instance, Adam Cusin, the primary scribe of the book, predominantly utilized Pb-based graphic lines in the early quires but more consistently employed a blunt tool in later gatherings. However, folio 45 v displayed a combination of both Pb and indentation rulings.

Writing Inks

An extensive investigation of the writing inks was performed by MSI, also using infrared false-color imaging (IRFC) and PCA image processing, in order to broadly identify the inks and assess the congruency across the various letter types: body text, display text, and large and small initial letters. The ink used in the main text (Figure 4a) displayed a dark brown hue under visible illumination, which appeared as red coloration

in IRFC images (Figure 4b), a behavior usually associated with the presence of iron-based inks [33].

The slight variation between the alignments of the written parts on either side of the folio offered the best areas for XRF analysis, clean from any other material applied on the other side. Although only one representative XRF spectrum of the text ink is shown in Figure 4h, all writing inks, including main text, display text, and initial letters, were found to have similar elemental compositions. The inks are mainly composed of Fe and S, with variable and small traces of Cu and Zn. Cu and Zn are usually associated with iron sulfate used in reaction with polyphenols to obtain an iron-based ink. However, as stated already, these elements are also detected in the writing support. Hence, a thorough quantitative analysis was performed on both the ink (150 spots) and parchment XRF spectra (81 spots). A similar content of Cu and Zn was found in clear parchment and inked areas.

As a result, it cannot be definitively concluded that Cu and Zn are exclusively attributed to the ink. Potassium (K) was ubiquitously present in inked areas at higher intensities than in clean parchment areas nearby, representing either a contribution from the binder (not analysed in this study) or an impurity in the iron compounds themselves [34,35].

Close observation of the MSI images revealed dishomogeneities in the appearance of the ink. This is shown by the display text images of Figure 4c–e, where individual letters displayed different hues of brown in the visible image, appearing as red and black or green and black in the IRFC and PCA images, respectively. The variation in color was ascribed to the different thicknesses of the ink application, with thicker deposition resulting in darker coloration. For example, it was noticed that the darker colors were often located on the serifs, which are an embellishment of the main strokes of the letter, corresponding to thicker applications. Thicker ink depositions would be more resistant to ageing, including abrasion and consequent fading in color. Although the persistence of a dark coloration in the IRFC image could potentially be linked to the presence of carbon (C) in the ink, this point could not be definitively proven during this investigation. Furthermore, it was observed that in laboratory-made samples, thick applications of iron-based ink were not completely transparent to IR (940 nm). A detailed analysis was also performed on selected large initials, which showed similar interesting characteristics, as

shown in Figure 4 f. Here, the letter “C” in folio 35 r was decorated with internal and external dots, following the shape of the C, all displaying the same brownish coloration. The optical microscopy image, inset of Figure 4i, showed a textured, thick application of dark material in the filling of the letter body, with a degradation pattern of cracking and flaking off the page. Similar to what has been observed for the display text, the assigned green and blue false colors in the PCA image (Figure 4g) suggest the presence of either one thicker application or various depositions of ink to thicken the letter body. In order to shed further light on the nature of used inks, Raman analysis was performed on a dislodged microsample from the body of the letter C. The spectrum recorded at 785 nm showed bands indicative of the presence of iron-based ink (Figure 4i). Specifically, Raman signature bands of iron-based ink were found at 1577 (broad), 1484 (strong), 1438 (shoulder), 1332 (broad) and 550–650 (broad) cm^{-1}, in agreement with literature data [36]. Intense peaks were observed in the 1200–1500 cm^{-1} region, corresponding to the major tannic acid vibrations. The spectrum also showed the shifting of the typical 1477 cm^{-1} band to 1484 cm^{-1}, possibly associated with the presence of other tannins in the ink other than gallotannin. Specifically, the presence of peaks at 1167 and 1277 cm^{-1} could be interpreted as lignin polyphenols and expected to be by-products of tannin extractions, especially if oak galls were substituted with other plant barks [37].

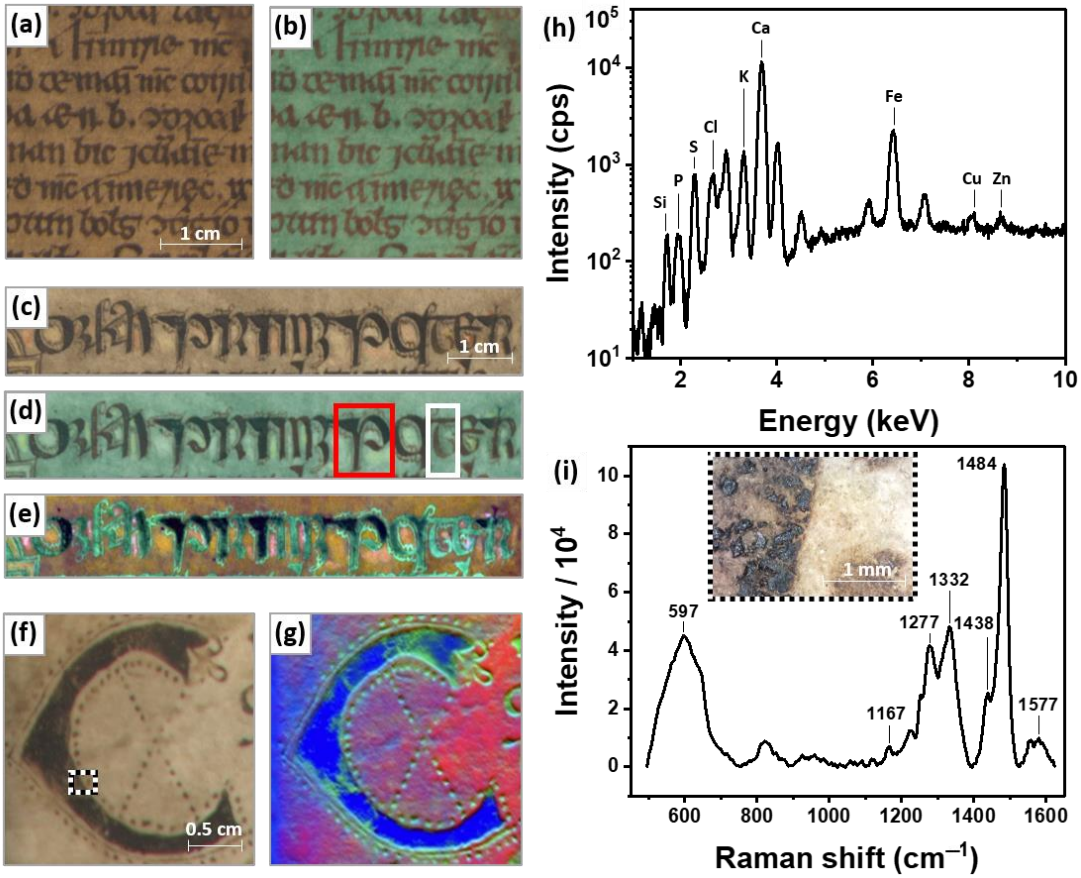

Figure 2.4. (a) Visible image and (b) IRFC image of a detail of folio 2 r showing body text; (c) Visible image, (d) IRFC image, and (e) Color composite image, based on PCA projections, of a detail of folio 48 r showing display text. Red box highlights a thick application of ink, while the white box highlights a thin application of ink; (f) Visible image; and (g) PCA image of a detail of folio 35 r showing the initial letter C. Dashed box highlights location of inset of (i); (h) Representative XRF spectrum of text ink, folio 2 r; (i) Raman spectrum of the letter body fragment taken at 785 nm. Inset shows an optical microscopy image of the area where the fragment dislodged.

Pigments

Two main colors were used throughout the book: red and yellow, albeit in different shades. Green in different hues was only used in one instance, for the decoration of folio 111 r.

Red rubrication was widely used throughout the manuscript for the decoration of large capital letters, initial letters and text in the genealogies. Visual inspection of such rubrication across the book revealed the presence of different shades of red, ranging from purple, dark red, orange-red, pink and metallic-lustrous gray with red particles visible to the naked eye. Therefore, XRF was performed on a number of representative red pigmentations to obtain insight into the nature of these colorations and their various ageing patterns. MSI imaging was performed in conjunction with XRF in order to extend

and attribute the XRF data to the folios that were not elementally characterized. A red-orange pigment was used in quires 1, 2, 9, 10, 11, 12, 13, 15, and 16. The elemental composition of that pigment is shown in the XRF spectrum of Figure 5a and was characterized by prominent peaks for mercury (Hg) and sulphur (S), indicative of the use of cinnabar or synthetic vermillion (mercury sulfide, HgS). Arsenic (As) peaks were also detected and interpreted as indicative of the presence of an arsenic sulfide, either realgar, pararealgar, or orpiment. The presence of Pb, which exhibits a main peak (Lα) that overlaps with As Kα, was excluded by considering the absence of its corresponding secondary peaks in the analysis. The red area in folio 48 r responded as yellow in IRFC (see insets of Figure 5a), further confirming the presence of vermillion as reported in the literature. FORS confirmed the presence of HgS due to the narrow and symmetric features centered at 590 nm in the first derivative spectra (Figure 5b) and a sharp s-shaped curve in the reflectance spectra indicative of a semi-conductor pigment [38]. In addition, Raman spectroscopic analysis of a dislodged red fragment in folio 50 r (Figure 5d) found in the gutter of the book was successful in firmly identifying cinnabar/vermilion as the red pigment (254, 282, 343 cm^{-1}). The minor peaks in the spectra (136, 154, 202, 291, 311, 353, and 382 cm^{-1}) showed an excellent match with natural orpiment (As_2S_3) [39]. Since other common arsenic sulfide pigments can be clearly distinguished by Raman spectroscopy, realgar and its alteration product, pararealgar, were ruled out. The intentional mixture of vermilion and orpiment is somewhat unusual and accounts for the yellow-orange appearance of these red decorations.

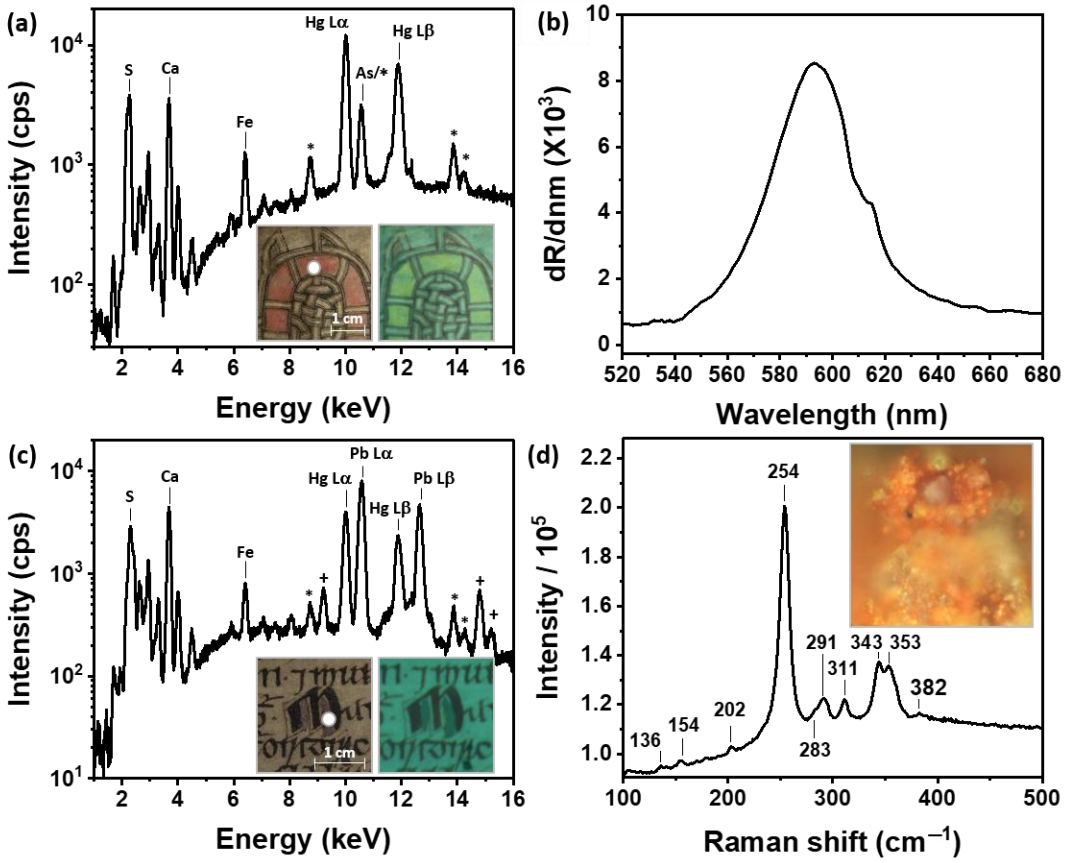

Figure 2.5. (a) XRF spectra of the red pigment cinnabar or vermilion. * represents other peaks for Hg. Insets show visible (left) and IRFC image (right) of the decorated initial letter in folio 48 r (quire 10). White dot in the visible image indicates where XRF analysis was performed; (b) FORS spectra confirming vermilion, folio 48 r; (c) XRF spectra of the red mixture of cinnabar/vermilion with Pb-based pigment/s. + indicates other peaks for Pb. Insets show visible (left) and IRFC image (right) of the decorated initial letter in folio 9 r. White dot in the visible image represents where XRF analysis was performed; (d) Raman spectrum, recorded using a 785 nm laser, confirms that cinnabar/vermilion and orpiment were used in mixture. Folio 50 r.

In contrast to what was found for the orange applications, the darker shades of red in quires 2, 5, 12, 18, 19, and 20 appeared as dark green in the corresponding IRFC image (see insets of Figure 5c), supporting the hypothesis that a different pigment mixture was used for these areas [40]. A representative XRF spectrum is shown in Figure 5c, performed on the rubricated letter M in folio 9 r. The spectrum was characterized by intense peaks for Hg and Pb, suggesting that for achieving these hues, cinnabar/vermilion was mixed with Pb-based pigment(s), more likely lead white [$2PbCO_3 \cdot Pb(OH)_2$] or minium (red lead; Pb_3O_4), which are known to degrade toward a gray color.

The elemental composition of the different red applications was plotted in a histogram where the relative (to Fe) concentrations of Pb, Hg, and As were plotted against the folios in the codicological order as it is today (Figure 6). This allowed two pigment

mixtures to be distinguished: a mixture of cinnabar/vermillion with orpiment (discussed above), which was used in quires 1, 2, 9, 10, 11, 12, 13, 15, and 16; and a mixture of cinnabar/vermillion with Pb-based pigment(s) in various ratios, used in quires 2, 5, 12, 18, 19, and 20. This clearly showed a correlation between the use of specific pigments and the structure of the Book Uí Mhaine by quire and scribal hand, in line with the fact that the quires composing the volume were meant to be stand-alone productions.

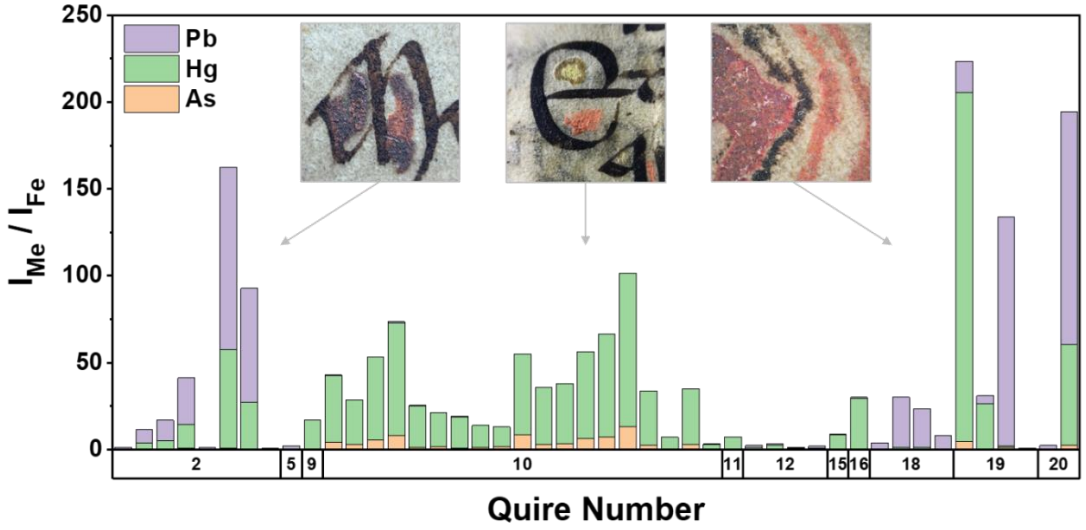

Figure 2.6. Histogram plotting the content of Pb, Hg, and As, ascribable to the presence of red cinnabar/vermilion, lead-based pigment(s), and orpiment (elements normalized to Fe). Insets: representative photographs of pigment applications in different red shades and yellow colorations.

Yellow decorations were found consistently in every folio of quire 10, written by Faelán, scribe, poet, and confidant of Bishop Ó Ceallaigh, for whom he prepared the most decorated gathering of the manuscript. Yellow applications were also found scattered in a few folios in quires 11, 12, 13, 14, 15, 16, 20, and 22. Yellow pigments were never found in conjunction with lead-based pigments in the same quires, but rather only in combination with vermilion. A total of twenty-six XRF spectra were obtained from yellow pigments throughout the book, revealing their similarity to one another. Figure 7a shows a representative XRF spectrum of a yellow pigment taken on an initial letter in folio 48 r. The elemental composition was characterized by prominent As and S peaks, indicating the use of an arsenic sulfide pigment. Fe, Ca, K, and Hg, along with traces of Cu and Zn, were also observed and were attributed to contributions from the background parchment or interpreted as contamination from adjacent ink and pigment areas. FORS

analysis of yellow-pigmented areas, in conjunction with XRF, confirmed the presence of orpiment due to a sharp peak at 480 nm in the first derivative spectra and a steep stair-step shape in the reflectance spectra indicative of semi-conductor pigments (see Figure 7b) [41]. Further analysis was carried out by MSI, which showed visible yellow areas shifting into ivory-white coloration in the IRFC images (Figure 7d), in line with the literature [13]. In some instances, the yellow application had become imperceptible to the naked eye. In such cases, XRF analysis played a crucial role in indicating the previous presence of orpiment in these areas. Notable examples can be observed in the yellow decorative line surrounding the initial letter (Figure 7c) and the line surrounding the text in the *probatio pennae* (Figure 7f) of folio 48 r. These specific details were elementally characterized using XRF for confirming As presence and subsequently emphasized through PCA processing. By processing the stack of 15 MSI images, 15 PCA images were generated. The selection of the PCA image that best captured solely the yellow applications was made by carefully examining both the visible image (which revealed remnants of orpiment decorations) and the PCA images together. By considering both sources of information in tandem, the most accurate representation of the yellow application was selected. In Photoshop, the grayscale PCA image was transformed into a yellow-scale image. Then the image histogram representing the color values of the image pixels was adjusted to exclude irrelevant pixels from the representation, such as those related to the background and/or the image noise. The resulting image was then superimposed onto the visible image of the corresponding folio, allowing for the reconstruction of the original positioning of the faded orpiment decoration (see Figure 7e,g). By overlaying the enhanced image onto the visible image, the original placement of the faded orpiment decoration was effectively restored and visualized.

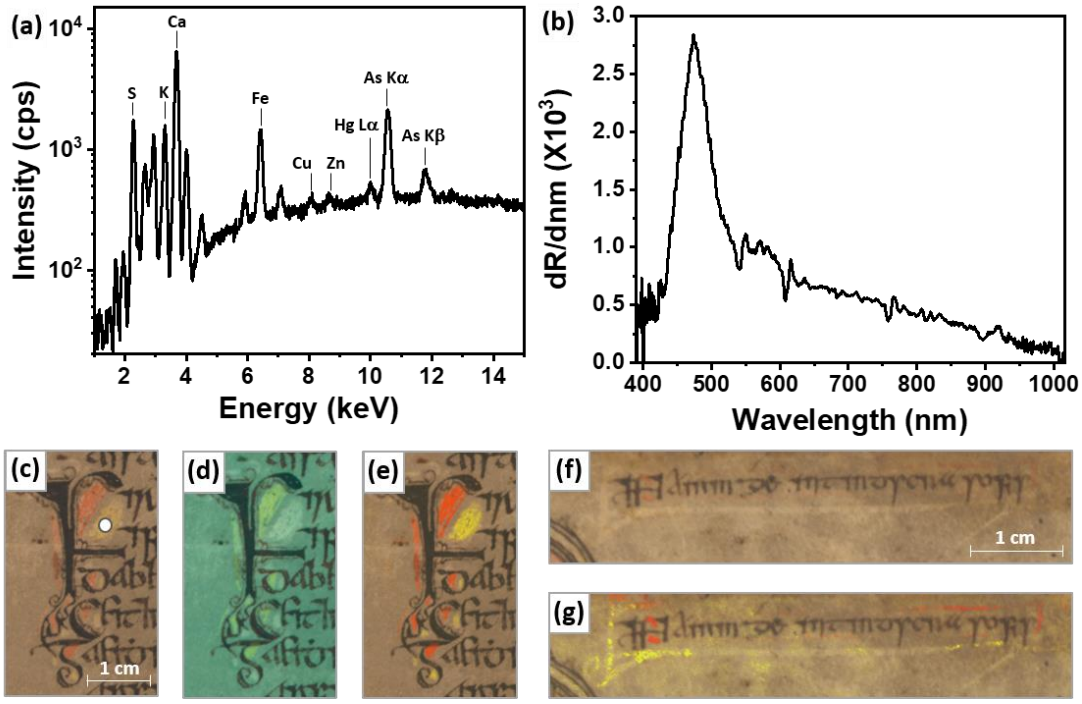

Figure 2.7. (a) XRF spectrum of a yellow pigment, folio 48 r; (b) Representative FORS spectrum of a yellow pigment, folio 54 v; (c–e) Visible image, IRFC, and PCA-based color reconstruction of the decoration of initial letter F (folio 48 r). White dot in visible image indicating the location where XRF spectrum was recorded; (f,g) Visible image and PCA-based color reconstruction of orpiment in *probatio pennae*, folio 48 r upper margin.

Given the somewhat unprecedented appearance of the mise-en-page of folio 111 r, and on the advice of codicologists and paleographers, further analyses were performed on this folio. In fact, the zoomorphic initial T (Figure 8a) stands alone in the decorative pattern of the book and presents a diverse palette of colors. For instance, it is the only decorated initial presenting green pigmentation. Its significance may be that it marks the beginning of the poem in praise of a famous Ó Ceallaigh chieftain, Uilliam Buidhe, who died in 1381.

The XRF spectrum of the warm red shade at the side of the animal head (Figure 8c, spot 16) showed intense peaks for Hg and Pb, suggesting that a mixture of cinnabar (bright red coloration) and Pb-based pigment(s) (dark coloration) was used. The XRF spectrum taken on the lighter red-pink hue of the figure (Figure 8d, spot 17) showed a similar ratio of Hg/Pb if compared to the darker red coloration. The overall lighter hue contribution could be associated with the presence of lead white, which was added to cinnabar to obtain the lighter red hue observed. Finally, the XRF of the purple/gray area (s18, Figure 8e) showed a prominent presence of Pb-based pigment(s), known to be prone to degradation towards brown and black colorations (galena, PbS) [42–44].

Six XRF spectra were performed on dark and light green on this folio. The elemental composition of these areas (see Figure 8f) highlighted that all greens were characterized by the presence of Cu and Pb. The lighter hues of green might have resulted from a lighter application or from a mixture with white pigment(s), either lead white or calcite, considering the more intense peak for Ca in these lighter areas when compared to darker green hues. However, as the analyzed light greens are thinner than the darker applications, it was difficult to exclude a substantial Ca contribution from the parchment. The presence of Fe was attributed to a contribution from the parchment background. Given that Hg was detected only in trace amounts, it was interpreted as contamination originating from the nearby vermilion applications, rather than being intentionally mixed with the green.

The green area appeared as blue in the IRFC image (Figure 8b), which aligns with the findings reported in the literature for most of the Cu-based greens. The FORS spectra (Figure 8g) exhibited a broad absorption centered at ~720 nm, indicating the likely presence of verdigris rather than other Cu-based pigments [45]. However, to fully confirm the presence of verdigris, further analysis would be necessary.

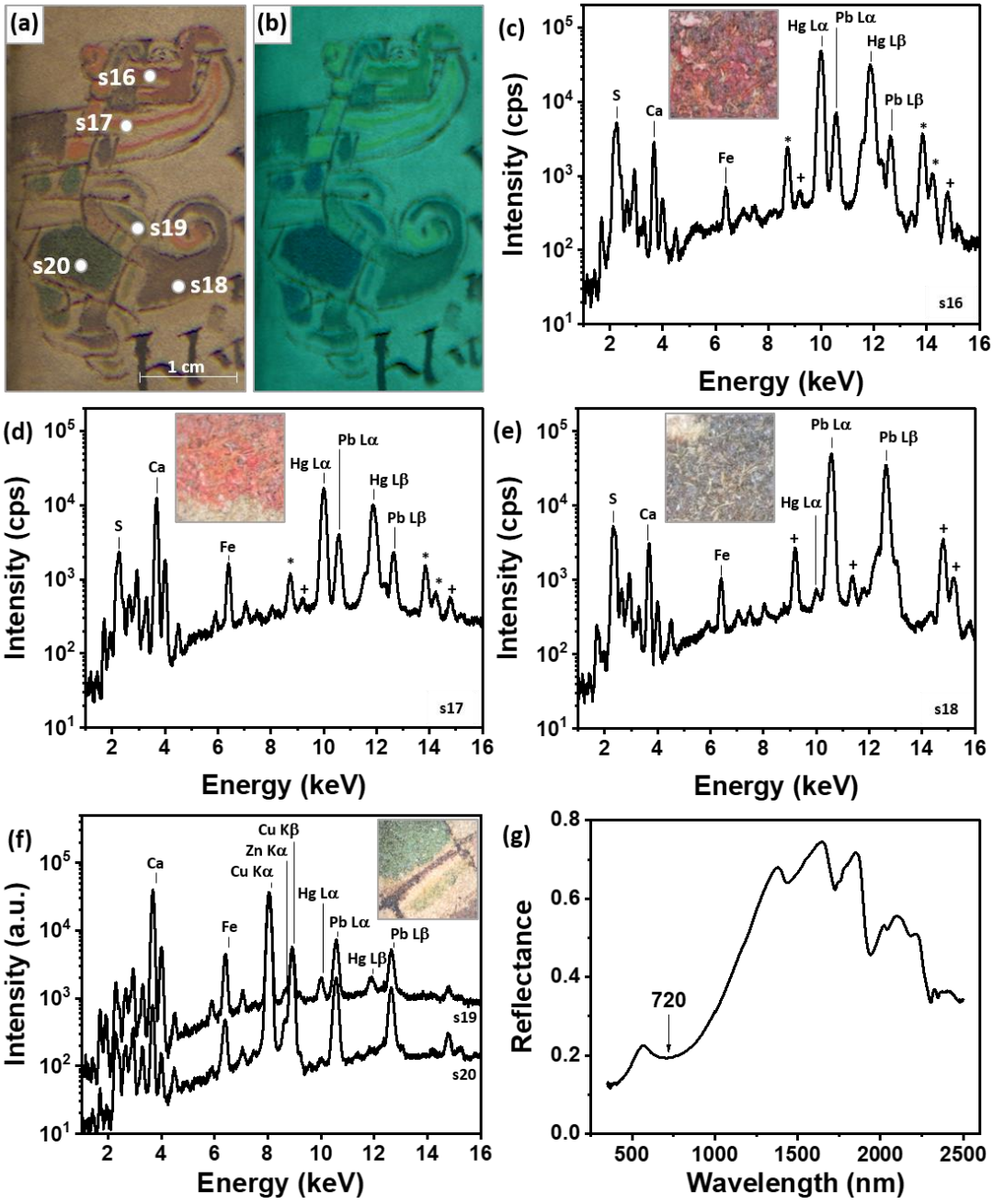

Figure 2.8. (a) Visible image and (b) IRFC of zoomorphic initial letter, folio 111r. White spots and numbering represent areas where XRF spectra were taken; (c–e) XRF spectra of spots 16, 17 and 18, respectively. Insets show microscopic optical images of the areas of analysis. * represents other peaks of Hg; + indicates other peaks for Pb; (f) XRF spectra of light green pigment (top spectrum, s19) and dark green pigment (bottom spectrum, s20); (g) FORS spectra of the dark green area (s20).

Pigment Degradation

Various causes of pigment degradation were identified and are highlighted in Figure 9.

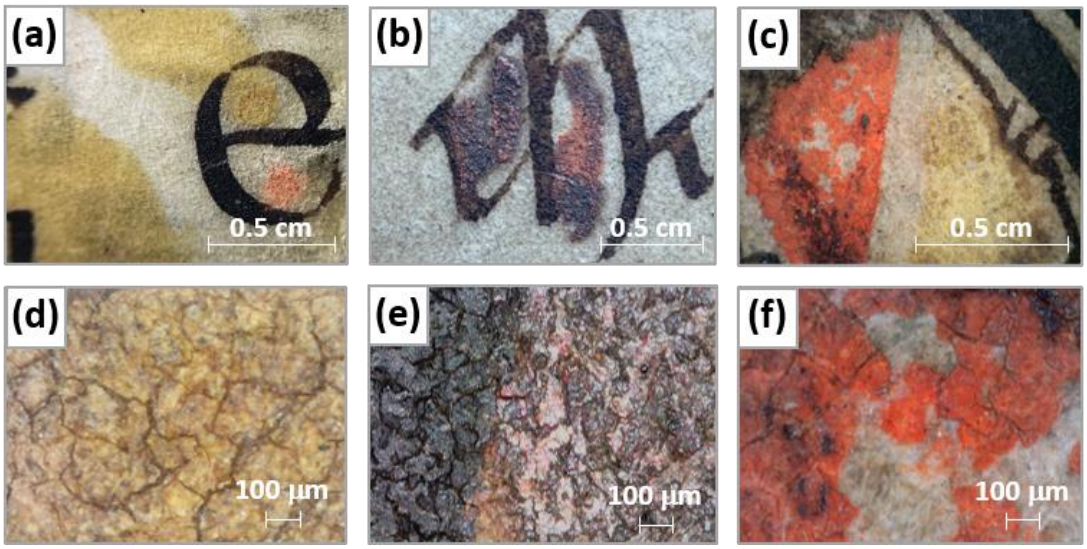

Figure 2.9. Optical microscopy images of pigment details across the book showing details of: (a,d) pigment migration and smudging; (b,e) pigment color change; (c,f) pigment detachment.

Degradation by spreading/smudges due to the water solubility of pigments exposed to humidity was observed (see Figure 9a and close-up Figure 9d), particularly accentuated in applications made of orpiment. Color degradation by color alteration was commonly observed. This process is shown in Figure 9b and 9e for the specific case of a red rubrication changing color into dark gray, a phenomenon likely associated with the chemical transformation of Pb-based pigments into galena (PbS). The other source of degradation observed was a color loss by detachment (see Figure 9c and close-up Figure 9f), likely associated with the degradation of the binding medium. This resulted in heavy cracking and flaking of the folios. This induced both poor adhesion to the support and loss of cohesion between particles, therefore resulting in detachment from the parchment support.

2.4 Conclusions

A multi-analytical approach was used for the first time to analyze the materiality of an Irish Gaelic manuscript from the medieval vernacular period. Protein analysis confirmed the use of skin from young calves in the production of the parchment. Additionally, a combination of XRF and MSI allowed the identification of writing inks, decorative practices for capital letters, and techniques for ruling the parchment prior to writing. The analysis of pigments using XRF, FORS and MSI allowed the identification of vermillion and Hg/Pb mixtures used for reds and the use of orpiment for yellows. Notably, a copper-based green was found solely in the decoration of a single folio. Several questions still remain unanswered, particularly regarding the origin of the Pb-based material used for ruling the folios and the cause behind the ink's persistent dark coloration in infrared images at 940 nm. Additionally, the cause of the degradation of the red pigment mixture (Pb/Hg), which displayed a shift in color towards a metallic purple/gray hue, is unknown. To address these queries, the use of sampling-based techniques would be beneficial. These techniques could provide valuable insights and help shed light on the uncertainties mentioned earlier. Moreover, obtaining samples would open up possibilities for understanding the organic components present in inks and pigments. Although this investigation focuses specifically on the Book of Uí Mhaine, the knowledge acquired from this research is anticipated to support future studies in the field by enhancing our understanding of the production of medieval manuscripts within the Gaelic tradition and beyond.

2.5 Experimental

Biomolecular Sampling (Proteins). Twenty-three samples were extracted using the kits sent by one of the authors (Sarah Fiddyment, University of Cambridge), according to a method described elsewhere [15]. Sample collection was undertaken on areas of the manuscript that had no writing and presented structural integrity. All the samples were stored at room temperature until required.

Biomolecular analysis. Protein mass spectrometry (ZooMS) was performed as already described in detail in reference [15]. Briefly, in order to collect collagen, collected eraser samples were centrifuged and solubilized in 0.05 M NH3CO3 (AmBic) buffer (pH 8) and 1 μL of trypsin (0.4 μg/μL) and incubated at 37 °C for 4 h. Samples were then centrifuged for 1 min, and 1 μL of 5% (v/v) TFA was added, followed by desalting and a concentration step in C18 resin (Millipore). Eluted peptides were mixed on a ground steel plate with 1 μL of α-cyano-4-hydroxycinnamic acid matrix solution [1% in 50% ACN/0.1% TFA (v/v/v)] and air-dried. Extracted peptides from the 23 samples were analyzed using a calibrated Ultraflex III (NLD1; Bruker Daltonics) MALDI-TOF instrument in reflector mode in 3 technical replicates. Spectral analysis was performed using the open-source cross-platform software mMass (www.mmass.org, 26/10/2022) [22], and individual peptides were identified manually according to Buckley et al. [23,24]. A FAM411 3 T-FV2W model microscope was used to acquire digital images at 50× and 200× magnification ratios. The instrument was equipped with visible LED lights and a digital camera with 1.3 Megapixel resolution.

Multispectral imaging was conducted using a Megavision system equipped with a 39-megapixel monochrome E6 camera (Kodak) with a CCD sensor (7216 × 5412 pixel ar-ray and a linear dimension of 6.8 microns). Illumination was provided by narrowband (FWHM between 6 and 20 nm) light-emitting diodes (LED) at 365, 400, 420, 450, 470, 505, 530, 560, 590, 615, 630, 655, 735, 850, and 940 nanometers (nm). Megavison, a hyperspectral lens having a focal length of 120 mm and a f-number of 4.5, color corrected from 350 to 1000 nm, was used and operated with an aperture of F11. The exposure times of the cam-era were adjusted for each narrow-band LED light via calibration to an in-scene Spectralon 99% diffuse white standard. Each capture is flat-fielded to correct for non-uniform illumination and variations of the lens and camera back. The exposure times of the camera were adjusted for each narrow-band LED light to ensure that the full dynamic range of the camera was used. Each capture is flat-fielded to correct for non-uniform illumination and variations in the lens throughput over the field of view. Files were captured as digital negative graphics (DNG), corrected for uniformity or artefacts using a flat fielding technique, and converted into 16-bit tagged image file format (TIFF) files. An X-rite color checker and Spectralon were used as reference standards. Image processing derived from multispectral image cubes was completed in the form of infrared false color (IRFC), substituting the red channel of the visible with the IR image at 940 nm, and principal component analysis (PCA). PCA images were obtained by processing all 15 MSI images.

X-ray fluorescence spectroscopy was performed with a portable, energy-dispersive XRF ELIO (XGLab, srl). The spectrometer was equipped with a Peltier-cooled Silicon Drift Detector with a resolution f 135 eV at the manganese (Mn) Kα line (5.9 keV). The excitation source was a low-power (4 W, 50 kV) transmission X-ray tube with a Rh anode. Measurements were performed with no filter under an air atmosphere in a range of 1–30 kV with a tube current of 130 uA. A collimator, allowing a ~1 mm-diameter focused spot size on the surface of the folio, was used to acquire XRF spectra. The distance from the folio was ~1 cm, and the acquisition time was 240 secs for representative spectra. A semi-quantitative approach to the XRF data was performed using the open-source software PyMca. The so applied fundamental parameter method (FPM) allowed estimating elemental concentrations based on observed peak intensities.

Raman spectra were taken with a Renishaw inVia Qontor Raman Spectrometer System equipped with a 785 nm laser with 300 mW laser power. For the spectra acquisition, 10% power was used to obtain maximum signal-to-noise ratio while avoiding laser-induced damage to the material. The collected polychromatic light was diffracted by 1800 lines/mm grating into its constituent wavelengths and captured on a Peltier-cooled (−70 °C) near-infrared enhanced, deep depletion CCD (1024 × 256 pixels). Spectra were obtained using ×100 objective (0.6 µm spot size)—30 accumulations of 30 s. Spectra were processed in Wire 5.5 using minimal smoothing, cosmic ray removal and baseline subtraction. Deconvolution uses Wire 5.5. mixed Gaussian/Lorentzian curves to identify relevant peaks. Additional Raman analyses were performed using a Renishaw InVia Raman system outfitted with a Leica DM2500 microscope, CCD detector, and Rayleigh edge filters. The laser excitation was 785 nm, and the grating was 1200 L/mm. Exposures ranged from 10 to 100 s at 0.45 or 0.24 mW power, using a 50× or 20× objective. Both instruments were calibrated to the 520.5 cm−1 line of Silicon. Reference Raman spectra for comparison were found on the IRUG website (www.irug.org, 23/01/2023).

FORS spectra were collected with an ASD FieldSpec 4 from 350 nm to 2500 nm with a collection area of ~3 mm. Spectral resolution is 3 nm at 700 nm and 8 nm at 1400 and 2100 nm. Ten spectra were averaged with a total acquisition time of <5 s. Reflectance was calibrated to a Spectralon 99% diffuse white standard (calibrated every 20 min during data capture). The bifurcated probe uses a halogen light source with a bulb temperature of 2900 K and a spot size of 10 mm.

2.6 References

1. Library, R.I.A. Catalogue of Irish Manuscripts in the Royal Irish Academy; Catalogue of Irish manuscripts in the Royal Irish Academy (28, fasc.); Royal Irish Academy: Dublin, Ireland; Figgis & Co.: Hodges, FL, USA; Williams & Norgate: London, UK, 1926; p. 3314.
2. O'Sullivan, W. The Book of Uí Maine formerly the Book of Ó Dubhagáin: Scripts and structure. *É*igse **1989**, 23, 151–166.
3. Lettner, M.; Sablatnig, R. Multispectral imaging for analyzing ancient manuscripts. In Proceedings of the 2009 17th European Signal Processing Conference, Glasgow, UK, 24–28 August 2009.
4. Hollaus, F.; Diem, M.; Fiel, S.; Kleber, F.; Sablatnig, R. Investigation of Ancient Manuscripts based on Multispectral Imaging. In Proceedings of the 2015 ACM Symposium on Document Engineering, in DocEng '15, Lausanne, Switzerland, 8–11 September 2015; Association for Computing Machinery: New York, NY, USA, 2015; pp. 93–96.
5. Weiskott, E. Multispectral Imaging and Medieval Manuscripts. In The Routledge Research Companion to Digital Medieval Literature; Boyle, J.E., Burgess, H.J., Eds.; Routledge: England, UK, 2018; pp. 186–196. Available online: https://www.academia.edu/35291754/Multispectral_Imaging_and_Medieval_Manuscripts (accessed on 6 April 2023).

6. Beeby, A. Spectral imaging of medieval manuscripts. In Hyperspectral Imaging and Applications; SPIE: Bellingham, WA, USA, 2020.

7. Cohen, Z.; Kindzorra, E.; Hahn, O.; Glaser, L.; Łojewski, T.; Rabin, I.; Cohen. 2015-Composition of the primary inks in medieval palimpsests–effects of ink removal. Opusc. Musealia **2016**, 23, 75–82.

8. Cohen, Z.; Olszowy-Schlanger, J.; Hahn, O.; Rabin, I. Composition Analysis of Writing Materials in Geniza Fragments: New Perspectives. In Jewish Manuscript Cultures; De Gruyter: Berlin, Germany, 2017.

9. Aceto, M.; Agostino, A.; Fenoglio, G.; Capra, V.; Demaria, E.; Cancian, P. Characterisation of the different hands in the composition of a 14th century breviary by means of portable XRF analysis and complementary techniques: Different hands in a 14th-century breviary by means of XRF analysis. X-ray Spectrom. **2017**, 46, 259–270.

10. Melo, M.; Otero, V.; Vitorino, T.; Araújo, A.R.D.S.D.; Muralha, V.S.; Lemos, A.; Picollo, M. A Spectroscopic Study of Brazilwood Paints in Medieval Books of Hours. Appl. Spectrosc. **2014**, 68, 434–444.

11. Leona, M.; Winter, J. Fiber Optics Reflectance Spectroscopy: A Unique Tool for the Investigation of Japanese Paintings. Stud. Conserv. **2001**, 46, 153.

12. Liu, W.; Li, M.; Wu, N.; Liu, S.; Chen, J. A new application of Fiber optics reflection spectroscopy (FORS): Identification of ‘bronze disease’ induced corrosion products on ancient bronzes. J. Cult. Heritage **2021**, 49, 19–27.

13. Ricciardi, P.; Delaney, J.K.; Facini, M.; Glinsman, L.D. Use of Imaging Spectroscopy and in situ Analytical Methods for the Characterization of the Materials and Techniques of 15th Century Illuminated Manuscripts. J. Am. Inst. Conserv. **2013**, 52, 13–29.

14. Aceto, M.; Agostino, A.; Fenoglio, G.; Idone, A.; Gulmini, M.; Picollo, M.; Ricciardi, P.; Delaney, J.K. Characterisation of colourants on illuminated

manuscripts by portable fibre optic UV-visible-NIR reflectance spectrophotometry. Anal. Methods **2014**, 6, 1488–1500.

15. Fiddyment, S.; Holsinger, B.; Ruzzier, C.; Devine, A.; Binois, A.; Albarella, U.; Fischer, R.; Nichols, E.; Curtis, A.; Cheese, E.; et al. Animal origin of 13th-century uterine vellum revealed using noninvasive peptide fingerprinting. Proc. Natl. Acad. Sci. USA **2015**, 112, 15066–15071.

16. Teasdale, M.D.; Fiddyment, S.; Vnouˇcek, J.; Mattiangeli, V.; Speller, C.; Binois, A.; Carver, M.; Dand, C.; Newfield, T.P.; Webb, C.C.; et al. The York Gospels: A 1000-year biological palimpsest. R. Soc. Open Sci. 2017, 4, 170988.

17. Fiddyment, S.; Teasdale, M.D.; Vnouˇcek, J.; Lévêque Binois, A.; Collins, M.J. So you want to do biocodicology? A field guide to the biological analysis of parchment. Heritage Sci. 2019, 7, 35.

18. Toniolo, L.; D'Amato, A.; Saccenti, R.; Gulotta, D.; Righetti, P.G. The Silk Road, Marco Polo, a bible and its proteome: A detective story. J. Proteom. 2012, 75, 3365–3373.

19. Cucci, C.; Bracci, S.; Casini, A.; Innocenti, S.; Picollo, M.; Stefani, L.; Rao, I.G.; Scudieri, M. The illuminated manuscript Corale 43 and its attribution to Beato Angelico: Non-invasive analysis by FORS, XRF and hyperspectral imaging techniques. Microchem. J. 2017, 138, 45–57.

20. De Viguerie, L.; Rochut, S.; Alfeld, M.;Walter, P.; Astier, S.; Gontero, V.; Boulc'h, F. XRF and reflectance hyperspectral imaging on a 15th century illuminated manuscript: Combining imaging and quantitative analysis to understand the artist's technique. Heritage Sci. 2018, 6, 11.

21. Calà, E.; Agostino, A.; Fenoglio, G.; Capra, V.; Porticelli, F.; Manzari, F.; Fiddyment, S.; Aceto, M. The Messale Rosselli: Scientific investigation on an outstanding 14th century illuminated manuscript from Avignon. J. Archaeol. Sci. Rep. 2019, 23, 721–730.

22. Strohalm, M.; Kavan, D.; Novák, P.; Volný, M.; Havlíˇcek, V. mMass 3: A Cross-Platform Software Environment for Precise Analysis of Mass Spectrometric Data. Anal. Chem. 2010, 82, 4648–4651.

23. Buckley, M.; Collins, M.; Thomas-Oates, J.;Wilson, J.C. Species identification by analysis of bone collagen using matrix-assisted laser desorption/ionisation time-of-flight mass spectrometry. Rapid Commun. Mass Spectrom. 2009, 23, 3843–3854.

24. Buckley, M.; Kansa, S.W.; Howard, S.; Campbell, S.; Thomas-Oates, J.; Collins, M. Distinguishing between archaeological sheep and goat bones using a single collagen peptide. J. Archaeol. Sci. 2010, 37, 13–20.

25. Lowe, E.A. Codices Latini Antiquiores: A Palaeographical Guide to Latin Manuscripts Prior to the 9th Century. Part 2, Great Britain and Ireland, 2nd ed.; Clarendon Press: Oxford, UK, 1972.

26. Moog, G.; Danforth, C. Skins and Hides for Making Parchment: An Overview of Parchment's Histologic Features that are Helpful when Identifying Raw Source Material. Art Transl. 2021, 13, 419–431.

27. Duran, A.; López-Montes, A.; Castaing, J.; Espejo, T. Analysis of a royal 15th century illuminated parchment using a portable XRF–XRD system and micro-invasive techniques. J. Archaeol. Sci. 2014, 45, 52–58.

28. Cains, A. The Vellum of the Book of Kells. Pap. Conserv. 1992, 16, 50–61.

29. Samidurai, S.; Khambhaty, Y.; Alagamuthu, T.S. Bio-preservation of raw hides/skins: A review on greener substitute to conventional salt curing. Environ. Sci. Pollut. Res. 2022, 29, 64513–64535.

30. Reed, R. Ancient Skins, Parchments and Leathers. In Studies in Archaeological Science; Seminar Press: London, UK, 1972; Available online: http://catalogue.bnf.fr/ark:/12148/cb353652597 (accessed on 28 February 2023).

31. Tanimoto, S.; Verri, G. A Note on the Examination of Silverpoint Drawings by Near-Infrared Reflectography. Stud. Conserv. 2009, 54, 106–116.

32. Balbas, D.Q.; Fovo, A.D.; Montalbano, L.; Fontana, R.; Striova, J. Non-invasive contactless analysis of an early drawing by Raffaello Sanzio by means of optical methods. Sci. Rep. 2022, 12, 1–10.

33. Havermans, J.; Aziz, H.A.; Scholten, H. Non Destructive Detection of Iron Gall Inks by Means of Multispectral Imaging Part 1: Development of the Detection System. Restaurator 2003, 24, 55–60.

34. Colini, C.; Hahn, O.; Bonnerot, O.; Steger, S.; Cohen, Z.; Ghigo, T.; Christiansen, T.; Bicchieri, M.; Biocca, P.; Krutzsch, M.; et al. The Quest for the Mixed Inks. H. Siegfried Stiehl (Eds.), Proceedings of the Second International Conference on Natural Science and Technology in Manuscript Analysis, Manuscript Cultures 11 (2018), 41–48. Available online: https://www.academia.edu/38120349/The_Quest_for_the_Mixed_Inks (accessed on 9 February 2022).

35. Fichera, G.V.; Malagodi, M.; Cofrancesco, P.; Weththimuni, M.L.; Guglieri, C.; Olivi, L.; Ruffolo, S.; Licchelli, M. Study of the copper effect in iron-gall inks after artificial ageing. Chem. Pap. 2018, 72, 1905–1915.

36. Edwards, H.G.M. Chapter 1. Analytical Raman Spectroscopy of Inks; Royal Society of Chemistry: Washington, DC, USA, 2018; pp. 1–15.

37. Piantanida, G.; Menart, E.; Bicchieri, M.; Strliˇc, M. Classification of iron-based inks by means of micro-Raman spectroscopy and multivariate data analysis. J. Raman Spectrosc. 2013, 44, 1299–1305.

38. Pallipurath, A.R.; Skelton, J.M.; Ricciardi, P.; Elliott, S.R. Estimation of semiconductor-like pigment concentrations in paint mixtures and their differentiation from paint layers using first-derivative reflectance spectra. Talanta 2016, 154, 63–72.

39. Cheng, H.; Zhou, Y.; Frost, R.L. Structure comparison of Orpiment and Realgar by Raman spectroscopy. Spectrosc. Lett. 2017, 50, 23–29.

40. Hayem-Ghez, A.; Ravaud, E.; Boust, C.; Bastian, G.; Menu, M.; Brodie-Linder, N. Characterizing pigments with hyperspectral imaging variable false-color composites. Appl. Phys. A 2015, 121, 939–947.

41. Villafana, T.; Edwards, G. Creation and reference characterization of Edo period Japanese woodblock printing ink colorant samples using multimodal imaging and reflectance spectroscopy. Heritage Sci. 2019, 7, 1–14.

42. Miguel, C.; Claro, A.; GonÃ, A.P.; Muralha, V.S.F.; Melo, M.J. A study on red lead degradation in a medieval manuscript LorvÃ£o Apocalypse (1189). J. Raman Spectrosc. 2009, 40, 1966.

2.7 Supplementary material

Classification of the Book of Uí Mhaine

Table A1. Classification of the Book of Uí Mhaine by scribe, quire, and folios according to William O'Sullivan. Key to understanding the "line" column of the table. First is listed the folio number, followed by either recto or verso; recto being indicated by "r" and verso by "v". What follows is the column in which the line of text is found, indicated by either "a", meaning the first column of text, or "b", indicating the second column of text. In cases where there are more than two columns on the folio, each column is listed as the succeeding letter, meaning column "c", column "d", etc. Finally, the last number indicates the line of text in said column. For example, f1ra1 means the first line of text in the first column of the recto of folio 1. O'Sullivan does not indicate at exactly which line on folio 112v scribe D6 turns over to scribe C, but does specify that scribe D6 returns again to finish the text from scribe C at line 10 of column "a" on folio 114r. This is indicated in the table with question marks (?). Scribe D6 concludes on column "a" of folio 114v, where the second column of text was left blank to be added to later by a secondary scribe.

Table 1 Table A1. Classification of the Book of Uí Mhaine by scribe, quire, and folios according to William O'Sullivan.

Scribe	Quire	Folio(s)
G2	1	f1
G1		f1-f2
C		f2-f6
	2	f7-f10
G2	3	f11-f12
G1	4	f13-f18
	5	f19-f22
C		f22
	6	f23-f24
?		f24
G2	7	f25-f27
G1		f27-f32
	8	f33-f38
C		f38
	9	f39-f47
F	10	f48-f55
C	11	f56
	12	f57-f64
	13	f65-f69
Secondary Scribe(s)		f69
C	14	f70-f74
Secondary Scribe(s)		f74-f75
G1	15	f76-f79
C		f79-f83

Scribe	Quire	Folio(s)
D1	16	f84
G1		f84-f90
D2		f90-f91
	17	f92
D3		f92-f99
C		f99
D1	18	f100-f101
D4		f101
D1		f101-f102
G1		f102
D3		f103-f107
	19	f108-f110
C		f110
D3		f111
D5		f111-f112
C		f112
D6		f112-?
C		?-f114
D6		f114
Secondary Scribe(s)		f114
C	20	f115-f122
	21	f123-f130
	22	f131-f139
	23	f140-f143
	24	f144-f151
	25	f152-f157

High-res photographs of stain patterns and ink transfer

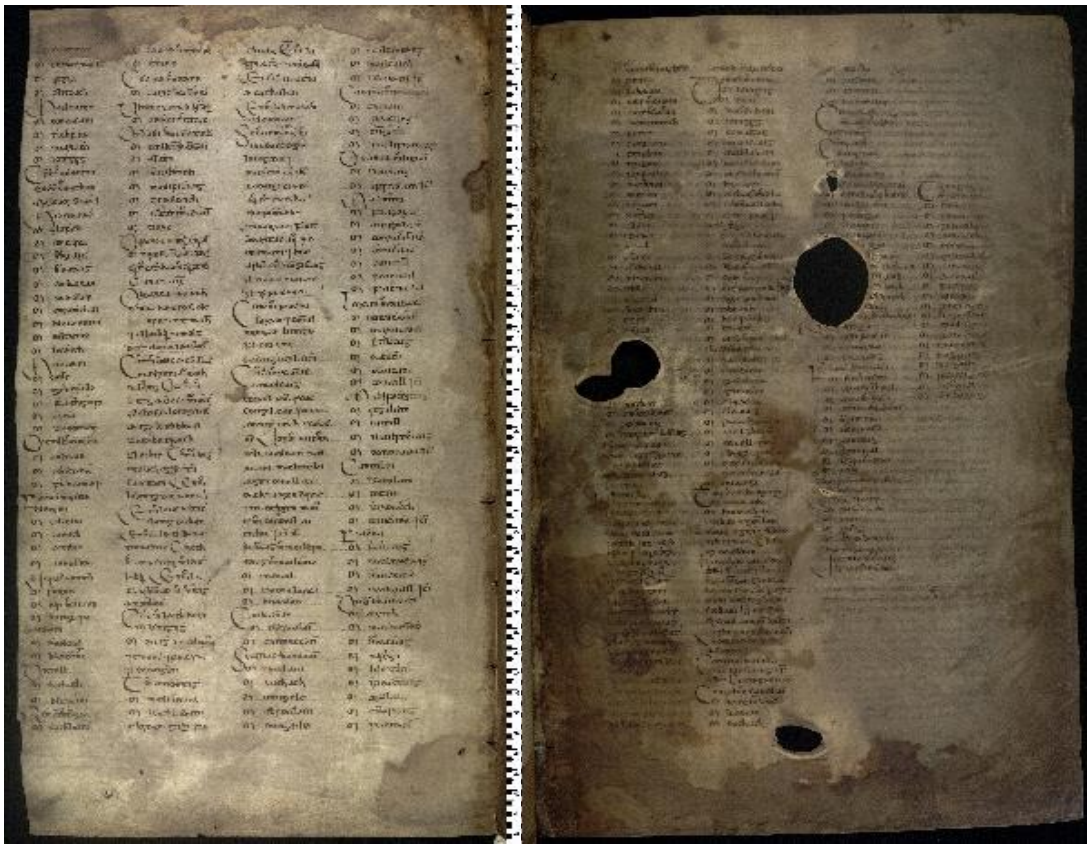

Figure. A1: High-res photographs of folio 18v (left) and folio 19r (right), corresponding to the transition from quire 4 to 5, showing dis-homogeneity in stain pattern. This break is probably the result of the loss of a single folio at this point.

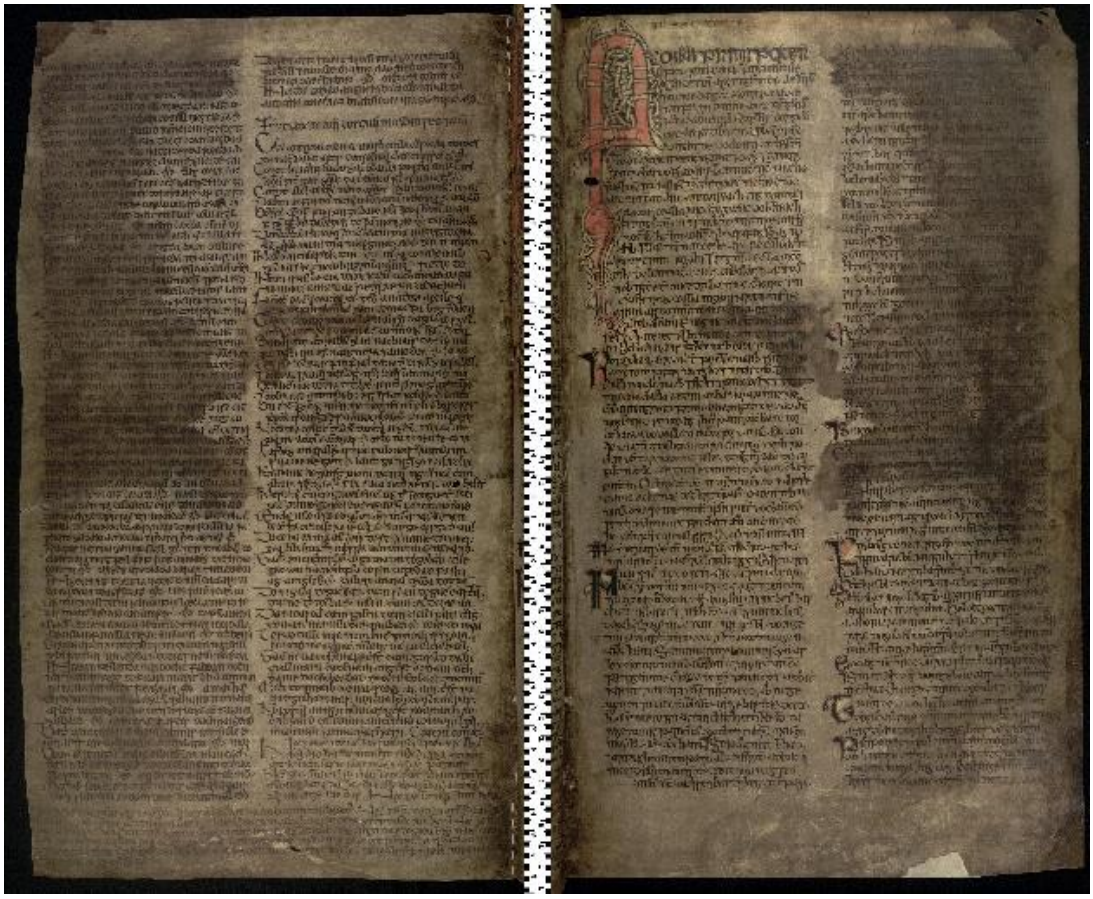

Figure A2: High-res photographs of folio 47v (left) and folio 48r (right), marking the transition from quire 9 to 10. This might be an indication that these two quires were housed together in a very similar environment even before they were bound together.

Ink transfer from f. 2v to f. 3r

Figure A3: Example of ink transfer induced by humidity from folio 2v (left) and folio 3r (right).

Ink transfer from f. 3v to f. 4r

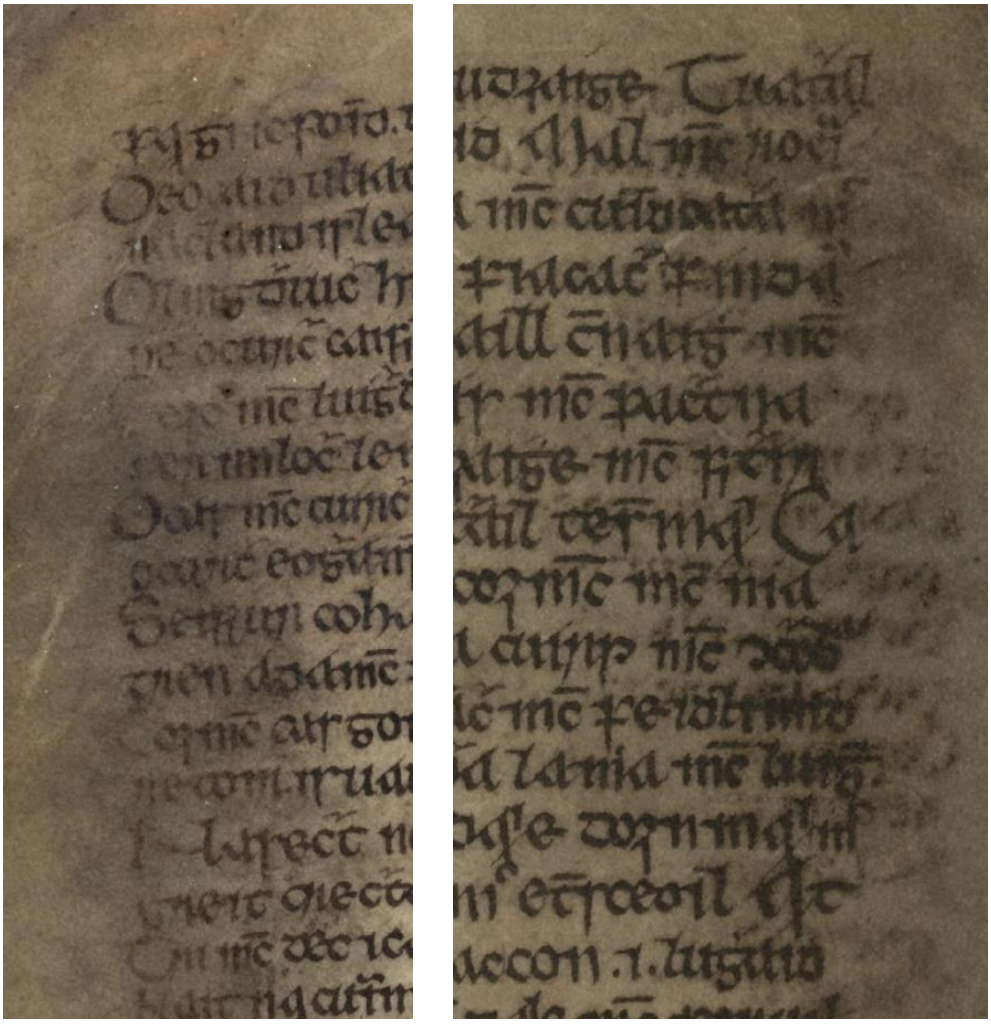

Fig. A4: Example of ink transfer induced by water-damage. Folio 3v (left) and folio 4r (right).

3. Establishing the original order of the poems in Harward's Almanac using paleography, codicology, X-ray fluorescence spectroscopy, and statistical analysis

---

As submitted to Journal of Cultural Heritage:

Author list: Veronica Biolcati, James Woolley, Élodie Lévêque, Andrea Rossi, Anna Grace Hoffmann, Andrea Visentin, Pádraig Ó Macháin, Daniela Iacopino

Title: Establishing the original order of the poems in Harward's Almanac using paleography, codicology, X-ray fluorescence spectroscopy, and statistical analysis

3.1 Abstract

This work presents the results of a transdisciplinary analysis performed on Harward's Almanac (Dublin, 1666), an extremely rare volume currently housed in the National Library of Ireland. The uniqueness and historical value of the Almanac is related to the presence of nineteen handwritten poems, entered by an anonymous scribe. These record textually important English clandestine satire circulating anonymously in Dublin in the late 17th and early 18th century. Following a comprehensive historical assessment, it appeared evident that the current order of leaves was incorrect. To reconstruct the correct order of the leaves, and hence the likely sequence in which the manuscript poems were inscribed, this study employed a codicological/paleographic analysis complemented by analytical (X-ray fluorescence, XRF) and statistical (Self Organizing Map, SOM) investigation. Specifically, point XRF analysis was carried out for each handwritten page of the Almanac, allowing identification of ink elemental compositions (iron-based ink) and successfully supporting the validity of historical hypotheses on the poems' order of inscription. The statistical organization of XRF data by SOMs allowed easy bi-dimensional visualization of the data set (54 points) and identification of ink similarities, once more validating the historical assessment.

3.2 Introduction

In 2020, the National Library of Ireland (NLI) acquired a volume of extreme rarity, the only known copy of a 1666 Dublin almanac compiled by Michael Harward and for convenience referred to as Harward's Almanac.[113] Almanacs of the period were commonly sold with blank interleaves and additional blank leaves – at the end of the volume – meant for the purchaser's notes and memoranda. In Harward's Almanac, most of these blank leaves, along with the blank regions of some of the printed leaves, remained blank during 1666, but they were later used by an unknown scribe to transcribe nineteen manuscript poems. Although it is known that these poems were composed between 1674 and 1711, it is less clear when they were copied into the Almanac.[114] When the Almanac was first reported in print in 1848, the handwritten poems were erroneously attributed to the Irish satirist Jonathan Swift (1667-1745). Although this attribution was later dismissed,[3, 4] the verse retains considerable interest. In fact, the manuscript writing preserves textually important English clandestine satire circulating anonymously in Dublin in the late 17th and early 18th century. Some of the most important poems are on Dublin topics, and three of them are not found in any other early manuscript or printed source ("The Gentlemen at Larges Litany," "To the Tune of Chivie Chace," and "The Picture of a Dublin Beau"). Much of the London verse centers on James II's Catholicism and the succession crisis caused by the 1688 birth of his son James Francis Edward, later known as the Pretender. These pieces are of interest in their own right and demonstrate the collection and possibly the circulation of London satiric verse in Dublin. No other Dublin manuscript poetical miscellany from the late 17th century has come to light, and this stands as the only example.[117] The Almanac was privately acquired sometime in the early 19th century and remained in the same Dublin family until it was sold at auction

in 2020. As it was received at NLI, Harward's Almanac was composed of 75 leaves (144 x 86 mm) in a 19th-century leather binding. Several leaves were detached from the structure and obviously not in the correct order. Early handwritten page numberings also appeared incorrect.

An extensive historical and codicological analysis was performed which established the original order of the Almanac leaves and thereby supported a plausible idea of the sequence of poem entries. During the 2021-22 conservation work performed by the NLI, the 19th-century binding was reused and, with minor exceptions, the leaves were restored in the possible order in which they were placed during the previous (19th-century) rebinding.

In parallel, X-ray fluorescence (XRF) analysis was performed to support the examination of the leaves and the reordering process. XRF analysis is a non-invasive method particularly useful in the examination of historical manuscripts and inks.[6, 7, 8] Among the diverse range of analytical methods used in heritage and conservation science, XRF stands out as a particularly valuable tool for the elemental characterization of materials. The technique offers numerous advantages, including its compatibility with portable instrumentation, which greatly facilitates *in situ* analysis. XRF requires minimal preparation of the material to be analyzed, making it an efficient and time-saving method. XRF permits qualitative analysis, providing valuable insights into the materials used in historical books and manuscripts. Furthermore, a semi-quantitative analysis of XRF data has been proven effective in uncovering ink patterns, as evidenced by previous studies that have successfully identified various writer contributions and manuscript corrections.[9, 10] The fundamental parameter (FP) is the preferred method for identifying the elemental concentration of heterogeneous samples in complex matrices, such as ink applications.[11, 12] The results obtained using FP quantification can be further analyzed using statistical methods, which can be highly valuable in identifying trends and correlations among samples. One such method is Self Organizing Map (SOM) clustering.[120] SOM mapping is a powerful technique for visualizing high-dimensional data and for clustering (grouping based on features' similarity) samples in datasets. Without requiring prior knowledge or labeled samples, SOM leverages unsupervised learning to discover the underlying structure and relationships in the data, providing insights and facilitating further analysis. SOMs are based on the concept of neural

networks and are inspired by the organization of neurons in the brain. SOMs consist of an array of artificial neurons arranged in a grid-like topology, where each neuron represents the representative point of a group. A successful example of SOM use in heritage science is the work of Lee *et al*., who classified a large number of paintings into different genres based on image features, including colors and composition characteristics.[14, 15]

In this paper we report the use of a transdisciplinary approach based on complementary historical, analytical, and statistical analyses to identify the possible order in which the poems were inscribed in Harward's Almanac. Following historical and codicological research, a systematic analytical investigation of the Almanac's handwritten poems was performed using point XRF and microscopy imaging. The ink and the paper support of every manuscript page were elementally characterized. This enabled the identification of calcium-based compounds and alum used for the preparation of the rag paper and iron-based inks for writing the poems. XRF semi-quantitative analysis of ink composition was performed and the resulting data were further analyzed by SOM, in order to identify relevant similarities associated with the stints of transcription. Following this novel approach, it was possible to confirm the historical hypotheses formulated during the Almanac's conservation work related to the correct leaf sequence and order of poem transcription. This study highlights the usefulness, in the conservation and preservation of heritage manuscripts, of a transdisciplinary approach, which in this specific case sits at the intersection of analytic bibliography, Irish studies, manuscript conservation, heritage science, and computer science.

3.3 Results and discussion

The initial phase of this analytical work involved conducting historical research on the printed Almanac. This was followed by a meticulous codicological observation during the 2021-22 conservation phase at the NLI. The disbound state of the volume during the conservation treatments provided access to typically concealed areas, including the spine sewing, the folding of the sheets, and the sewing holes. The combination of these two perspectives provided valuable information and laid the foundation for the complementary analytical and statistical investigation.

Background information: what we know about the book from historical and codicological analyses

The printed elements of the Almanac consisted of 48 unnumbered pages in three octavo (8-leaf) gatherings (A, B and C). Additionally, 14 blank interleaves plus an unknown number of appended blank leaves provided space for the purchaser's notes and memoranda; 11 of these appended leaves survive today. The structure of the Almanac is shown in Figure 1. In this schematic depiction, the double lines represent blank leaves, solid lines represent printed leaves, and dashed lines represent leaves now missing. Leaves are identified by handwritten page numbers, and printed leaves are also identified by gathering and leaf number. The diagrams show gatherings as viewed from the book's bottom edge with the book open. The base of the shallow "V" marks the fold or gutter through which the leaves would have been sewn when the volume was bound. In each gathering, the bottom leaf pair is outermost, the top pair innermost. So in the A gathering, p. 3 is the first, and the conjugate p. 34 is the last. Similarly, pp. 17-20 form the innermost pair of leaves or centerfold. Figure 1 shows that originally, each leaf in the volume was

one half of a bifolium. However, some leaves became detached and are at present non-conjugate. Additional appended bifolia may have originally been present, and it is no longer possible to establish how many blank leaves were originally present at the end of the volume.

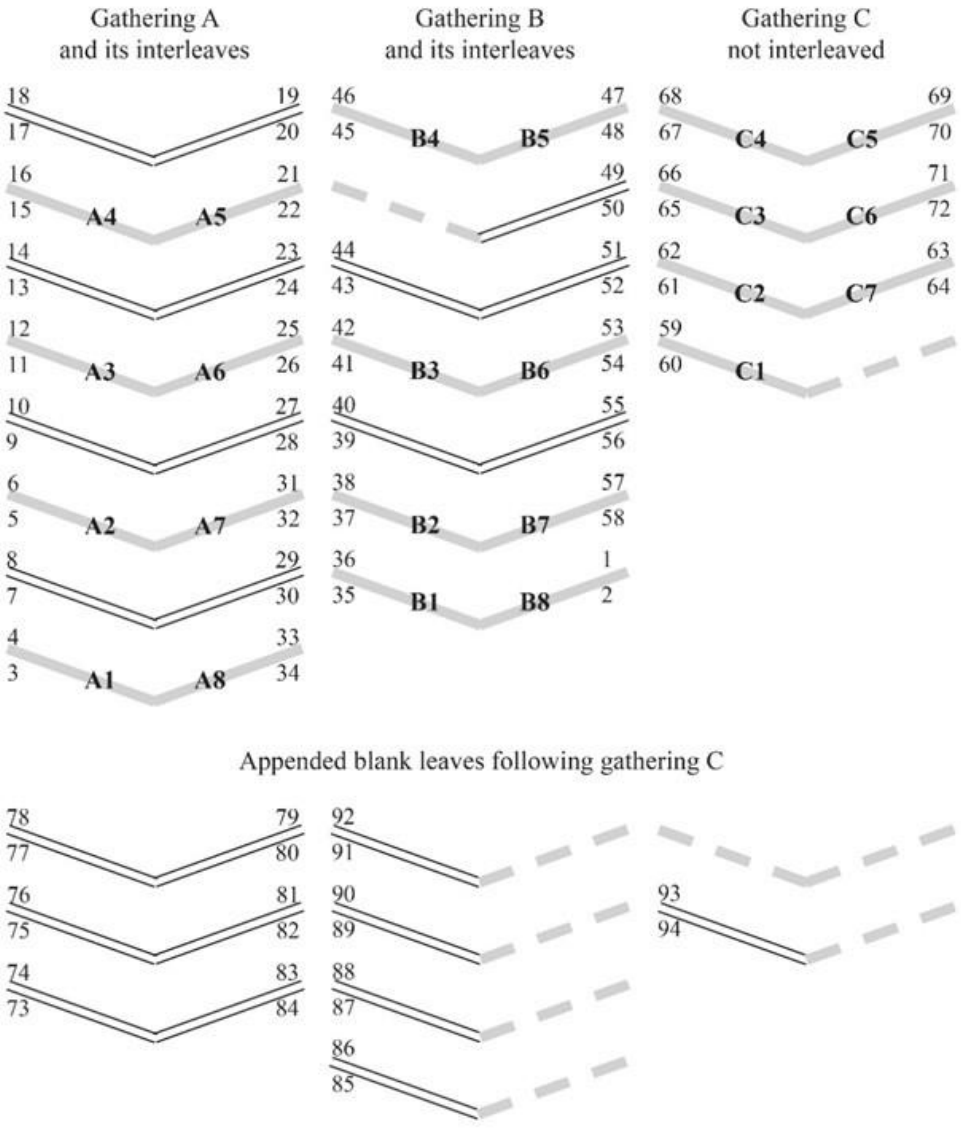

Figure 3.1. Structure of the Almanac gatherings, showing leaf pairs.

The book was sewn on three sewing supports. Five holes remaining in the spine folds (sewing stations) were recorded, evenly spaced and darker than the rest of the paper. It is likely that the three central ones were used for sewing the paper to the supports using linen thread and that the top and bottom holes were used for the kettle stitch. In addition,

on the leaf now numbered 94-93, remnants of stitching and leather marks from a previous cover supported the conclusion that there had been an earlier leather binding, predating the 19th-century one.

The paper support used across the entire volume (the printed sheets, the interleaves, and the appended blank leaves) was hand-made from 17th-century rag paper, the only type of paper produced in the West at the time. Rag paper is primarily made of cotton, hemp, or linen fibers from recycled fabric and is recognizable for its pronounced texture along with the presence of laid lines and chain-lines left by the paper mold.[18, 19]

Being octavo in format, the pages had vertical chain-lines and the watermarks were quartered across the upper gutter and the upper edge of four leaves, making it difficult to reconstruct the full watermark. However, one watermark was shared by both a printed page (pp. 47-48) and several blank leaves (interleaves 23-44, 51-52, and 55-56; appended blank leaves 77-78 and 85-86), suggesting that at least in these cases, the same paper stock was used for both components. The watermark was reconstructed as a fleur-de-lys above a post-horn bounded by a scroll, of a generic variety typified by Gravell §791.[125]

The volume's leaves seemed to have been reordered on at least two subsequent occasions. On the first, the pages were hand-numbered, presumably following a reordering, which implies that some leaves had already become detached from the structure. During a further reordering, possibly after the acquisition of the volume in the early 19th century, some of the earlier reordering was revised. The current (19th century) rebinding was seemingly assembled to protect the already damaged 17th century volume. The pages presented extensive damage with water stains, mold, tears, and losses (see Figure 2a, b, c, d).

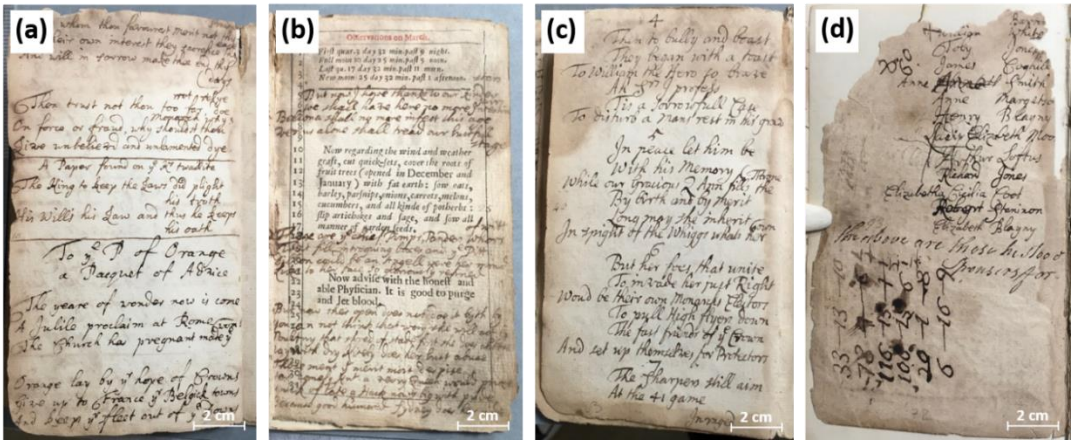

Figure 3.2. Pre-conservation photographs of damaged pages: (a) p. 10, (b) p. 25, (c) p. 40, and (d) p. 93. Reproduction rights owned by the NLI. The same applies to all the following photographs.

The sequence in which the poems were inscribed: historical analysis

In the late 17th and early 18th century, 19 poems were transcribed onto the blank interleaves and appended blank leaves as well as onto the blank areas of some of the printed leaves (see Figures 3a, b). What remains a topic of debate is the exact point at which the leaves had become loose, allowing the scribe to write noticeably farther into the gutter than would normally be possible in a bound volume (Figure 3c, and Figure S1 in the Supplementary Materials).

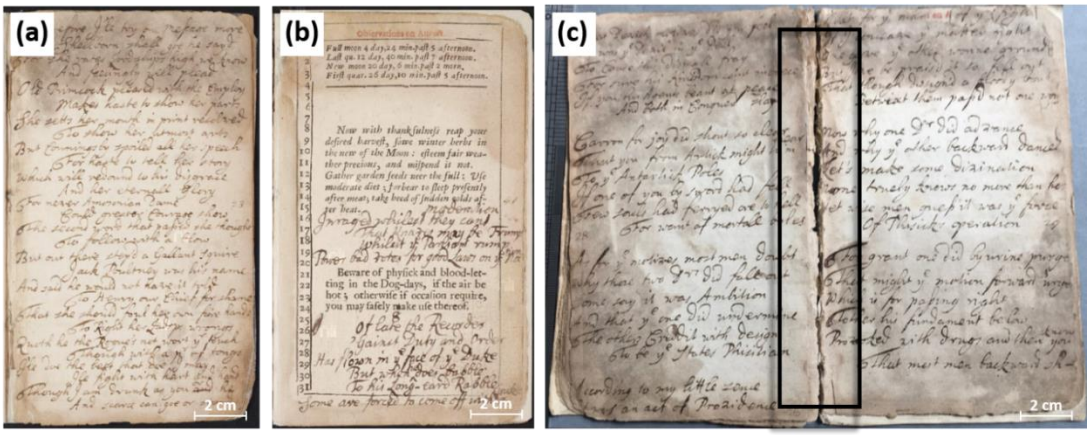

Figure 3.3. (a) The manuscript on an interleaf, p. 23; (b) The manuscript on a printed page, p. 25; (c) p. 28 and p. 29 before conservation. The black box shows the gutter with the writing running very close to the fold.

Detailed observation of the pages allowed recording several characteristics about the prior reordering of the pages (see Supplementary Materials). From a paleographical investigation of the handwritten sections, it appeared likely that a single scribe wrote all

the poems. However, notable variations in handwriting size, spacing, and color of the writing ink were observed across pages, leading to the assumption that the poems were entered in successive stints under varied circumstances, as the variations in ink elemental composition (discussed later) also suggest.

Based on the historical data regarding the poems' composition and circulation dates (between 1674 and 1711), it appeared likely that the compiler gathered some of the poems towards the end of the 17th century, over a span of approximately 15 years, and added poems during the early years of the 18th century. Circulation dates, textual content, and codicological assessment suggested that the scribe began adding poems using several appended blank leaves that followed the C gathering of the printed Almanac (pp. 77-88). Once these blank leaves were filled with poems dated to the late seventies of the 17th century, the scribe continued writing on interleaves 7-10, 13-14, 17-20, and 23-24. The scribe then continued on the unprinted areas of the printed p. 25 (see Figure 3b), before proceeding onto interleaves 27-30 (partly shown in Figure 3c). These poems (pp. 7-30) are dated to the late eighties and nineties of the 17th century. The poems on pp. 89-92 date from 1699 to 1709, while a poem dated to 1711 is found on pp. 39-51.

What is puzzling is why the scribe, having reached the bottom of what is now p. 88, then continued that poem at the top of p. 7. A possible explanation is that the scribe only then realized that there was far more material to copy into the book than the remaining appended leaves could accommodate and simply chose that moment to go to the early interleaves of the volume and continue writing there. For the belated use of pp. 39-51, the readiest explanation is that no other such stretch of blank pages remained available as late as 1711.

Based on the above historical assessment, an original sequence of poem insertion was proposed and it is shown in Table 1. This reconstructed sequence, as well as the open questions associated with the proposed order, established the basis for XRF and SOM analyses.

Table 3.1. Proposed original order in which the poems were transcribed in the Almanac

Page	Poem title	Composition date
77-78	Upon Nothing by y[e Earl o]f Ro[chester]	1678?
79-82	The Catholique Ballad or An Invitation to Popery	1674
83-87	Room for a Ballad, or A Ballad for Rome	1674

87-88	On Rome's Pardons by the E. of R.	1675-80
88 and 7	On the Composeing of a Prayer for the Unborne Prince of Wales	1688
7-9	The Miracle	1687
9-10	A Paper Put in the K's Shoo	1687?
10	A Paper Found on the K's Twallite [toilette]	1685-88
10, 13	To the P of Orange: A Pacquet of Advice	1688
14, 17	The Pacquet Boat Returned	1688
17-19	The Gentlemen at Larges Litany	1692-93?
19-20, 23-24	To the Tune of Chivie Chace	1692-93
24-25, 27	Mrs Butler to Mrs Bracegirdle	1692-93?
27-30	The Duel between 2 Phisitians	1693
30	A Pascall [pasquil] Lately Come from France	1696
89-90	[The Picture of a Dublin Beau]	1699
90-91	A Fable, yet a True Story	1700-01
92	The Thanksgiving	1709?
39-41, 43-44, 49-51	The Whiggs Lamentation. A Soar of Their Own Scratching	1711

Elemental composition of the book: XRF analysis

A total of 104 XRF spectra, comprising 37 of blank areas and 67 of handwritten inks, were taken during this study. XRF measurements were performed in the NLI laboratories, during the conservation of the Almanac, when the book was in a disbound state and access to areas otherwise not accessible was possible. XRF spectra were obtained for each handwritten page of the book. In cases where paleographical analysis suggested a change of poem or ink, multiple XRF spectra were captured per page. XRF analysis was also conducted on the blank areas of the paper to evaluate the elemental composition of the underlying support.

The XRF spectra of blank paper support recorded across the volume showed similar elemental features, with only small variations in elemental peak intensities. A representative XRF spectrum of blank paper is shown in Figure 4a. It was characterized by the presence of silica (Si), phosphorus (P), sulfur (S), potassium (K), calcium (Ca), manganese (Mn), iron (Fe), copper (Cu), and zinc (Zn).

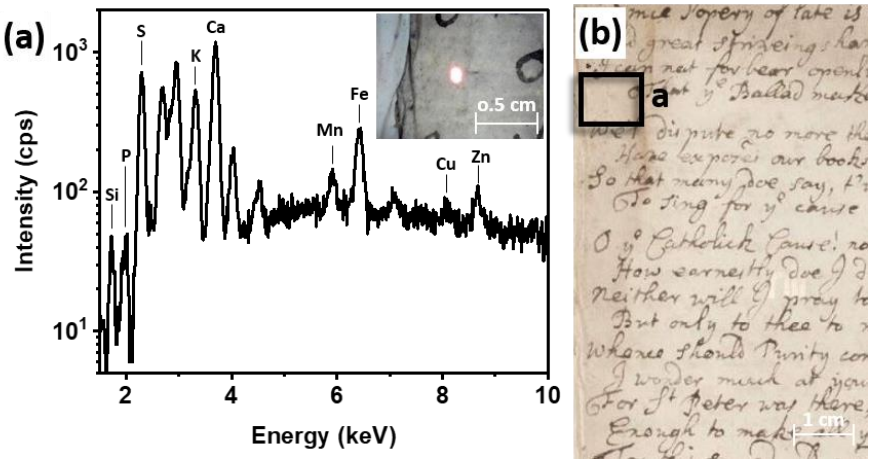

Figure 3.4. (a) XRF spectrum of blank paper taken at p. 79. Inset: microscopy image of the XRF illuminated area (bright spot) recorded with the internal camera of the XRF spectrometer; (b) photograph (detail) of the area where the XRF spectrum was taken, highlighted by the black box.

The presence of Ca was attributed to calcium-based compounds known to be used for inducing fermentation of rags. These could include lime (calcium hydroxide, $Ca(OH)_2$) or milk.[126] Considering the concomitant presence of S and Ca, gypsum ($CaSO_4$ x H_2O), a common ingredient used in paper making, could not be excluded. Ca could also be linked to the use of fillers such as calcium carbonate ($CaCO_3$), commonly employed in paper production.[126] The presence of S and K, often detected at similar or higher intensities than Ca, suggested the possible use of alum (potassium/aluminum sulfate, $KAl(SO_4)_2 \cdot 12H_2O$) liquor in the sizing of the paper. Records from the early 17th century indicate the addition of alum to gelatin size, as a preservative and stabilizer of the viscosity of the sizing liquor.[127] Additionally, alum salts were used to reduce the absorbency of the paper, by depositing in the interstices of paper fibers, leading to better writing performance.[21] Interestingly, alum-treated papers are more susceptible to ageing, due to the increased acidity, which leads to the degradation of cellulose through acid-catalyzed hydrolysis.[128] Calcium-based compounds were used, among other reasons, to counteract and neutralize the acidity of alum-treated paper, thereby providing a protective effect.[129] Accordingly, the most degraded and brittle leaves of the Almanac showed higher intensities of K compared to calcium Ca, in agreement with the observations above. It is important to note that the fragility of the water-damaged leaves may be attributed to both the higher K concentration and to the water-induced dissolution of the gelatin size, which served as a protective layer from environmental agents. Therefore, the weakening of the paper could potentially be a result of these combined

factors. Fe was observed in all recorded spectra and could be attributed to the presence of iron alum ($FeAl(SO_4)_2$ x $12H_2O$). Si was consistently detected though the book. The presence of Si in rag paper is reported in literature to be associated with the presence of straw, high in silicon dioxide (SiO_2).[130] Cu and Zn in minor concentrations were also identified in the XRF spectra. The presence of these elements could be related to the paper-production process, such as impurities from the water used for making the paper poultice or from contact with metallic tools – beater roll, mold, or press – employed during paper production.[126] Additionally, it is possible that these elements migrated from the printing and writing inks due to the extensive water damage observed.

In parallel with blank spots, spectra of handwritten text were taken. A representative XRF spectrum of an ink used for the handwriting is shown in Figure 5a.

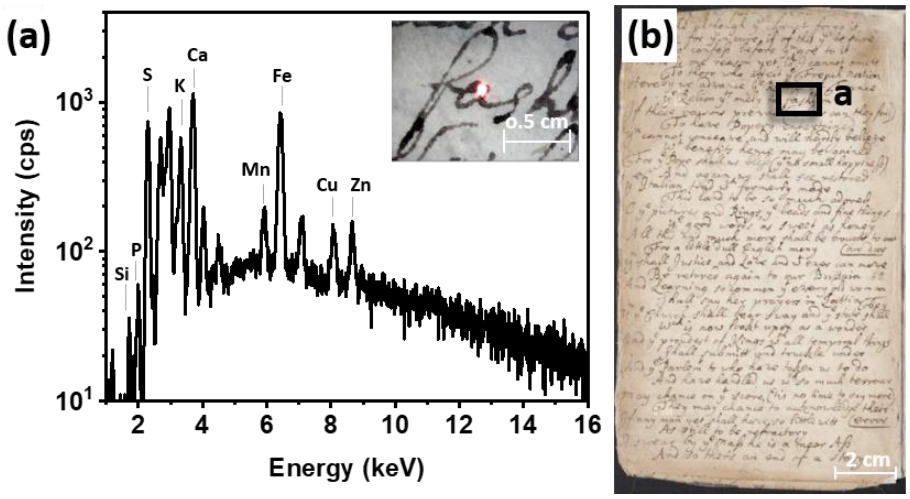

Figure 3.5. (a) XRF spectrum of an inked area, p. 82. Inset shows a microscopy picture of where the XRF spectrum was taken; (b) Photograph of p. 82. Black box shows the area of analysis.

The spectrum revealed the presence of several elements, including Si, P, K, Ca, Mn, Fe, Cu, and Zn. Si, P, and Mn were found at similar intensities in both the ink spectra and the paper spectra, suggesting that they were not diagnostic of the ink under analysis. On the other hand, S, K, Ca, Fe, Cu, and Zn exhibited higher peak intensities compared to the blank paper, indicating their association with the ink applications. The combination of S, Fe, Cu, and Zn suggests the presence of vitriol, a mixture of hydrated metal (Fe, Cu, and Zn) sulfates, associated with iron-based inks, one of the standard ink formulation extensively used in Europe between the 5th and 19th century.[26, 27, 28] These inks were obtained by combining vitriol with polyphenolic compounds such as tannic acid or gallic

acid. The reaction resulted in the formation of dark iron-polyphenol complexes, contributing to the distinctive dark color of iron-based ink.[119] The presence of K was attributed to the presence of gum arabic, commonly used in inks to improve viscosity and reduce bleeding.[80] It is worth noting that the presence of K may also be attributed to the presence of iron sulfate, as reported in studies on the chemical composition of iron-based inks.[30, 31] It was not possible to explain the increased Ca intensity in all the inked areas analysed. Further research and investigation is required to understand the reasons behind the increased Ca intensity in those particular areas.

The sequence in which the poems were inscribed: XRF analysis of three case studies

Following the general classification of writing inks as iron-based inks, a comprehensive qualitative elemental analysis was conducted on the spectra. The primary objective of this analysis was to explore the various composition of the writing inks, with a particular focus on the vitriol constituent elements. This examination aimed to find out whether evidence supports the order of poem insertion suggested by the historical analysis. Notably, previous studies have highlighted the significance of observing variations in content of Mn, Cu, and Zn (relative to Fe) in XRF spectra of inks. These ratios are specific to each vitriol source or extraction method,[80] which allows for the identification and classification of different inks.[32, 33. 34] Three case studies further illustrate these findings.

The **first case study** focused on the proposed starting point of the transcribed text, where the scribe filled pp. 77-88 and continued writing on interleaf p. 7. On p. 88 (Figure 6a), it was discernible that a horizontal line marked the conclusion of the poem “On Rome's Pardons by the E. of R.,” which circulated between 1675 and 1680, followed by the commencement of “On the Composeing of a Prayer for the Unborne Prince of Wales” (1688). XRF spectra collected for these two segments exhibited similar compositions (Figures 6b, c), particularly the ratio of Cu Kα and Zn Kα intensities (I_{Cu}/I_{Zn}), which was found to be ~1.2 for both spectra. This was observed also for all the previous pages (pp. 77-88), and suggested that these areas were likely penned using the same ink or inks of very similar composition.

The I_{Cu}/I_{Zn} of these spectra closely resembled the ratio obtained from the upper section of p. 7 (Figure 6e). This consistency in elemental composition of ink between page 88 and 7 supported historical and codicological data.

When examining p. 7 (Figure 6d), several differences between the text in the first and second half of the page became apparent. These differences included variations in color, thickness of the ink line, and size of writing. By comparing the elemental composition of these two sections (Figure 6e, f), a noticeable disparity was observed. The beginning of the poem "The Miracle" in the second half of p. 7 presented a I_{Cu}/I_{Zn} ratio of ~4.0, which is different from ~1.2 found in the previous sections (discussed above). These discrepancies strongly indicates that two different inks were used to write the first and second half of p. 7.

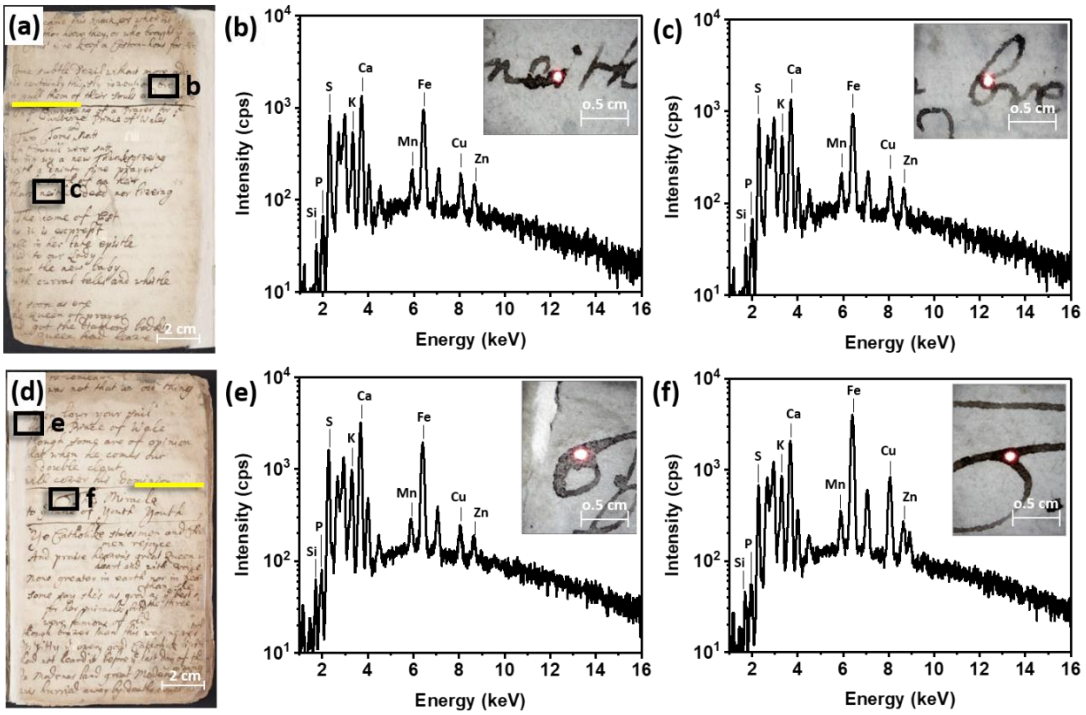

Figure 3.6. (a) Photograph of p. 88; (b) XRF spectrum of ink in poem "On Rome's Pardons by the E. of R." (1675-80) on p. 88; (c) XRF spectrum of ink in poem "On the Composeing of a Prayer for the Unborne Prince of Wales" (1688), p. 88; (d) Photograph of p. 7; (e) XRF spectrum of ink in poem "On the Composeing of a Prayer for the Unborne Prince of Wales" (1688), p. 7; (f) XRF spectrum of ink in poem "The Miracle" (1687), p. 7. In the photographs, the yellow line shows the break between the two different poems and the black boxes show where the XRF analysis was performed. The inset in the XRF spectra show a magnified image of the analyzed area.

The **second case study** was related to the phase of inscription spanning pp. 7 to 31. The codicological assessment did not uncover discernible features that would indicate a disruption or break in the writing process. However, XRF analysis revealed a

discontinuous elemental composition within the writing ink (see Figure 7). All these leaves presented a constant trace of Zn; therefore that element was not considered indicative of the ink applications. Figure 7b exhibits an XRF spectrum taken from the upper section of p. 17 (Figure 7a), demarcated by a horizontal line, following the conclusion of the poem “The Pacquet Boat Returned” (1688). The ink used for writing this poem contained ink diagnostic peaks corresponding to Fe, and Cu. In contrast, the XRF spectrum taken in the lower section of page 17 (Figure 7c), below the horizontal line, and featuring the poem titled “The Gentlemen at Larges Litany” (1692-93), was characterized by S and Fe only, indicating that a different ink was used for penning this section. What is apparently the same ink continued to be used until the completion of the poem titled “To the Tune of Chivie Chace" (1692-93) (first half of p. 24, see Figure 7e). In contrast, a new ink composition, featuring S, Fe and Cu, was observed in the second half of p. 24 in the “Mrs Butler to Mrs Bracegirdle” poem (from 1692-93, Figure 7f).

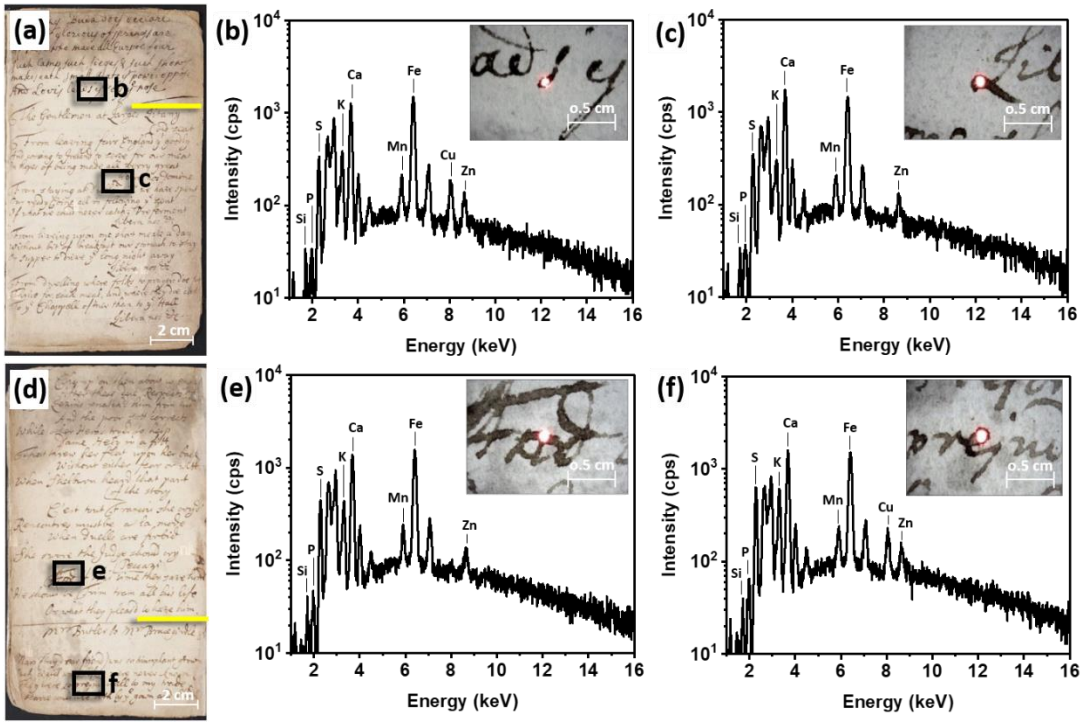

Figure 3.7. (a) Photograph of p. 17; (b) XRF spectrum of ink in poem “The Pacquet Boat Returned” (1688), p. 17; (c) XRF spectrum of ink in poem “The Gentlemen at Larges Litany”, (1692-93), p. 17; (d) Photograph of p. 24; (e) XRF spectrum of ink in poem “To the Tune of Chivie Chace” (1692-93), p. 24; (f) XRF spectrum of ink in the poem “Mrs Butler to Mrs Bracegirdle” (1692-93), p. 24. In the photographs, the yellow line shows the break between the two different poems and the black boxes show where the XRF analysis was performed. The inset in the XRF spectra show a magnified image of the analyzed area.

The **third case study** focused on the analysis of the most recent additions to the Almanac, dating from the end of the 17th to the early years of the 18th century. Specifically, the following poems were analyzed: “The Whiggs Lamentation. A Soar of Their Own Scratching”, dated 1711, pp. 39-51 (p. 41 in Figure 8a); “The Picture of a Dublin Beau”, from 1699, pp. 89-90 (p. 90 in Figure 8b); “A Fable, yet a True Story,” from 1700-01, pp. 90-91; “The Thanksgiving,” probably from 1709, p. 92 (Figure 8c).

In terms of ink composition, the XRF analysis of the ink on p. 41 (Figure 8d), which represents the inked areas of “The Whiggs Lamentation. A Soar of Their Own Scratching”, revealed the presence of only S and Fe. The high concentration of Zn was also detected in the XRF spectra of the unwritten paper, making it difficult to solely attribute it to the ink. Nonetheless, the consistency in ink composition throughout the poem on pp. 35-51 supports the findings of previous case studies, indicating that the writer likely used the same ink for each individual poem or small groups of these.

Pp. 89-90-91, compared with pp. 39-51, show variations in color, thickness of the ink line, and size of writing. No noticeable differences were observed in their ink elemental fingerprint. Once again, the ink in that section (pp. 89-90-91) was characterized by the presence of S and Fe, with Zn being ascribable to the paper content (see representative XRF spectrum in Figure 8f). However, it is important to note that the chemical composition of the ink in p. 92 (Figure 8g) has shown discontinuity from the previous short poems in pp. 89-90-91, displaying traces of Cu and lead (Pb). This suggests that a different ink may have been used for the poem “The Thanksgiving.”

In summary, the performed XRF analysis showed that different types of inks were used to compile the poems. Based on the available information, it is likely that all these short poems were written sequentially, roughly adhering to a chronological order. However, they were likely transcribed in several stints, a new stint sometimes entailing a different ink. This suggests a pattern of writing and compilation that deviates from a continuous, uninterrupted flow, and rather follows a periodic grouping approach with a variety of inks over time.

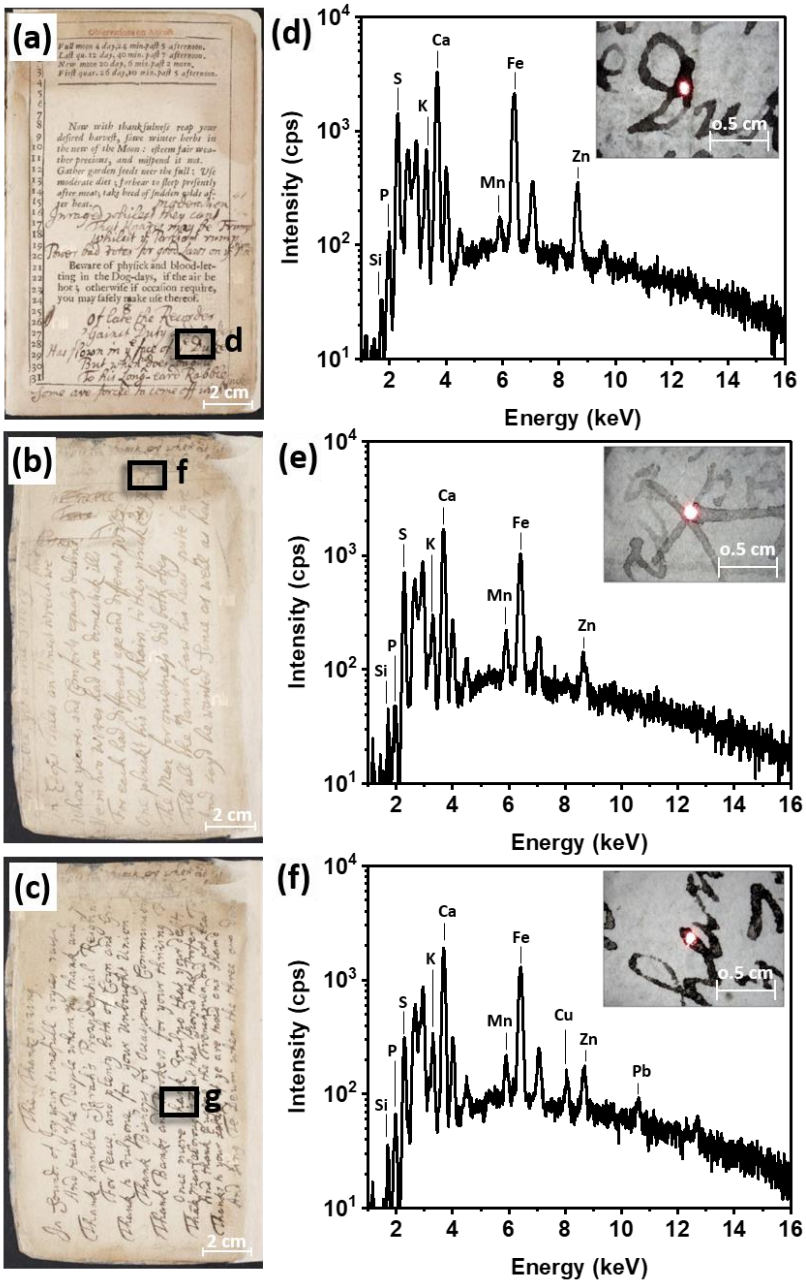

Figure 3.8. Photograph of (a) p. 41, (b) p. 90, and (c) p. 92; (d) XRF spectrum of ink in "The Whiggs Lamentation. A Soar of Their Own Scratching", p.41; (e) XRF spectrum of ink in "The Picture of a Dublin Beau", p 90; (f) XRF spectrum of ink in "The Thanksgiving.". The black boxes in the photographs show where the XRF analysis was performed. The inset in the XRF spectra show a magnified image of the analyzed area.

XRF quantification and statistical analysis

The quantification of elements present in the XRF spectra of both blank paper and inked areas was obtained using the FP algorithm integrated in the PyMca software.[64] This approach facilitated the extraction of quantitative values for the identified elements (Si, P, Cl, S, K, Ca, Mn, Fe, Cu, and Zn) in each recorded spectrum. To account for the inherent variability resulting from the heterogeneity of ink applications and paper substrate, and to enable easier comparison between spectra, it was decided to express elemental concentrations relative to Fe.

Compared to other popular clustering techniques, such as K-means,[136] SOM was selected for its ability to identify non-linear relationships between the samples, as it uses a neural network approach that can capture and represent complex data structures in a lower-dimensional space while preserving the main features of the original data. This capability was well-suited for the three case studies, as the variability of elemental peak intensities, relative to each other in various analysis spots, is influenced by multiple factors including composition, acquisition geometry, and thickness of the analysed ink.

In the context of XRF data analysis, SOM maps took the form of a 2D grid-like structure consisting of neurons. Each neuron represented a specific location in the map, and its weight vector corresponded to the elemental composition associated with that neuron. The statistical analysis pipeline began with feature extraction using Principal Component Analysis (PCA) on a dataset of 54 selected XRF spots, which identified Cu and Zn as the main chemical elements explaining the majority of the variance. This result was expected, as these two elements were already used in prior qualitative analysis as representatives of the vitriol sources. The elemental concentrations of Cu and Zn were then used to iteratively adjust the weights of the neurons during the training phase, which employed the Kohonen algorithm. This adjustment process involved computing the similarity of concentrations (W_{Cu}/W_{Fe} and W_{Zn}/W_{Fe}) to the weight vectors associated with each neuron, with the goal of capturing and organizing the elemental composition patterns of the samples.

The clustering in Figure 9 depicts four groupings, indicated by different colors, broadly representing four classes of inks. The green dots represent inks with a medium content of Cu and a high concentration of Zn ($W_{Zn}/W_{Fe} > W_{Cu}/W_{Fe}$), while the purple dots represent inks with a high content of Cu and medium content of Zn ($W_{Cu}/W_{Fe} > W_{Zn}/W_{Fe}$).

The solid-line circle encompasses these two clusters as they make up the majority of the analyzed inks in the poems written during the early stage of the transcription. These satiric verses date from 1674 to 1692-93 (pp. 77-88, 7-17, 24-31, previously approached in case study 1). On the other hand, the dash-line circle groups the majority of analyzed areas from poems written from 1699 to 1711 (pp. 39-51 and pp. 89-92; case study 3). Within this area, the algorithm recognized two groups: one comprising inked areas with low concentration of both Cu and Zn ($W_{Cu}/W_{Fe} \approx W_{Zn}/W_{Fe}$, represented by red dots), and another group with low content of Cu and high concentration of Zn ($W_{Cu}/W_{Fe} < W_{Zn}/W_{Fe}$, represented by blue dots). Interestingly, the spots representing the ink analyzed in case study 2 (pp. 17-24) were scattered outside the outlined circles. The findings from the analysis provided evidence supporting the reliability of SOM maps as a robust method for the initial categorization of data on elemental concentration of inks. It is important to note that when a larger amount of data is incorporated into the SOM maps, they are even more dependable for effectively organizing and categorizing complex datasets. While this approach was applied to Harward's Almanac only, it is expected to be tested on larger datasets which comprise thousands of XRF spectra of ink.

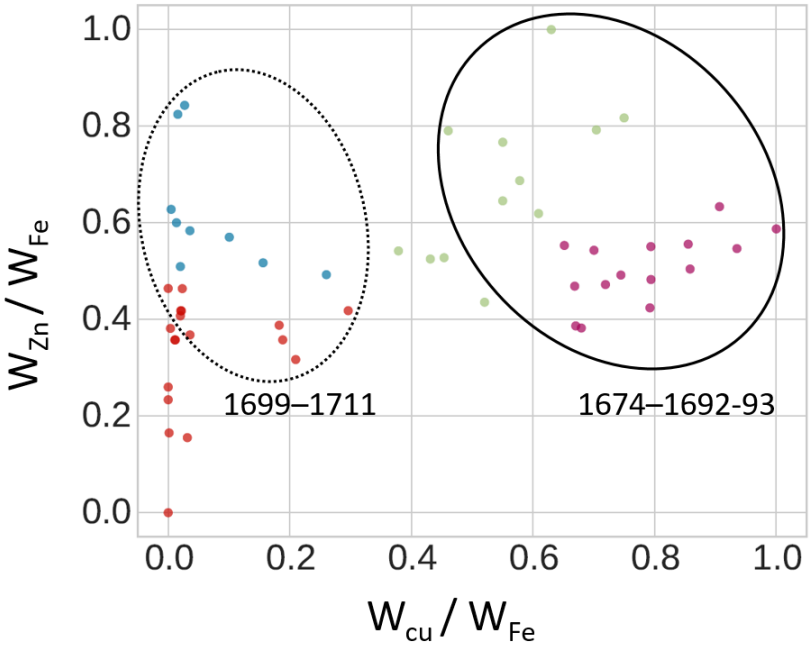

Figure 3.9. 2x2 SOM-based clustering showing the date of composition of the poems.

3.4 Conclusion

We have presented a transdisciplinary approach to the investigation of Harward's Almanac, an Irish almanac of extreme rarity preserving important and, in some cases, unique texts of late 17th-century Irish poems. The investigation was conducted while the book was in a disbound state during conservation. This allowed historians to gain unique insight into the book's manufacture, its subsequent binding and rebinding, and the reordering of the leaves as well as to formulate a hypothesis on the original order of the poems' entry. The complementary XRF analysis performed on each handwritten page was key to confirming the validity of the historical hypotheses on the poems' inscription and dating based on codicological and paleographic investigation. Finally, statistical analysis of all XRF data allowed the identification of four classes of iron-based inks, based on variable quantities of Cu and Zn. The statistical clustering allowed easy bi-dimensional visualization of all collected XRF data and provided further insights into ink similarities, which could be associated with date of circulation.

3.5 Experimental

X-ray fluorescence spectroscopy (XRF)

XRF was performed with a portable, energy-dispersive XRF ELIO (XGLab, srl). The spectrometer was equipped with a Peltier-cooled Silicon Drift Detector with a resolution of 135 eV at the manganese (Mn) Kα line (5.9 keV). The excitation source was a low-power (4 W, 50 kV), transmission X-ray tube with a Rh anode. Measurements were performed with no filter, under air atmosphere in a range 1 – 25 kV. The tube current was kept at 160 μA. A collimator, allowing a ~1 mm diameter focused spot size on the surface of the pages, was used to acquire XRF spectra. The distance from the folio was ~1 cm and the acquisition time was 120 sec. A semi-quantitative approach to the XRF data was performed using the open-source software PyMca. The so-applied fundamental parameter method (FPM) allowed estimating elements' concentration based on observed peak intensities. The elemental concentrations of the blank paper areas were subtracted from the ones in inked areas.

Semi-quantitative XRF analysis using fundamental parameter (FP)

In order to discriminate writing inks and identify manuscript passages containing inks of similar elemental composition, a standardless semi-quantitative approach was applied to the XRF spectra. The conversion of peak intensities to elemental concentration was obtained by applying a FP approach to spectral analysis using the open-source software PyMca. The XRF spectrometer was fully characterized elsewhere, and a configuration file for data processing via PyMca was provided to the authors.[64] The fit parameters were tailored based on the experimental parameters. After having ensured proper fitting for every spectrum, the "batch fitting" and the "RGB correlator" tools were

used in order to batch fit the spectra and to find relative ratios of elements. For better comparison, all XRF data were normalized with respect to Fe K (not separating Kα and Kβ lines).

SOM-based clustering

In the analysis, all the characteristic elements in inked areas were subjected to initial analysis using SOM clustering. However, for the final clustering, only the relative concentrations (in relation to Fe) of trace elements Cu and Zn were considered, as these were considered significant to obtain ink distinction. The analysis was conducted using Google Colab with Python 3.10. The Pandas package was utilized for data handling and pre-processing, while Scikit-learn was employed for machine learning and data reduction implementations. The SOM clustering algorithm was implemented using the MiniSom package, and visualizations were generated using Matplotlib. To ensure reproducibility, the code used in the analysis has been made freely available.[137]

3.6 References

1. M. Harward, A new almanack for the year of our Lord, 1666 : Being the second after bissextil or leap year, and from the creation of the world, 5615 ... Dublin: Printed by John Crook, printer to the kings most excellent majesty, and are to be sold by Samuel Dancer bookseller in Castle-street, 1666. NLI MS 42,680.

2. J. Woolley and S. Karian (eds), The Cambridge Edition of the Works of Jonathan Swift, vols. 3-6 (Poems). Cambridge: Cambridge University Press, (forthcoming).

3. Stephen Gwynn, A Manuscript Assigned to Swift. The Athenaeum, no. 3605, 1896. [Online]. Available: https://archive.org/details/sim_athenaeum-uk_1896-11-28_3605

4. H. Williams (ed.), The poems of Jonathan Swift. Oxford: Clarendon Press, , 1937. vol. 3, pp. 1058-68, 1071-72, 1075-77, 1083-84.

5. J. Woolley, "The circulation of verse in Jonathan Swift's Dublin," Eighteenth-Century Irel. Iris an udá chultúr, vol. 32, pp. 136–150, 2017.

6. C. Luízar Obregón, M. A. Zamalloa Jara, F. L. Rojas Arizapana, Y. J. Chura Huayllani, J. F. Gonzales Bellido, and J. Olivera Olivera, "XRF elemental analysis of inks in South American manuscripts from 1779 to 1825," Herit. Sci., vol. 9, no. 1, p. 147, Nov. 2021, doi: 10.1186/s40494-021-00619-9.

7. O. Hahn, "Analyses of Iron Gall and Carbon Inks by Means of X-ray Fluorescence Analysis: A Non-Destructive Approach in the Field of Archaeometry and Conservation Science," Restaur.-Int. J. Preserv. Libr. Arch. Mater. - Restaur., vol. 31, pp. 41–64, Jan. 2010, doi: 10.1515/rest.2010.003.

8. O. Hahn, B. Kanngießer, and W. Malzer, “X-ray Fluorescence Analysis of Iron Gall Inks, Pencils and Coloured Crayons,” Stud. Conserv., vol. 50, pp. 23–32, Jan. 2005, doi: 10.1179/sic.2005.50.1.23.

9. G. Nehring, “Writing and Correcting a Torah Scroll in Germany of the Thirteenth and Fourteenth Centuries,” 2021.

10. G. Nehring, N. Gordon, and I. Rabin, “Distinguishing between seemingly identical inks using scanning μXRF and heat maps,” J. Cult. Herit., vol. 57, pp. 142–148, Sep. 2022, doi: 10.1016/j.culher.2022.07.007.

11. I. Szalóki, D. G. Lewis, C. A. Bennett, and A. Kilic, “Application of the fundamental parameter method to the in vivo x-ray fluorescence analysis of Pt,” Phys. Med. Biol., vol. 44, no. 5, pp. 1245–1255, May 1999, doi: 10.1088/0031-9155/44/5/012.

12. J. Kawai, K. Yamasaki, and R. Tanaka, “Fundamental Parameter Method in X-Ray Fluorescence Analysis,” in Encyclopedia of Analytical Chemistry, John Wiley & Sons, Ltd, 2019, pp. 1–14. doi: 10.1002/9780470027318.a9666.

13. M. M. Van Hulle, “Self-organizing Maps,” in Handbook of Natural Computing, G. Rozenberg, T. Bäck, and J. N. Kok, eds., Berlin, Heidelberg: Springer, 2012, pp. 585–622. doi: 10.1007/978-3-540-92910-9_19.

14. S.-G. Lee and E.-Y. Cha, “Style classification and visualization of art painting’s genre using self-organizing maps,” Hum.-Centric Comput. Inf. Sci., vol. 6, no. 1, p. 7, Jun. 2016, doi: 10.1186/s13673-016-0063-4.

15. K. Kadokura and Y. Osana, “Image (Artwork) Retrieval based on Similarity of Touch by Self-Organizing Map with Refractoriness”.

16. V. A. Solé, E. Papillon, M. Cotte, Ph. Walter, and J. Susini, “A multiplatform code for the analysis of energy-dispersive X-ray fluorescence spectra,” Spectrochim. Acta Part B At. Spectrosc., vol. 62, no. 1, pp. 63–68, Jan. 2007, doi: 10.1016/j.sab.2006.12.002.

17. A. Rossi, A. Visentin, and V. Biolcati, “Code used in the analysis of the elemental concenration value of inks.” https://bit.ly/almanac-inkandskin

18. D. Hunter, Papermaking: the history and technique of an ancient craft. New York: Dover Publications, 1978. Accessed: May 02, 2023. [Online]. Available: http://catdir.loc.gov/catdir/enhancements/fy0707/77092477-d.html

19. P. Ó. Macháin, Paper and the Paper Manuscript: A Context for the Transmission of Gaelic Literature. Published by Cló Torna, Department of Modern Irish, University College Cork, 2019.

20. Mosser, Daniel W., Sullivan, Ernest W., Hatfield, Len, and Radcliffe, David H., “The Thomas L. Gravell Watermark Archive. 1996.” https://memoryofpaper.eu/gravell/ (accessed Jul. 17, 2022).

21. Permanence/Durability of the Book—VII. Physical and Chemical Properties of Book Papers, 1507-1949. Richmond: W. J. Barrow Research Laboratory, 1974.

22. E. J. Labarre, Dictionary and Encyclopaedia of Paper and Paper- Making. Oxford University Press, 1952.

23. M. Jablonský and J. Šima, “Stability of Alum-Containing Paper under Alkaline Conditions,” Molecules, vol. 25, no. 24, p. 5815, Dec. 2020, doi: 10.3390/molecules25245815.

24. E. L. Graminski and E. J. Parks, “The Effect of Calcium Carbonate on the Stability of Acid Treated Papers,” J. Res. Natl. Bur. Stand., vol. 86, no. 3, pp. 309–315, 1981, doi: 10.6028/jres.086.012.

25. A. Dragojević, D. Gregor-Svetec, J. Vodopivec Tomažič, and B. Lozo, “Characterization of seventeenth century papers from Valvasor’s collection of the Zagreb Archdiocese,” Herit. Sci., vol. 9, no. 1, p. 35, Mar. 2021, doi: 10.1186/s40494-021-00507-2.

26. R. J. Díaz Hidalgo et al., “New insights into iron-gall inks through the use of historically accurate reconstructions,” Herit. Sci., vol. 6, no. 1, p. 63, Dec. 2018, doi: 10.1186/s40494-018-0228-8.

27. V. Corregidor, R. Viegas, L. M. Ferreira, and L. C. Alves, “Study of Iron Gall Inks, Ingredients and Paper Composition Using Non-Destructive Techniques,” Heritage, vol. 2, no. 4, pp. 2691–2703, Sep. 2019, doi: 10.3390/heritage2040166.

28. M. J. Melo et al., “Iron-gall inks: a review of their degradation mechanisms and conservation treatments,” Herit. Sci., vol. 10, no. 1, p. 145, Sep. 2022, doi: 10.1186/s40494-022-00779-2.

29. C. Krekel, “The chemistry of historical iron gall inks: understanding the chemistry of writing inks used to prepare historical documents,” 1999. Accessed: Jul. 17, 2023. [Online]. Available: https://www.semanticscholar.org/paper/The-chemistry-of-historical-iron-gall-inks%3A-the-of-Krekel/c5bae6e449a9ab22380a48ff6fa7e7aa9f8514ca

30. G. Fichera et al., “Study of the copper effect in iron-gall inks after artificial ageing,” Chem. Pap., vol. 72, Feb. 2018, doi: 10.1007/s11696-018-0412-z.

31. C. Colini et al., “The Quest for the Mixed Inks,” Christ. Brockmann Oliver Hahn Volker Märgner Ira Rabin H Siegfried Stiehl Eds Proc. Second Int. Conf. Nat. Sci. Technol. Manuscr. Anal. Manuscr. Cult. 11 2018 41-48, Jan. 2018, Accessed: Feb. 09, 2022. [Online]. Available: https://www.academia.edu/38120349/The_Quest_for_the_Mixed_Inks

32. O. Hahn, W. Malzer, B. Kanngiesser, and B. Beckhoff, “Characterization of iron-gall inks in historical manuscripts and music compositions using x-ray fluorescence spectrometry,” X-Ray Spectrom., vol. 33, no. 4, pp. 234–239, 2004, doi: https://doi.org/10.1002/xrs.677.

33. I. Rabin, “Material Studies of Historic Inks: Transition from Carbon to Iron-Gall Inks,” in Traces of Ink, Brill, 2021, pp. 70–78. doi: 10.1163/9789004444805_006.

34. I. Rabin et al., “Identification and classification of historical writing inks in spectroscopy: a methodological overview,” Jan. 2012, doi: 10.25592/uhhfdm.509.

35. X. Jin and J. Han, “K-Means Clustering,” in Encyclopedia of Machine Learning and Data Mining, C. Sammut and G. I. Webb, Eds., Boston, MA: Springer US, 2017, pp. 695–697. doi: 10.1007/978-1-4899-7687-1_431.

3.7 Supporting information

Details of the reordering of the pages from codicological studies

Detailed observation of the pages enabled the recording of several characteristics about the prior reordering of the pages. An interleaf, formerly conjugate with pp. 43-44, is missing (apparently torn out), though its spine fold, along with some handwriting, was visible when the volume was disbound for conservation. The poem on pp. 39-51 (with catchword on p. 44 leading to p. 49) is complete. When the pages were hand-numbered, the part-title to the second printed section, entitled "A Prognostication for the Year of Our Lord God 1666," was mistakenly numbered 1-2 and evidently placed ahead of the actual title page, which is numbered 3-4. Leaf C1, evidently loose, was turned the wrong way and numbered 60-59. Leaf C7 was mislocated and numbered 63-64. These errors were corrected in the 19th-century rebinding. By that time, or perhaps later, leaf C8 was lost. The catchword "*From*" leading to C8 remains at the foot of leaf C7v. This lost leaf, which almost certainly ended the Almanac, was the conclusion of the section entitled "The High-Wayes of Ireland." The interleaf bifolium consisting of pp. 7-8 and 29-30 once stood between pp. 4-5 and 32-33 (as shown in Figure S3), that is, not in its 19th-century position between *A*2-3 and *A*6-7 but between *A*1-2 and *A*7-8. Evidence of this is of two kinds. First, the lines of "The Duel between 2 Phisitians" are in the wrong order when the 29-30 interleaf is misplaced in its 19th-century position but in the correct order if it is moved to follow p. 32, as is readily seen from comparison of the Almanac text with that published in *The Counter-Scuffle* (Dublin: E. Waters for M. Gunne, 1708), sig. B7r-v (copy in Boston College library). Second, when the interleaf is moved to the correct position, ink from the interleaf is mirrored in offset on facing pages of the printed Almanac. For example, Figure S1a,b shows photos of pp. 6 and 9 side by side. It can be noticed that

several ink spots in the inner margin of p. 6 are offset from areas of heavy ink on the facing manuscript interleaf, p. 9 on the printed page (see detail in Figure S1c). In order for the ink spots on p. 6 to mirror the accumulated ink on p. 9, there would have to have been some give in the binding, or the page may have been loose, allowing the interleaf to slip up and down relative to the printed leaf. Such looseness may explain why the edges of leaves in the book are often tattered. The structure was simply not securely held together with thread, even as early as the inscription of p. 9.

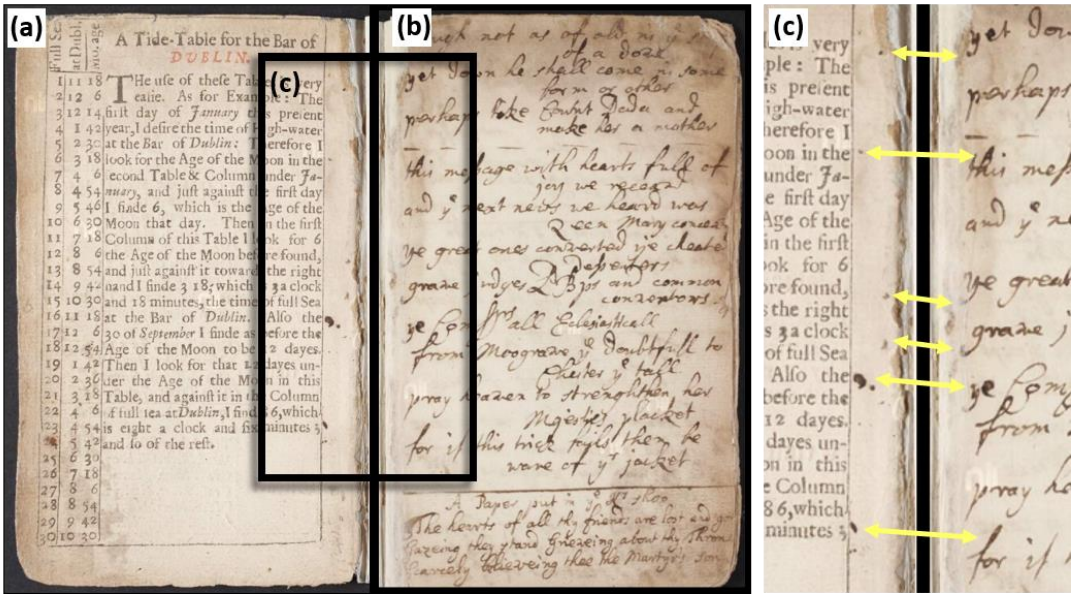

Figure B1. (a-b) Pre-conservation photographs of pp. 6 and 9; white box represents the location of the detail in (c); (c) Detail of the inner margins of pp. 6 and 9, side by side, showing the slight offset of the ink stains from the manuscript (p. 9, right) onto the printed page (p. 6, left). Yellow arrows indicates areas of ink offset.

Placing photos of pp. 32 and 29 side by side appears to reveal several small instances of ink offset from 29 onto 32 (see Figure S2). In the gutter of 32 opposite the lines for 21 and 26 May, there are spots of brown ink that appear to match the excess ink on the capital F of "For," 6 lines from the bottom of p. 29, and the excess ink of the capital T of "Tother," 3 lines from the bottom of 29. A small spot of brown ink in the outer margin of 32 against 30 May probably is a vestige of the completion of the last word on 29, the last letter or letters of which are now lost ("sh—t" or "sh—te"). In order for the ink spot between lines 6 and 7 of p. 32 to mirror the accumulated ink on the "d" of "passd" on p. 29, there would have to have been some play in the binding, allowing the interleaf to slip up and down relative to the printed leaf. In the 19th-century rebinding, the last leaf

(pp. 94, 93) was turned over, reversing the original numberer's sense of which side came first. An undetermined number of the final blank leaves following the last printed leaf C8 have disappeared, along with the missing C8.

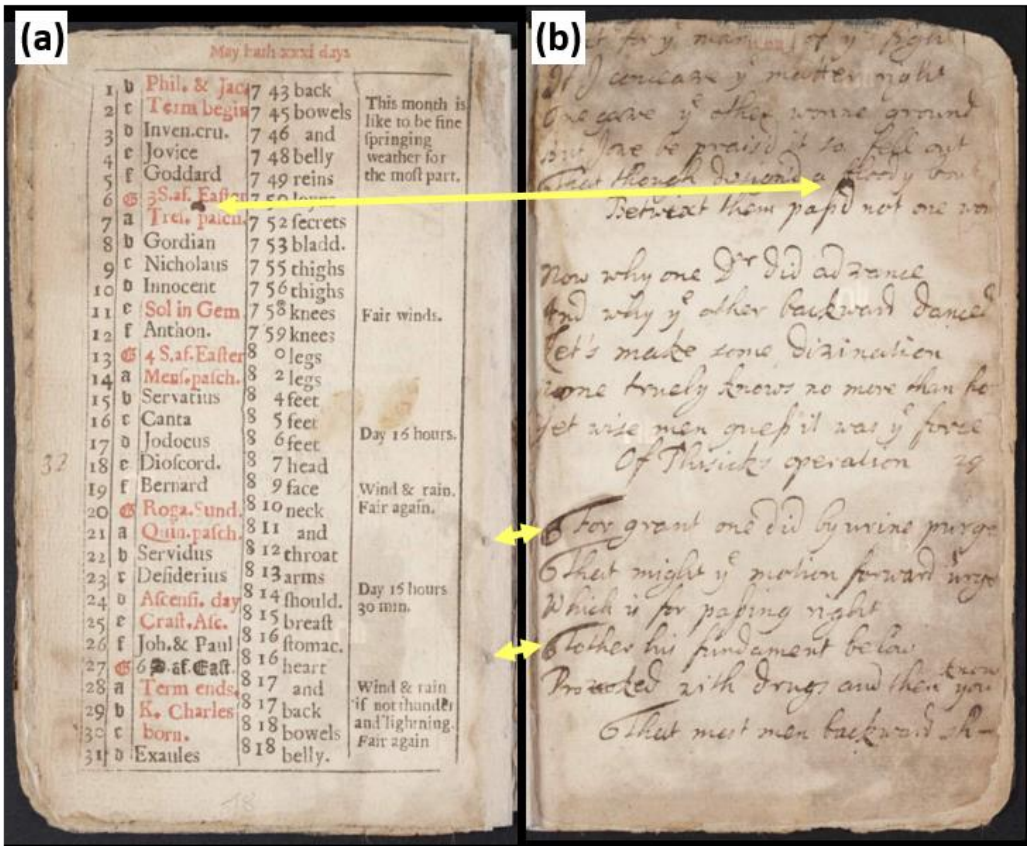

Figure B2. (a) Photograph of p. 32; (b) photograph of p. 29. Yellow arrows indicates areas of ink offset.

Structure of the book, with leaves in their pre-19th-century order

Table B1. The sometimes incorrect hand-numbering of the pages perhaps occurred in the late 18th or early 19th century. That mistaken ordering of the pages was the understandable consequence of wear and tear, loose and failing stitching, and the detaching and faulty relocation of several leaves or bifolia. Some of the mistakes were corrected for the 19th-century rebinding. In the table below, two additional ordering revisions are noted on the basis of the present investigation:

- the pages erroneously numbered 7-8 are correctly placed between pp. 4 and 5; and
- the pages erroneously numbered 29-30 are correctly placed between pp. 32 and 33.

The printed elements of the Almanac form three gatherings: the first (notionally *A*) is unsigned, the second signed "B," and the third "C." Page numbers use the handwritten pagination. Cells containing handwriting are highlighted in light gray.

Table 2 Table BI Structure of the book, with leaves in their pre-19th-century order

Leaf	**Page**	**Topic or title (portions on blank leaves are in *italics*)**
*A*1	3	[Title page]
	4	Woodcut relating parts of the body to signs of the Zodiac
	7	*On Rome's Pardons by the E. of R.* (1675-80) [continued from p.88]
	7-8	*The Miracle* (1687)
*A*2	5	A Note to Know When the Four [law] Terms Begin and End
	6	Tide-Table for the Bar of Dublin
	9	*The Miracle* [continued from p. 8]
	9-10	*A Paper Put in the K's Shoo* (1687?)
	10	*A Paper Found on the K's Twallite* [*toilette*] (1685-88)
	10	*To the P of Orange: A Pacquet of Advice* (1688)
*A*3	11	A Table Whereby to Know the Age of the Moon
	12	January hath xxxi days
	13	*To the P of Orange: A Pacquet of Advice* [continued from p. 10]
	14	*The Pacquet Boat Returned* (1688)
*A*4	15	Observations on January
	16	February hath xxvii days
	17	*The Pacquet Boat Returned* (1688) [continued from p. 14]
	17-19	*The Gentlemen at Larges Litany* (1692-93?)
	19-20	*To the Tune of Chivie Chace* (1692-93)
*A*5	21	Observations on February
	22	March hath xxxi days
	23-24	*To the Tune of Chivie Chace* [continued from p. 20]
	24-25	*Mrs Butler to Mrs Bracegirdle* (1692-93?)
*A*6	25	Observations on March
	26	April hath xxx days
	27	*Mrs Butler to Mrs Bracegirdle* [continued from p. 25]
	27-28	*The Duel between 2 Phisitians* (1693)
*A*7	31	Observations on April
	32	May hath xxxi days
	29-30	*The Duel between 2 Phisitians* [continued from p. 28]
	30	*A Pascall* [*pasquil*] *Lately Come from France* (1696)
*A*8	33	Observations on May
	34	June hath xxx days

B1	35 36	Observations on June July hath xxxi days
B2	37 38	Observations on July August hath xxxi days
	39-40	*The Whiggs Lamentation. A Soar of Their Own Scratching* (1711)
B3	41 41 42	*The Whiggs Lamentation* [continued from p. 40] Observations on August September hath xxx days
	43-44	*The Whiggs Lamentation* [continued from p. 41]
	--	[*interleaf deleted before pages were numbered*]
B4	45 46	Observations on September October hath xxxi days
B5	47 48	Observations on October November hath xxx days
	49-51 52	*The Whiggs Lamentation* [continued from p. 44] [*blank*]
B6	53 54	Observations on November December hath xxxi days
	55-56	[*blank interleaf*]
B7	57 58	Observations on December Upon the Year, 1666 [poem]
B8	1 2	Part title to "A Prognostication for the Year of Our Lord God 1666" Of the Four Quarters of the Year (catchword to C1)
C1	"60" [59] "59" [60]	Of the Eclipses this presen[t] year 1666 (catchword to C1v) The Principal Fairs of Ireland
C2	61-62	The Principal Fairs of Ireland [continued]
C3	65-66	The Principal Fairs of Ireland [continued]
C4	67-68	The Principal Fairs of Ireland [continued]
C5	69-70	Fairs That Are upon Moveable Feasts
C6	71-72	The High-Wayes of Ireland
C7	63-64	The High-Wayes of Ireland [continued]; formerly placed after C2. C7v catchword ("*From*") to C8, which is missing
C8		[missing; presumably C8 was the final printed leaf of the Almanac]
	73-74	[*financial jottings*]
	75-76	[*financial jottings* + *blank*]
	77-78	*Upon Nothing by y*[*e Earl o*]*f Ro*[*chester*] (1678)
	79-82	*The Catholique Ballad or An Invitation to Popery* (1674)
	83-87	*Room for a Ballad, or A Ballad for Rome* (1675-80)
	87-88 88	*On Rome's Pardons by the E. of R.* (1675-80) *On y*^{e} *Composeing of a Prayer for y*^{e} *Unborne Prince of Wales* [continuing to p.7]
	89-90	[*The Picture of a Dublin Beau*] (1699), title and first two lines lost

	90-91	*A Fable, yet a True Story* (1700-01)
	92	*The Thanksgiving* (1709?)
	--	[*leaf or leaves missing before pages were numbered*]
	"94" [93] "93" [94]	[*financial jottings*] *List of "those he stood sponser for" ("he" presumably being the compiler)*

4. X-Ray Fluorescence analysis of three late medieval silver chalices associated with Ireland

---

As submitted to Journal of Cultural Heritage:

Author list: Veronica Biolcati, Richard Keyes McDonnell, Anna Grace Hoffmann, Pádraig Ó Macháin, Małgorzata Krasnodębska-D'Aughton, Daniela Iacopino

Title: X-Ray Fluorescence analysis of three late medieval silver chalices associated with Ireland

4.1 Abstract

This paper presents the results of the first X-ray fluorescence (XRF) investigation conducted on three late medieval chalices associated with Ireland: the Ó Learghusa chalice, auctioned as medieval Irish in 2021, does not have a confirmed provenance; the de Burgo-O'Malley chalice, dated 1494, and the TP-IEP chalice, dated 1589, both of Irish provenance. The analysis revealed that both the Ó Learghusa and de Burgo-O'Malley chalices were crafted from a silver-copper alloy and adorned using a fire-gilding technique. The blue and green enamels on the de Burgo-O'Malley chalice were found to be constituted by cobalt and iron/copper glasses, respectively. In contrast, the TP-IEP chalice exhibited a more intricate structure, being a composite object with partial silver gilt and with the bowl and base made of a ternary silver-copper-gold alloy. The TP-IEP chalice's knop displayed glass, simulating gems with transparent, blue, and purple colorations. XRF analysis allowed identification of lead-potash glass, while the red glass displayed a rich iron content and was identified as soda-lime glass. The analysis allowed concluding that the de Burgo-O'Malley chalice had retained its original condition, including its original gilding and enamels, while the Ó Learghusa and TP-IEP chalices appeared to have undergone refurbishment. These significant discoveries contribute to a deeper understanding of the historical context and artistic craftsmanship behind these late medieval chalices, shedding light on their unique stories within Irish art and history.

4.2 Introduction

Chalices played a key role in medieval liturgy and were requisites for the celebration of the Eucharist, as they contained consecrated wine, which together with the host, represented the real presence of Christ's blood and body on the altar.[138] Early Christian chalices were made of various materials, including glass and bronze. However, by the late eighth century, the western Church stipulated that sacred liturgical objects be made of gold (Au) and silver (Ag), because Christ's blood and body should only be contained within objects created of the most precious materials.[139] These liturgical objects were often composed of a copper–silver (Cu-Ag) alloy as base metal. Cu was added to Ag for increasing the strength and wear resistance of the alloy.[140] For aesthetic reasons, and to add preciousness, chalices' metal surface was overlaid with an Au layer, a process called gilding. Among various procedures, fire-gilding was the most popular technique in the middle ages. It consisted in the application of a paste of Au powder in liquid mercury (Hg), followed by firing of the artifact at high temperature to induce the evaporation of Hg and leaving a solid layer of Au behind.[141], [142] As the choice of chalice materials changed over the centuries – from glass to precious metals – so did the shape of these objects. Early medieval chalices with a wide bowl, a short stem and a circular foot gave way to later medieval chalices with a narrower bowl, a slender stem, a bulbous knop and a polygonal foot, usually hexagonal or octagonal.[143]

XRF has been extensively applied to the characterization and investigation of historical metal alloys, whereby it was shown of key importance to support hypotheses regarding manufacturing techniques, contemporaneity of the production of various components within the object, later additions, and conservation interventions.[86], [144]–[147] Advantages of XRF include speed of analysis, no requirements for sample

preparation, non-invasiveness, capability to return a precise elemental composition with an approximation of the relative concentrations of constituent elements, also in traces.[91], [148]

To date, no chalice of proven Irish provenance and date has been subjected to XRF analysis. As a result, no data regarding the elemental composition of liturgical artifacts produced in late medieval Ireland is available. The absence of such information severely limits the understanding of the materials and techniques employed in crafting chalices during that historical period in Ireland. The primary objective of the presented work was to fill this gap by the investigation of three chalices performed through a complementary approach which combined stylistic and historical information with an in-depth study of materials and manufacturing techniques. Therefore, following historical analysis, the composition of the chalices metal alloy, the gilding layer, and the enamels and glass (where present), were investigated by XRF. The qualitative examination of XRF data lead to highly valuable insights into the choice and use of materials and manufacturing techniques. For instance, the analysis of minor and trace elements of the chalices provided insights into the specific raw materials employed in the alloying process. These elements served as indicators of the sources of ore used.[147]

4.3 Results and discussion

Comparative stylistic analysis of analyzed chalices

Figure 1 shows photographs of the three chalices analyzed in this work. The Ó Learghusa chalice (1a), named as such for the purpose of this paper to reflect the family connection of its last owner. This chalice, auctioned in 2021 by Duke's Auctioneers in Dorchester, was described in the auction catalog as "an exceptionally rare Irish silver gilt chalice, circa 1480". The absence of any inscriptions or hallmarks posed a challenge in assigning a specific provenance or date. The de Burgo-O'Malley chalice (1b), is a gilded chalice with enamels, securely dated to the late fifteenth century. It was probably produced in Galway for the Dominican priory at Burrishoole, Co. Mayo.[149] The inscription at the base identified Thomas de Burgo and Grainne O'Malley as its donors and provides the date of 1494.[150] The third chalice analyzed was the Irish TP-IEP chalice dated by the inscription to 1589 (1c). It was a gilded chalice embellished with colored glass on the knop. Its donors may be identified as Thomas Purcell and his wife Joanna Fitzpatrick.[151] One facet of the foot beard the image of the Paschal Lamb with a cross.[150]

The Ó Learghusa, the de Burgo, and the TP-IEP chalices have been chosen for this study for the similarity of some of their stylistic features. For instance, lozenge designs, one of the common features of Gothic chalices, appear on all three chalices analyzed (see detailed descriptions in SI). Such designs also featured on late medieval chalices made across continental Europe, for example, in Germany, the Low Countries and Poland, and were present on pre-Reformation English chalices. In Ireland, the lozenge motif continued well into the early modern period where, despite the arrival of a new

Baroque style, many Irish silversmiths continued to employ conservative medieval styles in liturgical ware.[1] Such is the case of the TP-IEP chalice, dated 1589 but still executed in Gothic style. Similar to lozenges, the lancet window design was another international motif, featuring on liturgical objects created in Ireland and elsewhere in medieval Europe and observed in the Ó Learghusa's knop and in the de Burgo-O'Malley's stem.

Figure 4.1. Photographs of analyzed chalices: (a) Ó Learghusa; (b) de Burgo-O'Malley; (c) TP-IEP.

Elemental analysis of the chalices

The elemental composition of the Ó Learghusa chalice gilding layer (representative spectrum in Figure 2a) was found consistent across the three parts of the chalice (base, knop and bowl). It was characterized by high concentration of Au and relatively high intensities of Hg, confirming the amalgam method of gilding.[152] The presence of Ag and Cu in all the spectra strongly indicated the presence of an Ag/Cu binary alloy, composing the base of the chalice. Despite the inability to quantify the XRF spectra, the interpretation of the peak areas provided valuable and interesting information. When comparing various spots of analysis, the intensities of Au were inversely proportional to those of Ag and Cu. This observation confirmed that Ag and Cu were localized to the subsurface layer, underneath the gilding layer, and suggested the presence of different thickness gilding layers on different parts of the chalice.

Figure 2b displays three representative XRF spectra of non-gilded areas. The knop and the base were characterized by the presence of Cu, Ag, Au, Hg, and Pb, whereas the bowl exhibited Cu, Ag, Au, Hg, and traces of zinc (Zn) but no detectable Pb. Au and Hg are either remnants of the now worn-out gilding layer or detected from adjacent gilded areas. The detection of Pb in the knop and base can be interpreted as an impurity within Ag, as it was never detected in the gilding layer, arising from Ag extraction through cupellation.[147] This observation suggested that different raw materials were used for the manufacturing of the bowl compared to the knop and the base. Figure 2c displays a comparison of the XRF spectra of gilded (orange line) and non-gilded areas (black line) of the knop. A significant variation in the ratio between Au and Hg was evident. The gilded region predominantly consisted of Au, while non-gilded areas (resulting from abrasion of the gilding layer) exhibited a higher concentration of Hg compared to Au. This finding indicates an enrichment of Hg at the interface of fire-gilded silver substrates, attributed to the process of amalgam/Hg diffusion into the silver substrate.[142]

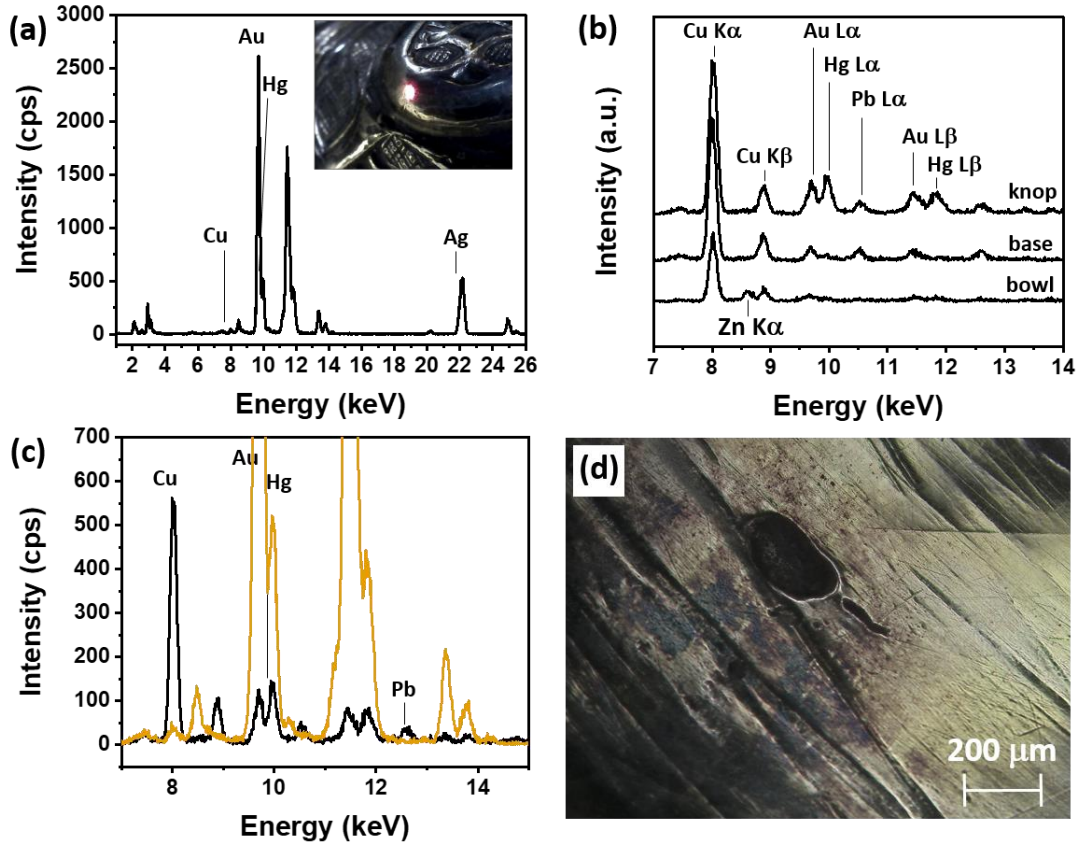

Figure 4.2. (a) Representative XRF spectrum of gilded areas (taken on the knop); (b) Representative XRF spectrum of non-gilded areas of the knop, the base, and the bowl of the chalice; (c) Comparison of XRF spectra from

gilded (orange line) and non-gilded (black line) areas. Au peaks have been cut for highlighting trace elements in the region of interest; (d) Photographic detail of the deterioration of the gilding layer.

Upon closer visual examination, it was observed that both the bowl and the base of the chalice exhibited small imperfections on the gilding layer, as depicted in Figure 2d. These imperfections, taking the form of cavities of varying sizes and shapes, were less present in the knop. Notably, these cavities were observed to be filled with a dark reddish-brown corrosion material ascribable to cuprite (Cu_2O). The presence of corrosion products formed within the Ag-Cu alloy potentially caused eruptions through the gilding layer at various locations, leading to displacement or deformation of the gilded surface.[153] Another form of deterioration, characterized by a dark corrosion layer on the gilding, was also extensively present. This dark layer indicates the formation of silver and copper sulfides (chalcocite, Cu_2S; acanthite, Ag_2S), which deposit on the surface of the gilding layer contributing to its tarnishing.[154], [155] This particular appearance is in line with literature and results from the interaction of environmental gases, primarily hydrogen sulfide (H_2S) and carbonyl sulfide (COS), with the Ag-Cu alloy.

Figure 3 summarizes the elemental characterization of the de Burgo-O'Malley chalice. The elemental composition of both the gilding and base alloy in the base, knop, and bowl of this chalice were similar to each other, suggesting that these components were produced using similar techniques and materials. The XRF spectra of the gilded areas (represented by the orange line in Figure 3a) confirmed the presence of Au and Hg, indicative of the Hg/amalgam technique utilized for gilding the artifact. Additionally, the presence of Ag and Cu indicated the use of an Ag-Cu alloy for the base, with inclusion of Pb impurities likely originating from the extraction ore (represented by the black line in Figure 3a), similar to the findings in the Ó Learghusa chalice, where cupellation was used for extracting Ag from argentiferous lead.

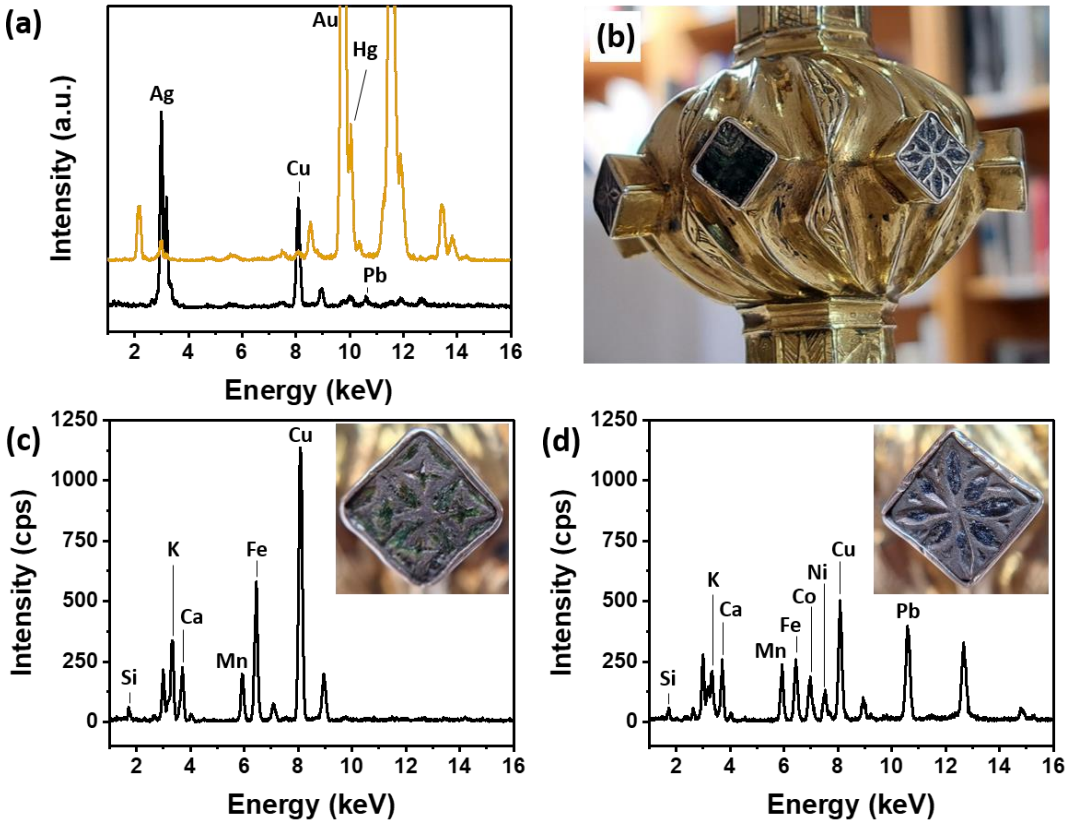

Figure 4.3. (a) Comparison of the XRF spectra from gilded (orange line) and non-gilded (black line) areas. Au peaks have been cut for highlighting trace elements in the region of interest; (b) Photographic detail of the chalice knop; (c) XRF spectrum of green enamel; (d) XRF spectrum of blue enamel. Insets in (c) and (d) show the analyzed areas.

The chalice's enamels underwent elemental investigation. The technique of decorating metals using enamels is a sophisticated craft, and in the case of this silverware, either the *champlevé* or the *basse-taille*.[156], [157] technique was used. This was observed through the marks left by the enchasing tool on the metal that remained uncovered after the loss of the enamel layer. The enamels were damaged to the extent that it was not possible to determine if they were originally meant to be transparent or opaque. Figure 3c displays the XRF spectrum of green enamels, revealing the detection of silica (Si), potassium (K), calcium (Ca), manganese (Mn), iron (Fe), and Cu. Although the Si content is dominant in enamels, representing their matrix made from aluminosilicate, Si peak intensity is very low as the XRF analysis was performed in air. The high concentration of Ag in the background of the analysis area posed a challenge in assessing K, because of the proximity of Ag L lines with K Kα line in the spectrum. However, a semi-quantitative approach using PyMca software allowed to detect K despite the interference, and its presence was attributed to the use of potash in the glass production.

The presence of Ca, Mn, and Fe, along with K, were suggestive of the use of various fluxing agents to lower the melting point of the siliceous matrix.[158], [159] Cu, detected at higher intensities than the Ag-Cu alloy in background, suggested the use of Cu-based colorant for obtaining the green color of the glass. Considering the high intensity for Fe, it cannot be excluded that a Fe-based mineral was also use for imparting a green color to the glass.[160] Cu alone may impart a bluish hue, and the addition of Fe compound(s), yellow in color, may serve to shift the overall color towards a greener shade. Figure 3d displays an XRF spectrum taken on blue enamel. Si, K, Ca, Mn, and Fe, detected at different relative ratios compared to the green enamel, were ascribed to the ingredients composing the glass matrix. Cobalt (Co), detected at relative high intensity, is known to have been used since antiquity as blue colorant in historical glasses.[161] Nickel (Ni) – detected at a similar intensity compared to Co – was interpreted as impurity in the source of Co. The contemporary presence of Co and Ni suggests the use of smalt for the blue coloring of this enamel. Studies highlighted that presence of traces elements, alone or in combination, associated to Co may suggest a provenance of the mineral.[162] For example, it is known that Co from European ores contains arsenic (As). The absence of Arsenic (As) detection excluded the use of such mineral.[163] However, more data would be needed to ascertain the exact mining sites. Pb, detected at a relatively high intensity, strongly suggested the use of a Pb-based material as an opacifier and/or for lowering down the melting point of the flux (PbO?). Evaluating the concentration of tin (Sn) was challenging due to the interference of intense peaks from Ag Kβ lines (detected from the background alloy). Nevertheless, traces of Sn were observed through a weakly intense peak at ~28.48 KeV, corresponding to Sn Kβ.

During visual assessment of the TP-IEP chalice, it was noticed that the typical porous surface texture commonly associated with fire-gilding, caused by the evaporation of Hg, was absent. Additionally, the same uniform texture of the surface was observed on the bottom of the base, which also appeared to have a golden color (see Figure 4a). This was intriguing, as areas usually hidden from view were typically not embellished with precious and expensive gold. This observation led to the suggestion that a different manufacturing technique or alloy might have been used for the TP-IEP chalice, setting it apart from the Ó Learghusa and the de Burgo-O'Malley chalices. In contrast, it was observed that the color of the alloy beneath the gilding of the knop was instead silver-

gray (visible in the photographic detail in Figure 4b), indicating that Au was applied on top of the surface and not mixed within the alloy. These findings supported the theory that the chalice had its base and bowl refurbished, possibly along with the colored decorative glass mounted in the lozenges of the knop (as observed in Figure 4a-d).

The elemental analysis of the base and the bowl (Figure 4e) revealed the presence of Ni, Cu, Zn, Au, Pb, and Ag. Considering the intensity ratio of these elements, the absence of Hg in the spectra, the uniform surface texture, and the color of the metal, it was concluded that the TP-IEP chalice was crafted using a ternary Ag-Cu-Au alloy with impurities of Ni, Zn, and Pb. Interestingly, the upper part of the base of the chalice was fire-gilded, possibly in an attempt to uniform its color to the knop. Figure 4f displays the XRF spectra of the gilding of the upper part of the base and the knop. It is visible that both spectra show the presence of Au and Hg, suggesting the detection of Hg/amalgam in both areas. However, the intensity ratios of Au vs Hg in these two parts of the chalice were found to be different suggesting a different manufacturing process. In addition, the gilding of the knop did not contain traces of Ni, Zn, and Pb (possibly from the background alloy). Unfortunately, it was not possible to access areas of the knop without gilding, therefore the composition of the base alloy is still unknown.

The decorative transparent glass, along with the blue and the violet glasses (represented by the blue, black, and orange line in Figure 4g, respectively), were characterized by the presence of major concentrations of Pb, Si, K, Ca, Mn, Fe, and Ni. Pb, Si, and K suggest the general composition of lead glasses, which were not produced before 1674,[164] are composed mainly by silica, lead oxide, and potash. The presence of Ni, found in constant concentration in all three samples, was considered a trace element of potash within the glass matrix.[165] Ca was attributed to the use of CaO as a stabilizing component of the flux.[166] Fe was present in minor concentration in all samples. The main difference among the samples lied in the content of Mn, which was found in discrete concentration in both the transparent and purple glass and was absent in the blue glass. It is known that Mn was used to achieve different effects, serving as a decoloring agent in small amounts or providing a purplish color when used in higher quantities.[167] Ag, Cu, and Au in transparent glass were interpreted as interference for the surrounding area (gilded silver).

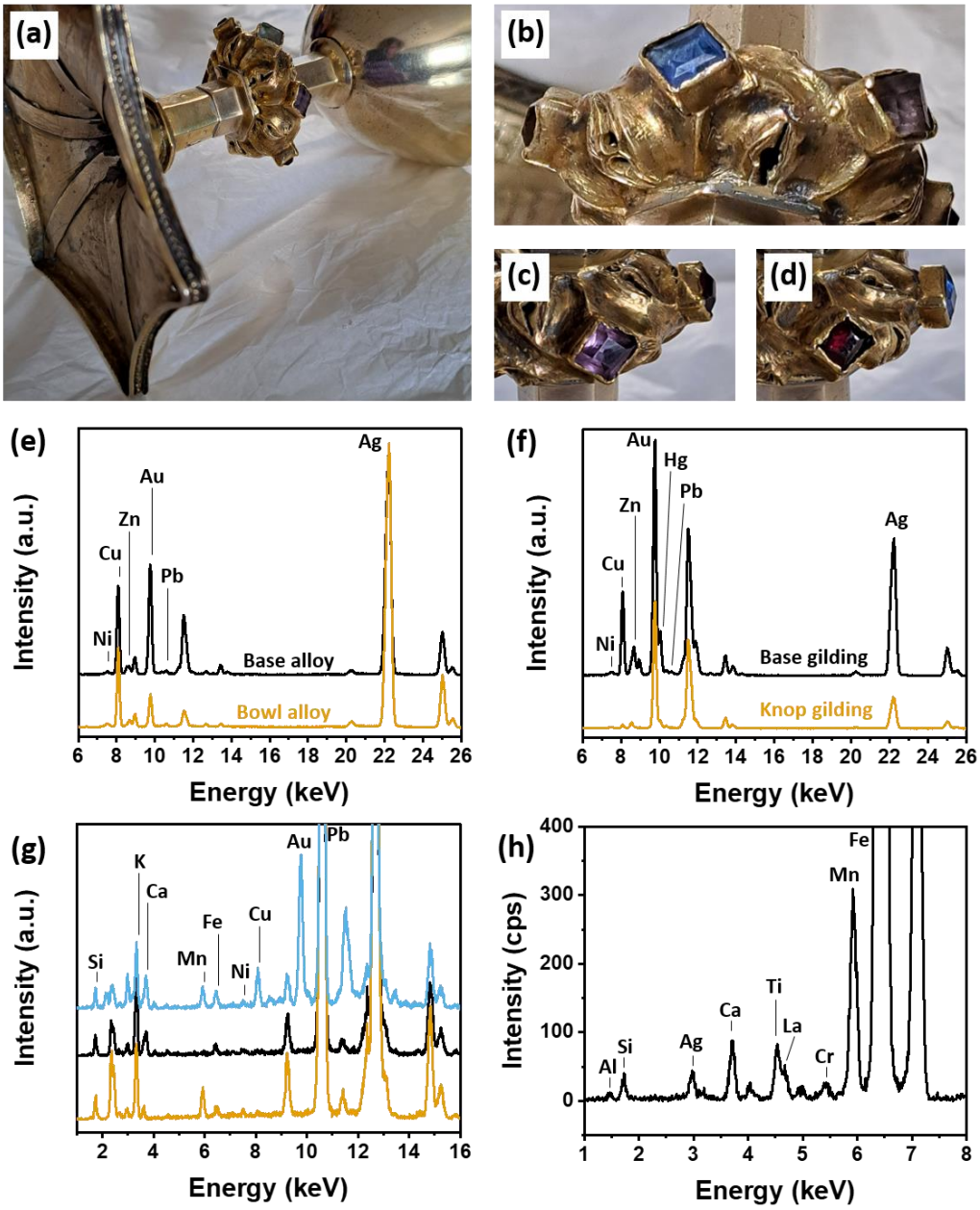

Figure 4.4. (a) Photographic detail of the TP-IEP chalice, view form below; (b) Detail of the knop with the silver-gray alloy visible, as well as the blue glass; (c) Detail of the purple glass; (d) Detail of the red glass; (e) Comparison of the XRF spectra from the bowl alloy (bottom orange line) and base alloy (top black line). (f) Comparison of the XRF spectra from the knop gilding (bottom orange line) and base gilding (top black line); (g) Comparison of the XRF spectra from the transparent glass (top blue line), blue glass (middle black line) and purple glass (bottom orange line); (h) XRF spectrum of red glass. Pb and Fe peaks in (g) and (h) were cut for highlighting traces elements in the region of interest.

4.4 Conclusions

This study presents the pioneering XRF investigation of three significant late medieval chalices associated with Ireland. Both the Ó Learghusa and de Burgo-O'Malley chalices were found to be crafted from a silver-copper alloy and decorated using the fire-gilding technique. In contrast, the TP-IEP chalice showcased a more complex construction, featuring both silver gilding and a ternary alloy composition. The analysis also extended to examining the blue and green enamels on the de Burgo-O'Malley, revealing their composition based on Co and Fe/Cu glass. The analysis of the TP-IEP chalice colored glass allowed identification of lead-potash glass. Transparent, blue, and purple colorations were likely achieved by using different concentrations of Mn. The red glass showed a notable presence of iron. These groundbreaking findings shed light on the diverse manufacturing methods employed in creating historically significant chalices, offering valuable insights into the artistic craftsmanship of medieval Ireland.

4.5 Experimental

Optical microscopy was carried out with a Zeiss Stemi 508 (Carl Zeiss MicroscopyGmbH, Jena, Germany) stereo-microscope equipped with an Axiocam 208 digital camera with 8 Megapixel resolution. The instrument was equipped with visible LED ring illuminator lights.

X-ray fluorescence spectroscopy was performed with a portable, energy-dispersive XRF ELIO (XGLab, srl). The spectrometer was equipped with a Peltier-cooled Silicon Drift Detector with a resolution f 135 eV at the manganese (Mn) K line (5.9 keV). The excitation source was a low-power (4W, 50 kV) transmission X-ray tube with a Rh anode. Measurements were performed with no filter under an air atmosphere in a range of 1–50 kV with a tube current of 10 A. A collimator, allowing a ~1 mm-diameter focused spot size on the surface of the metal, was used to acquire XRF spectra. The distance from the analyzed areas was ~1 cm, and the acquisition time was 90 secs for all spectra. The elemental characterization of the chalices encompassed both gilded and non-gilded areas of the base, knop, and bowl of each chalice. Colored enamels and glass were also characterized. For each point of analysis various measurements were taken (10 for the Ó Learghusa, 3 for the de Burgo-O'Malley, and 3 for the TP-IEP). This approach was chosen for averaging the spectra of each area to obtain a more accurate approximation of the concentration of constituent elements. XRF analysis was performed without any sample treatment (usually abrasion of the area of analysis).

4.6 References

[1] M. Krasnodebska-D'Aughton, *"Me fieri fecit: Franciscan chalices 1600-1650."* 2011.

[2] I. Krueger, *On Chalices and Ciboria of Glass*, Journal of Glass Studies, vol. 58, 2016, pp. 105–133, at p. 105.

[3] N. H. Gale and Z. A. Stos-Gale, "Ancient Egyptian Silver," J. Egypt. Archaeol., vol. 67, no. 1, pp. 103–115, Aug. 1981, doi: 10.1177/030751338106700110.

[4] P. A. Lins and W. A. Oddy, "The origins of mercury gilding," *J. Archaeol. Sci.*, vol. 2, no. 4, pp. 365–373, Dec. 1975, doi: 10.1016/0305-4403(75)90007-2.

[5] R. Margreiter, J. Baumann, I. Mantouvalou, M. Radtke, U. Reinholz, and E. Strub, "Investigations on fire-gilding," *Archaeometry*, vol. 64, no. 6, pp. 1465–1478, 2022, doi: 10.1111/arcm.12797.

[6] F. Cabrol, ed., *Dictionnaire d'archéologie chrétienne et de liturgie*. Paris, Letouzey et Ané, 1910, pp. 42-47

[7] L. Beck, S. Bosonnet, S. Réveillon, D. Eliot, and F. Pilon, "Silver surface enrichment of silver-copper alloys: a limitation for the analysis of ancient silver coins by surface techniques," Sep. 2020.

[8] E. HALL, "Surface-Enrichment of Buried Metals," *Archaeometry*, vol. 4, pp. 62–66, Aug. 2007, doi: 10.1111/j.1475-4754.1961.tb00535.x.

[9] A. N. Shugar and J. L. Mass, *Handheld XRF for Art and Archaeology*. Leuven University Press, 2012.

[10] D. A. Scott, *Metallography and microstructure of ancient and historic metals*. Marina del Rey, CA: Getty Conservation Institute in association with Archetype Books, 1991.

[11] P. Craddock, “Production of Silver across the Ancient World,” *ISIJ Int.*, vol. 54, no. 5, pp. 1085–1092, 2014, doi: 10.2355/isijinternational.54.1085.

[12] J. Mass and C. Matsen, “Quantitative non-destructive analysis of historic silver alloys: X-ray fluorescence approaches and challenges,” *Handheld XRF Art Archaeol.*, pp. 215–248, Jan. 2012.

[13] M. Ferretti, C. Polese, and C. Roldán García, “X-ray fluorescence investigation of gilded and enamelled silver: The case study of four medieval processional crosses from central Italy,” *Spectrochim. Acta Part B At. Spectrosc.*, vol. 83–84, pp. 21–27, May 2013, doi: 10.1016/j.sab.2013.02.001.

[14] I. Delamer, *500 years of Irish silver : an exhibition at the National Museum of Ireland /*. in National Museum of Ireland monograph series; p. 33 Wordwell in association with the National Museum of Ireland, 2005.

[15] J. J. Buckley, *Some Irish altar plate: a descriptive list of chalices and patens, dating from the Fourteenth to the end of the Seventeenth Century, now preserved in the National Museum and in certain churches*, vol. 1, 9 vols., pp. 22-23, Dublin: Royal Society of Antiquaries of Ireland, 1943.

[16] Information provided by Dr Edith Andrees, “National Museum of Ireland database,” Apr. 27, 2023.

[17] K. Anheuser, “The practice and characterization of historic fire gilding techniques,” *JOM*, vol. 49, no. 11, pp. 58–62, Nov. 1997, doi: 10.1007/s11837-997-0015-6.

[18] D. A. Scott, “The Deterioration of Gold Alloys and Some Aspects of Their Conservation,” *Stud. Conserv.*, vol. 28, no. 4, pp. 194–203, 1983, doi: 10.2307/1505967.

[19] T. E. Graedel, “Corrosion Mechanisms for Silver Exposed to the Atmosphere,” *J. Electrochem. Soc.*, vol. 139, no. 7, p. 1963, Jul. 1992, doi: 10.1149/1.2221162.

[20] J. Ortíz-corona and F. J. Rodríguez-gómez, “Role of copper in tarnishing process of silver alloys in sulphide media,” *Trans. Nonferrous Met. Soc. China*, vol. 29, no. 12, pp. 2646–2657, Dec. 2019, doi: 10.1016/S1003-6326(19)65171-X.

[21] D. Buckton, “Enamelling on gold,” *Gold Bull.*, vol. 15, no. 3, pp. 101–109, Sep. 1982, doi: 10.1007/BF03214613.

[22] M. Campbell, *An Introduction to Medieval Enamels*. H.M. Stationery Office, 1983.

[23] "Enamels of Limoges, 1100–1350 - MetPublications - The Metropolitan Museum of Art." https://www.metmuseum.org/art/metpublications/enamels_of_limoges_1100_1350 (accessed Jul. 26, 2023).

[24] M. T. Wypyski, "Technical Appendix: Compositions of Enamels on the George Watch," *Metrop. Mus. J.*, vol. 35, pp. 150–7, 2000, doi: 10.2307/1513031.

[25] V. Van Der Linden *et al.*, "Deeply coloured and black glass in the northern provinces of the roman empire: differences and similarities in chemical composition before and after AD 150," *Archaeometry*, vol. 51, no. 5, pp. 822–844, 2009, doi: 10.1111/j.1475-4754.2008.00434.x.

[26] G. Van der Snickt, O. Schalm, J. Caen, K. Janssens, and M. Schreiner, "Blue Enamel on Sixteenth - and Seventeenth-Century Window Glass," *Stud. Conserv.*, vol. 51, pp. 212–222, Jan. 2006, doi: 10.1179/sic.2006.51.3.212.

[27] B. Gratuze, I. Pactat, and N. Schibille, "Changes in the Signature of Cobalt Colorants in Late Antique and Early Islamic Glass Production," *Minerals*, vol. 8, May 2018, doi: 10.3390/min8060225.

[28] P. Colomban, B. Kırmızı, C. Gougeon, M. Gironda, and C. Cardinal, "Pigments and glassy matrix of the 17th–18th century enamelled French watches: A non-invasive on-site Raman and pXRF study," *J. Cult. Herit.*, vol. 44, pp. 1–14, Jul. 2020, doi: 10.1016/j.culher.2020.02.001.

[29] D. Dungworth and C. Brain, "The 'Invention' of Lead Crystal Glass," *34th Int. Symp. Archaeom. 2006-01-01 ISBN 84-7820-848-8 Pags 453-458*, Feb. 2015.

[30] Z. Cílová and J. Woitsch, "Potash – a key raw material of glass batch for Bohemian glasses from 14th–17th centuries?," *J. Archaeol. Sci.*, vol. 39, no. 2, pp. 371–380, Feb. 2012, doi: 10.1016/j.jas.2011.09.023.

[31] Z. Zlámalová Cílová, M. Gelnar, and S. Randáková, "Trends in Colouring Blue Glass in Central Europe in Relation to Changes in Chemical Composition of Glass from the Middle Ages to Modern Age," *Minerals*, vol. 11, no. 9, Art. no. 9, Sep. 2021, doi: 10.3390/min11091001.

[32] B. Lockhart, “The Color Purple: Dating Solarized Amethyst Container Glass,” *Hist. Archaeol.*, vol. 40, no. 2, pp. 45–56, Jun. 2006, doi: 10.1007/BF03376725.

4.7 Supplementary material

Description of the chalices.

The Ó Learghusa chalice is relatively small, standing at 16cm in height, with its bowl being 10.3cm in diameter and its foot 12.2cm in diameter. The stem with the knop is the most ornate part of the chalice. Around the middle part of the knop there are twelve lozenges (rhombus shapes) filled with plant motifs, which intersect to form the x shape; one of the lozenges bears the sign of the cross. Above and below the lozenges there are twelve lobes (six on either side of lozenges), each decorated with a leaf design. Between the lobes there are designs that look like elongated Gothic lancet windows. The foot of the chalice is circular with a flattened rim: three small holes and a rivet suggest that the foot bore a figure of Christ crucified or the cross, a typical representation for the liturgical plate at that time. The absence of any inscriptions or hallmarks on the chalice posed a challenge in assigning a specific provenance or date to the artifact. The foot is circular, where typically a polygonal shape (hexagonal or octagonal) is a feature in chalices dating from the later medieval period. These non-typical shapes of the bowl and the foot suggest that the Ó Learghusa chalice may be a composite object.

The de Burgo-O'Malley chalice measures 20.3cm in height, its wide bowl is 10.5cm in diameter and its foot is 16.2cm wide. The chalice has an octagonal stem with chased decoration and a knop with eight projecting lozenges, each with translucent enamel. The stem is engraved with different designs: four undecorated walls of the stem above the knop alternate with four panels decorated with lancet window designs; below the knop four stem panels display lancet window designs that alternate with plant motifs. The foot is octagonal with incurved angle and base lines. The foot is engraved with the

sacred monogram (IHC) and the Latin inscription that reads “Thomas de Burgo et Grania Ni Malle me fieri fecerunt Anno Domini MCCCCLXXXXIIII”.

The TP-IEP chalice measures 15cm in height, the bowl is 9.6cm in diameter and the foot is 11.9cm wide. The bowl of the chalice is wide and splayed. A plain stem is hexagonal in section with a flattened knop. The knop is embellished with openwork designs and six projecting lozenges, each filled with color glass. The foot is a flattened hexagonal pyramidoid with incurved angle and base lines. It is inscribed with the words: ‘TP ET IEP ME FIERI FECERVT QVORVM ANIMABVS MISERIATVR OMNIPOTENS 1589’. One facet of the foot bears the image of the Paschal Lamb with a cross. The gilding on the bowl and on portions of the stem appear paler than the knop and the foot suggesting that these parts may be later replacements.

Conclusion and Recommendations

The Inks & Skins project (I&S) has played a pivotal role in shaping the foundation and direction of this thesis. Through its interdisciplinary approach, merging the fields of humanities and scientific research, I&S aimed to unlock the mysteries concealed within medieval Irish Gaelic books written on animal skin. The primary objective was achieved through a comprehensive investigation that combined codicological studies, advanced analytical techniques, and collaborative efforts across multiple fields.

The preliminary examination of the Book of Uí Mhaine, conducted with state-of-the-art scientific methodologies, led to a deeper understanding of the materiality and composition of the manuscript. This analytical approach not only supported the conjectures formulated during the visual and codicological assessment but also provided valuable insights into the availability, origins of materials, and the techniques employed by scribes in their creation.

Through the exploration of this target manuscript, insights were gained into the Gaelic manuscript tradition. This offered a tool for conducting comparative analyses of medieval manuscripts in the same tradition, as well as manuscripts belonging to other medieval Irish traditions. This newfound understanding provides a solid foundation for conducting further comparative analyses.

To advance this research, it is recommended to expand the array of Irish manuscripts, a path already initiated during the course of this thesis. This entailed subjecting to scientific analysis 27 other medieval Irish manuscripts written on animal skin.

The scope of the study should encompass the parallel Irish traditions of making manuscripts: the Ecclesiastical tradition within monastery settings and the Municipal

tradition in administrative contexts, such as the books produced in cities under English administration. By applying the examination protocol exemplified in the published article on the Book of Uí Mhaine to a comprehensive selection of manuscripts, the potential for drawing broader conclusions regarding shared materials and technologies in distinct temporal, political, and geographical contexts will become evident. The integration of statistical methodologies could further enhance the accuracy and depth of these conclusions, thereby enriching our understanding of the intricate fabric of Ireland's manuscript heritage.

The fusion of analytical methods with humanities was an essential ingredient in the successful unraveling of historical narratives. I&S project exemplified this integration, showcasing the importance of collaborative efforts from fields like material science, analytical bibliography, paleography, conservation, and codicology in forming accurate conclusions. Collaborations with institutions and libraries, enriched the project and underlined the significance of interdisciplinary teamwork.

As evidenced by the exploration of the Harward's Almanac and the late medieval Irish chalices, this thesis has further demonstrated the advantages of multifaceted approaches. A holistic research approach that combined material analysis, historical context, and visual assessment yielded more comprehensive and accurate results. Therefore, future researchers should place emphasis on gathering a diverse range of data sources and integrating them to form a complete picture of Irish books on paper, as well as medieval artefacts made of metals.

Similarly to what was suggested for continuing the research on Irish manuscript traditions, the possibility of studying a larger sample set is pivotal for having an accurate representation of the artistic production and metallurgical methodologies employed in medieval Ireland. This principle of broadened analysis is equally relevant when examining Irish books produced on paper during later epochs.

In all cases, researchers should invest significant effort in data treatment, interpretation, and contextualization. Historical research provides crucial insights into the provenance, production techniques, and aging processes of materials, while visual assessment and scientific analysis aid in identifying patterns and anomalies. By delving into historical context, conservation reports, and comparable artworks, scholars lay the foundation for a robust scientific protocol, which is strongly driven by their research

questions. Neglecting these crucial elements can lead to misleading analytical data and misguided interpretations.

Future researchers should prioritize open access publications and knowledge dissemination. Sharing research findings, methodologies, and datasets with the scholarly community and the public contributes to the advancement of knowledge and encourages broader engagement.

The preservation of cultural heritage artifacts is a shared responsibility. Institutions, researchers, scientists, and conservators should collaborate to develop and implement effective long-term preservation strategies. This includes proper storage conditions, conservation treatments, and ongoing monitoring to safeguard the integrity of artifacts for future generations. All these are informed by the deep knowledge of the materials to preserve, again, underscoring the importance of material studies.

In conclusion, the recommendations outlined above serve as guiding principles for future research endeavors in the intersection of humanities and scientific investigation. The lessons learned from I&S project and the collaborative efforts undertaken in this thesis provide a roadmap for researchers seeking to unlock the secrets of the past and reshape our understanding of Irish cultural heritage. By embracing interdisciplinary collaboration, advanced analytical techniques, and a holistic research approach, scientists and scholars can continue to push the boundaries of knowledge and contribute to the preservation and interpretation of our shared history.